PLEASE NOTE:

In all cases this material has been filmed in the best possible way from the available copy. Problems encountered with this document have been identified here with a check mark ✓.

1. Glossy photographs _____
2. Colored illustrations _____
3. Photographs with dark background _____
4. Illustrations are poor copy _____
5. Print shows through as there is text on both sides of page _____
6. Indistinct, broken or small print on several pages ✓ throughout _____
7. Tightly bound copy with print lost in spine _____
8. Computer printout pages with indistinct print _____
9. Page(s) _____ lacking when material received, and not available from school or author _____
10. Page(s) _____ seem to be missing in numbering only as text follows _____
11. Poor carbon copy _____
12. Not original copy, several pages with blurred type _____
13. Appendix pages are poor copy _____
14. Original copy with light type _____
15. Curling and wrinkled pages _____
16. Other _____

University Microfilms International

300 N. ZEEB RD., ANN ARBOR MI 48106 (313) 761-4700

THE UNIVERSITY OF OKLAHOMA

GRADUATE COLLEGE

DEVELOPMENT OF SMALL SCALE LIQUID IGNITION TEST

A DISSERTATION

SUBMITTED TO THE GRADUATE FACULTY

in partial fulfillment of the requirements for the degree of

DOCTOR OF PHILOSOPHY

BY

KOU-CHU YIIN

Norman, Oklahoma

1979

DEVELOPMENT OF A SMALL SCALE

LIQUID IGNITION TEST

APPROVED BY

C. M. Stevenich

K E Starling

Sub Gollahalli

J M Townsend

Krishna Kumar

DISSERTATION COMMITTEE

ABSTRACT

The principal objective of this work was to develop an apparatus and experimental procedure for small scale liquid flammability tests. N-tridecane, n-tetradecane and four mixtures of normal paraffins, from n-$C_{12}H_{26}$ to n-$C_{15}H_{32}$, were used to demonstrate the feasibility and effectiveness of the test apparatus. Both piloted and unpiloted ignition tests were conducted by using external radiant energy (heating source) supplied by tungsten filament lamps. The results indicate that the ignition times are primarily functions of incident irradiance (energy per unit area per unit time) for both piloted and unpiloted ignitions. As has been observed previously for the ignition of solids, the reciprocal of the ignition time for liquids also varies linearly with the incident irradiance; the minimum incident irradiance below which ignition did not occur (in infinite time) was found to be 0.06 cal/cm^2-sec for liquid n-tridecane and 0.078 cal/cm^2-sec for liquid n-tetradecane respectively.

The results obtained also show that the rate of heat loss has a significant effect on the ignition time as was demonstrated by two experiments: (1) varying the volume of

the liquid sample and (2) inserting a water cooled radiometer in the liquid sample.

The fraction of incident irradiance absorbed by the liquid increased exponentially with the depth of the liquid, reaching a value of about 40 percent absorbed for a depth of 1.7 cm, while the fraction reflected at the liquid surface was about 17 percent. The maximum surface ignition temperature obtained for liquid n-tridecane and n-tetradecane are 200 and 210°F, respectively. The various mixtures of four normal paraffins, from n-$C_{12}H_{26}$ to n-$C_{15}H_{32}$, show very little difference in their maximum surface ignition temperatures (in piloted ignition tests with temperature measured at the center of the liquid surface) which ranged from 190 to 200°F according to their compositions.

ACKNOWLEDGMENTS

I would like to express my gratitude and appreciation to a number of persons who have contributed to this research effort.

Dr. C. M. Sliepcevich, George Lynn Cross Research Professor of Engineering, for providing the opportunity to conduct this research and for his invaluable guidance and untiring assistance throughout the whole course.

Dr. S. R. Gollahalli for his kind help in many areas.

Dr. K. M. Sista for his patience and untiring assistance.

Dr. K. E. Starling and Dr. F. M. Townsend for their service on my graduate committee.

Dr. W. E. Martinsen, Dr. D. W. Johnson, Dr. J. R. Welker, Dr. V. V. Hathi, Mr. L. C. Higginbottom, Mr. P. E. Miller and Mr. K. Hudson for the assistance in the development of the experimental apparatus and techniques.

Miss Trish Brown for the preparation of the manuscript.

I am grateful to the Chemical Engineering Department, U. S. Coast Guard and University Technologists, Inc. for providing financial support during this long period.

And finally, it has been my family who have sacrificed the most. My parents, my parents-in-law, my wife, and my

brothers furnished the incentive for this work. Without their encouragement and support there would have been little reason for its completion.

Kou-Chu Yiin

TABLE OF CONTENTS

LIST OF TABLES

LIST OF ILLUSTRATIONS

DEVELOPMENT OF A SMALL SCALE LIQUID IGNITION TEST

CHAPTER 1

INTRODUCTION

In the early days a small procelain dish of oil was slowly heated and at regular intervals a flame (pilot) was passed through the vapor evolved, to check whether they caught fire or not. This "flash point" determination at first was carried out in the "naphtometre" of Parrish (1865), later by Tagliabue (1870), Abel (1880) and Luchaire (1880). In the last two decades of the nineteenth century, the determination of the ignition temperature of flammable gas (or vapor) was the subject of many experimental investigations, in which, one of the two following methods was employed. Either the gas was passed through a tube which was heated from a low initial to a definite temperature, or it was enclosed in a small vessel and plunged into a bath of known temperature. Mallard, LeChatelier, Meyer, Krause, Emich and many others are the well known pioneer investigators.

The earliest determination of the spontaneous ignition temperature (S.I.T.) of a fuel was undertaken in 1906 by Falk

at the suggestion of Nerst; a rapid adiabatic compression apparatus was used with cylinder diameters ranging from 1 to 2 inches to determine the S.I.T. of hydrogen-oxygen mixtures. Since then, over a period of 40 years improvements in the above methods and many developments of other methods have taken place in many countries to measure ignition temperatures of liquid fuels. Countries which have published extensively in this area of investigation include France, Germany, Japan, Russia, United Kingdom and United States. A description of these various methods together with summaries of the test results and conclusions are available from many sources, such as Lewis and von Elbe (52), Coward and Jones (22), Mullins (56), NACA report 1300 (10), Rix, Strother and Woodbridge (63), Penner and Mullins (61), Zabetakis and Burgess (85), Zabetakis (84), etc.

Although ignition of solids (wood, fabrics, polymers, solid propellants) by applying external radiation from hydrocarbon diffusion flames, electric arcs, solar furnaces, gas-fired panels, electrical coils and tungsten lamps has been studied extensively, ignition of liquids by external radiation has not received much attention. The principal contribution in relating incident radiant energy to the flammability of liquid fuels was by Ormandy and Craven (60) who applied infrared radiation in S.I.T. measurements of n-heptane by Moore's ignition meter in 1926. Except for this paper no others appear in recent ignition literature, despite

the fact that liquids, as well as solids, are exposed to external heat by radiation from nearby fires in real life situations. The objective of this study, therefore, was to develop a test apparatus and experimental procedures for quantifying the ignition of liquids exposed to external radiation.

In an effort to achieve a more quantitative measurement of the ignition behavior of solids, the University of Oklahoma Flame Dynamics Laboratory developed a vertical ignition test cabinet in 1965. The radiative heating source selected was a liquid hydrocarbon (usually benzene) diffusion flame or, alternatively, tungsten filament lamps. For some plastics or polymers which drip during the preheating period before ignition, this cabinet could not be utilized. Therefore, University Engineers, Inc. (a private consulting engineering firm associated with the Flame Laboratory) subsequently devised a horizontal ignition test cabinet for this purpose, using a tungsten lamp as the radiation source. Originally, it was intended to use this horizontal ignition cabinet for the present studies on ignition of liquids. However, after preliminary experimentation, it became evident that a new cabinet would have to be designed and fabricated for accommodating liquids. In the present work, the specially designed and fabricated apparatus for liquid fuels was used to measure ignition times for liquids exposed to different levels of incident irradiances. In addition the temperature

of the liquid at the ignition point was obtained and was compared to the conventional flash point temperatures reported in the literature. The important distinction is that the flammability characteristics as obtained by the irradiance method developed in this study contains the additional information on the elapsed time required for ignition to occur as well as the temperature at ignition. In assessing fire hazards, the time parameter is of more substance than temperature.

In discussing the flammability of liquids, a terminology has evolved which is identified with the following definitions:

1. Spontaneous Ignition Temperature (S.I.T.) was defined by Moore (54) as the minimum temperature of a fuel at which ignition occurs without the assistance of any external flame or spark. For spontaneous ignition to occur, the liquid must be heated at a rate to evolve a sufficient amount of volatiles which mix with the surrounding air to form a combustible mixture.

2. Flammability Limits (61) define the minimum and maximum concentrations of the combustible vapors admixed with air (or the specified oxidant) for which the application of a strong external ignition source is only just capable of producing a sustained flame in a given test apparatus.

3. Flash Point (61) is defined as the minimum temperature at which a liquid will evolve a flammable vapor when

admixed with air and contacted with a small, naked flame (called a pilot). The flash point temperature is quite sensitive to the heating rates applied externally to the containment vessel and to the precise manner in which the experimental details are conducted.

4. Piloted Ignition (80) refers to an ignition which is actuated by inserting a naked, piloted flame or spark, or any form of a piloter into the volatile fuel-oxidant mixture, as contrasted to spontaneous or unpiloted ignition.

5. Unpiloted Ignition, exclusively used in this work, refers to an ignition not initiated by a naked pilot flame. (In this study, however, so-called unpiloted ignition is actually piloted by the hot, inert surface of the tungsten lamps.)

6. Spontaneous Ignition Delay or Ignition Delay (61) is the time interval between the moment a homogeneous combustible mixture suddenly attains a given initial temperature and the moment when spontaneous ignition or spontaneous radical ignition occurs.

7. Ignition Time as introduced in this work is the elapsed preheating time by the external radiation source (tungsten lamps) to bring the liquid from a preset condition--such as ambient temperature and pressure--to the condition where a sustaining flame appears near the surface of the liquid as a result of either unpiloted or piloted induced ignition.

As emphasized before, relatively little work has been done on the ignition of liquid fuels by external, radiant heating. Even though the physical properties, phase transitions and subsurface heat transfer mechanisms between liquid and solid fuels are quite different, it can be anticipated that the ignition of solids and liquids are fundamentally very similar. As the radiant energy impinges in the surface of either a solid or liquid fuel which is initially at a temperature below its flash point (or fire point), the fuel temperature will gradually increase with time. Simultaneously, volatile products are evolved by either pyrolysis or evaporation. The evolved volatiles or active fragments mix with oxygen in the air and ignition can occur when the lower flammability limit is reached. Since ignition actually occurs in the vapor phase near the surface for both liquids and solids, the basic mechanisms should be alike. One concept of ignition of solids is that the surface must reach a characteristic (ignition) temperature before it will ignite. Correspondingly, and by definition, liquids must reach their flash points before ignition can occur.

The principal factors governing the ignition of liquids have been investigated experimentally in this study. The experimental techniques, experimental data, correlations and ignition criteria are presented in subsequent sections.

CHAPTER II

REVIEW OF PREVIOUS WORK AND THEORIES

In this review of the literature on the flammability of liquid, the ignition of solids and gases will also be covered to the extent that it impacts on the ignition of liquids.

Ignition Process and Criteria

Brown (13) concluded that if a combustible material is heated gradually in the presence of sufficient air, a very slow reaction first takes place between the fuel and oxygen. As the rate becomes faster with increasing temperature, the heat of reaction evolved further increases the temperature and promotes the reaction itself. At the same time there is heat loss from the material to the environment through conduction, convention and radiation. At a certain temperature the rate of reaction is sufficiently rapid such that the resulting rate of heat generation exceeds that of heat loss. Consequently, the temperature of the material rises much faster than it would otherwise by external heating alone. Thus, the reaction accelerates itself and very rapid heating follows, the end result of which is visible evidence

of ignition, such as a glow or flame. Brown lists the following requirements for ignition to take place:

1. A combustible material must be present.

2. A source of oxygen, such as air or other, must be available within certain concentration limits relative to the combustible.

3. Heat must be evolved as a result of the combustion reactions.

4. The reaction must proceed rapidly over a certain temperature range.

5. The reaction must be accelerated by a rise in temperature.

6. A supply of energy, sufficient to the point where the reaction becomes autogenious, is necessary.

Brown also points out that ignition is a process requiring time rather than being an event in time; in other words ignition does not imply a discontinuity between the rate of the reaction and temperatures. He further emphasizes that ignition cannot be considered synonymous with the appearance of glow or flame, as sometimes held, since these phenomena can not occur unless the ignition process is first carried out. Based on this concept, he defines the ignition temperature as being the temperature in the center of the surface of the combustible material for which the rate of heat generated by the reactions inducing ignition just exceed the rate at which heat is dissipated by all causes under the

given conditions. The ignition point defined by Brown is, therefore, identified as the inflection point on the temperature-time curve.

Simms (8) classified the factors influencing the ignition process of materials into two categories, internal and external. Thermal properties, pyrolysis characteristics, the absorptivity of the irradiated surface, diathermancy, size of the irradiated area and moisture content of the fuel are considered as internal factors which are mainly the properties of the solid. Factors such as irradiance, time of exposure, areas of uniform energy flux, the type of ignition, draft and specimen preheating are recognized as external factors.

Glassman et al (28, 29, 53), in their flame spreading studies, have summarized the postulated physical processes involved as follows:

1. Heat transfer from the flame and (the source of radiation) to the atmosphere.

2. Heat transfer from the flame to the fuel surface below the flame.

3. Heat transfer from the flame to the fuel surface ahead of the flame.

4. Heat transfer from the precursor to the fuel surface below the precursor.

5. Heat transfer from the flame to the edges of the containment vessel or tray.

6. Heat transfer from the surface of the fuel to the bulk of the fuel.

7. Heat transfer from fuel under the flame to the fuel ahead of the flame.

8. Heat transfer from the fuel layer to the water layer (where fuel is suspended over water) and thence to the tray.

9. Heat transfer from the fuel layer to the walls of the tray.

10. Heat transfer from the tray rim to the bulk of the tray and thence to the table top.

11. Heat transfer from the tray to the fuel layer.

12. Evaporative mass transfer of fuel from the surface.

13. Mass transfer upwards of the hot combustion products.

14. Mass transfer of air into the flame (or the plume) both ahead of the spreading flame and over the tray edges.

Some of these processes represent heat losses which slow down the propagation of flame.

Hallman (32) has concluded that the ignition phenomena for solids can be generalized as a function of many variables.

$$I_g = f(T_z, \bar{T}, T_s, T_o, T_g, H_f, H_z, E_s, C_p, k, t, L, h, \rho, M, A, \varepsilon_\lambda, \nu_\lambda, \alpha_\lambda, H_i, ---) \quad \text{(II-1)}$$

where

I_g = ignition criteria

T_g = gas film temperature

$\overline{T}$ = source temperature

T_z = pyrolysis temperature

T_s = source temperature of the material

T_o = ambient temperature

E_s = activation energy of the material

C_p = specific heat

k = thermal conductivity

t = time

L = thickness of the material

h = convective heat transfer coefficient

M = molecular weight

ε_λ = emittance of source for each wavelength involved

ν_λ = attenuation factor for each wavelength involved

λ = wavelength

ρ = density

H_i = incident irradiance

H_f = heat of fusion

H_z = heat of pyrolysis

A = area of the material under test

α_λ = surface absorptance for each wavelength involved

The complexities of ignition phenomena are illustrated by the number of variables shown in Equation II-1.

Kanury (38), in his review, lists the following conditions for ignition to occur:

1. Attainment of a fixed critical temperature T* by the exposed surface is an adequate criterion to predict transient flame ignition for radiative as well as convective heating. If ignition is spontaneous, the concept of critical exposed surface temperature is expected to be associated with some type of critical thermal phenomenon. If the ignition is piloted, attainment of the critical temperature by the exposed surface is expected to be a passive indication of attainment of a critical pyrolysis rate.

2. If the enthalpy content of the solid at the instant of termination of the external heating exceeds a critical lower limit enthalpy, persistent flaming is assumed. The critical lower limit enthalpy is roughly $2L\rho C(T_p - T_o)$, where ρC is the volumetric heat capacity of the solid, $2L$ is the thickness of the fuel bed, T_p is a temperature related to the pyrolysis kinetics (may be taken as approximately 320°C for cellulosic solids) and T_o is the initial temperature.

3. As the slab thickness becomes small, the thin fuel bed limit is approached. In this limit, once ignition occurs, it is persistent. Therefore, for thin bodies, fulfillment of the T* criterion automatically fulfills the critical enthalpy content criterion.

These deductions for solids apply as well to liquids.

From studies of the spreading of flame over a liquid by Burgoyne et al (14, 15), Glassman et al (28, 29, 53) and others (68, 69), it can be concluded that flame spreading is a series of continuous ignition processes. For liquids at temperatures initially below the fire (or flash) point, an igniter must first heat the surface in its neighborhood to this temperature. The ignition delay with a liquid pool may be appreciable, owing to fluid motion apparently induced by buoyant and/or surface tension forces. Thus, a greater mass must be heated to the flash point than with a less mobile system. In general, flash or ignition is initiated in the plume, near the condensed fuel, which has been observed in many experiments and has been theoretically predicted by Kashiwagi (38), Kumar and Hermance (46), Kindelan and Williams (41, 42, 43), Law (48, 49) and other.

A considerable problem exists in the study of ignition mechanisms due to various definitions and criteria for ignition. The exact state of ignition is itself an ill-defined concept, but ignition delay can be evaluated only by defining in advance some criterion of runaway. In most experiments, the measurements of ignition delay time are based on the detection of light emission or sound explosion. However, such criteria cannot be applied solely as the theoretical ignition delay unless detailed values of the parameters for the chemical reaction kinetic mechanisms are well understood. Although at present the available information related to the

mechanisms of complex chemical reactions are limited, it is believed that the ignition criterion should include the effect of the chemical reaction process in addition to the conventional thermal criterion.

In general, there are six well-established gas phase ignition criteria available mathematically (39):

1. The total gas phase reaction rate becomes equal to or greater than a constant "C_1."

$$\int_0^\infty (\text{reaction rate})\ dy \geq C_1 \qquad \text{(II-2)}$$

2. The minimum local gas phase reaction rate becomes equal to or greater than a constant "C_2."

$$\text{Minimum reaction rate} \geq C_2 \qquad \text{(II-3)}$$

3. The maximum local gas phase reaction rate becomes equal to or greater than a constant "C_3."

$$\text{Maximum } (\theta) \geq C_3 \qquad \text{(II-4)}$$

Where θ is a non-dimensional temperature parameter.

4. The total heat release rate of the exothermic gas phase reaction becomes equal to or larger than the rate of radiant energy absorption in the condensed phase.

$$Q \int_0^\infty (\text{reaction rate})\ dy \geq I_o(1-r) \qquad \text{(II-5)}$$

where

Q = heat of combustion per gram of fuel consumed

I_o = incident radiant flux

r = reflectivity

5. The acceleration of the total gas phase reaction rate becomes equal to or greater than a constant "C_4."

$$\frac{\partial}{\partial t} \int_0^\infty (\text{reaction rate})\, dy \geq C_4 \qquad \text{(II-6)}$$

6. The temperature gradient of the gas phase at the fuel surface becomes zero or positive.

$$\left(\frac{\partial \Theta}{\partial \eta}\right)_{\text{surface}} \geq 0 \qquad \text{(II-7)}$$

where

η = non-dimensional coordinate normal to the surface

Mullen et al (55), Kumagai and Kirmura (45) and Adomeit (1) have made significant contributions by their experimental investigations on the subject of ignition of flowing gases over hot bodies, such as electrically heated circular rods. Adomeit (1) correlated these experimental data in terms of the influence of rod diameters, rod temperature, free flow velocity, etc.

Chambre (19) studied analytically the ignition of a planar, stagnation flow. An explicit expression for the ignition temperature was derived for the case of Lewis number (Le = Sc/Pr) equal to unity and with a very large dimensionless activation energy $(E/RT_w) >> 1$, where E = activation energy, R = universal gas constant and T_w = wall temperature. The assumption of a large activation energy is required in order to make the reaction zone very thin and close to the surface of heating source so that an estimate of the temperature gradient needed in his calculation can be made from the results of earlier, non-reacting, boundary layer flow

calculations. The derived ignition criterion $(\partial T(x,0)/\partial y) = 0$ has been widely applied in later work on ignition study at the stagnant point or surface. Sharma and Sirignano (66), using a second order rate law of chemical reaction, have solved numerically the governing equation for the planar and axisymmetric stagnant flows. The surface temperature of the wall (T_w or equivalent to ignition temperature) was obtained for a limited range of the first Damkohler number (defined as the ratio of convective time to chemical time). Alkidas and Durbetaki (5) extended the range of the first Damkohler number beyond which ignition is impossible. The incompressible fluid-dynamic approximation was used in their analysis. Alkidas and Durbetaki (6) have applied numerical methods to study the ignition and extinction characteristics of the stagnation flow of premixed gases in steady-state systems. (This approach is commonly referred to as the absolute theory.) The incompressible fluid-dynamic approximation was adopted to study the effect of the Damkohler similarity parameter on the surface heat transfer of a premixed gas in the stagnation region of a blunt body. They used this model in a subsequent study (7) to examine the steady-state theory of ignition of a premixed gaseous mixture by a hot surface. They found that for incompressible flow conditions the first Damkohler number (D_I) was very sensitive to changes in the ignition temperature; for instance, the difference between the absolute theory and the van't Hoff criterion of ignition can be as large as 57 percent when the dimensionless ignition

temperature at the surface of a blunt body is 3.5. But, the calculated dimensionless ignition temperatures were not sensitive to the variation of the first Damkohler numbers. for example, when D_I value is larger than 10^{10}, the differences of calculated ignition temperatures between the above two approaches are only about 2 percent. Smith et al (70) have also applied the absolute theory to study the extinction characteristics of the stagnation flow of premixed gases. They focus their attention to the extinction phenomena of a carbon monoxide - humid air mixtures at the stagnation region of a heated plate.

Law (49) presented a mathematical analysis of the ignitability of a cold premixed combustible at the stagnant point of an isothermal hot surface in the limit of large activation energy. Asymptotic analytical solutions were obtained for the first order perturbation, resulting in explicit expressions for the heat transfer at the wall, the temperature and species profiles, and most importantly an ignition criterion which states that ignition is expected to occur when a suitably defined (reduced) Damkohler number exceeds unity. It is further demonstrated that this state corresponds to the case of zero heat transfer from the walls, which was intuitively used in the work by Chambre (19) as the ignition criterion of an inert, stagnant, hot surface.

Measurements of Flammability of Liquid Fuels

The evaluation of fire hazard or flammability of liquid fuels is most frequently obtained via measurements of flash point or fire point, spontaneous ignition temperatures and flammability limits.

Flash Point

The flash point temperature of liquid is obtained by means of a standard test apparatus which is classified as either closed cup or open cup method. Closed cup testers confine the liquid and ensuing vapor within a cover which is equipped with a shuttered aperture that can be opened periodically to allow insertion of an external, naked flame into the vapor space. The most popular types are the Pennsky-Martens (ASTM D93-73), Tag (ASTM D1310) and Abel (most used in the United Kingdom). Open cup flash point temperatures can be determined with Pennsky-Martens apparatus by removing the cover or by the Cleveland open cup apparatus (ASTM D92-72). In the open cup method, after the flash point is determined, the heating rate is continued at approximately 10°F/minute until application of the piloted flame causes the liquid to ignite and continue to burn for a period of at least five seconds. The temperature of the liquid at this point is called the fire point temperature. With many low boiling petroleum or other organic liquids, the fire points are almost the same or only a few degrees above the flash point. Higher boiling, less volatile oils and fluids exhibit a wider

difference between the flash and fire points. Among the flash point testers, the closed cup usually gives better repeatability, but variations of 5°to 20°F among the different types of testers are not uncommon.

The flash point of a fuel is strongly dependent upon the fuel vapor pressure which is a function of its temperature. Williams (82) for instance, demonstrated a linear correlation between flash point and the logarithm of fuel vapor pressure at 20°C for a range of petroleum products. With the Pennsky-Martens apparatus Butler et al (17) derived an equation relating flash point and volatility for a large number of hydrocarbon fuels.

$$T_f = 0.683\ T_b - 119.0 \qquad \text{(II-8)}$$

They also showed that flash occurred for pure components when

$$M\ P_v = 15.19 \qquad \text{(II-9)}$$

for mixtures;

$$\sum_i X_i M_i P_{vi} = 15.19 \qquad \text{(II-10)}$$

where

T_f = flash point in °F (closed cup)

T_b = boiling point in °F

M = molecular weight

P_v = vapor pressure in psi

X = mole fraction in liquid phase

i = species

Later Lenoir (50) modified this equation with equilibrium ratio instead of vapor pressure above; with this modification, it predicts flash points of fuels with higher volatility more accurately than the previous equation.

Burgoyne and William-Leir (16) developed an equation for estimating both flash point and fire point of a single flammable substance or a mixture of two single liquids of which one is flammable and one non-flammable. Values determined in this manner are generally slightly lower than those determined by the standard laboratory methods. The equation was derived from the partial pressure equation

$$P\ y = 100\ p \qquad \text{(II-11)}$$

where

P = atmospheric pressure (usually taken as one atmosphere)

y = volume percent flammable vapor in air

p = saturated vapor pressure at T °K

and an approximation equation correlating the liquid temperature and its vapor pressure

$$\log_{10} p = -A/T + B \qquad \text{(II-12)}$$

where A and B can be determined by inserting the known data of temperature and corresponding vapor pressure of that substance to obtain

$$T = A/(2 + B - \log_{10} Py) \qquad \text{(II-13)}$$

By using the above relation, four extreme conditions can be recognized;

1. Lower flammability limit and closed cup flash point.

2. The corresponding fire or flame point temperature when the vapor pressure is larger than the lower flammability limit.

3. Upper flame point (or fire point) with corresponding vapor fraction.

4. Upper limit of flammability and upper flash point temperature.

Flash point dependence on pressure is discussed by Mullins (57).

Spontaneous Ignition Temperature

Spontaneous ignition temperatures of liquid fuels have been studied by numerous investigators with reference to (a) determining the suitability of fuel oils for use in diesel engines, (b) estimating the tendency of automotive fuels to pre-ignite in the engine, (c) specifying temperatures above which various combustibles will constitute a fire or explosion hazard from the standpoint of spontaneous combustion. Principally four methods have been employed, which may be designated as the adiabatic compression method, dynamic tube method, crucible method and bomb method. In these methods three criteria have been choosen for indicating the ignition point-namely, inflammation of the mixtures, the sound of the explosion, and the rapid rise in pressure of the system. It seems reasonable to assume that these three phenomena may happen almost simultaneously.

The first determination of the spontaneous ignition temperatures (S.I.T.) of a fuel were undertaken in 1906 by Falk (26). A rapid adiabatic compression apparatus was used, with cylinder diameters ranging from 1 to 2 inches. Dixon et al (23) were the first group to recognize, some eight years later, that this apparatus did not provide evidence of the phenomena of ignition delay. The adiabatic compression device, designed by them, involves the rapid compression, and therefore heating, of a homogeneous combustible mixture. Considerable improvements have been achieved over the years on this type of apparatus. One such improvement uses the technique in which the piston is a gas and the flammable mixture is ignited by a shock wave. Steinberg and Kaskan (72) have discussed the use of shock tubes in measuring ignition delays and ignition temperatures; they have also presented some data for propane-air and hydrogen-oxygen mixtures.

The dynamic tube method (also known as flow method) is particularly suitable for measuring ignition temperatures of gaseous fuels. It simply regulates the mixtures of fuel-air or fuel-oxygen passing through the heated tubes, the temperature being raised until explosion occurs. Dykstra and Edgar (24) have given the details of the apparatus and procedures and also have examined the variables involved. Two other dynamic tube methods were developed which are known respectively as N.G.T.E. (National Gas Turbine Establishment, U. K.) method and N.A.C.A. (National Advisory Committee for

Aeronautics, U.S.A.) method. These two methods are capable of operating with a wide range of ignition delays.

The heated crucible method was adopted in an elementary form by Holm (33) in 1913; it is especially suitable for liquids. In the same year Constam and Schlapfer (20) experimented with liquid fuel droplets falling into a platinum crucible located in a gas-heated sand bath. In 1917, Moore (54) developed a form of ignition tester while engaged in a study of diesel fuels. This method of measuring ignition temperature has been widely used and is still in vogue although it has been continuously modified to acquire the accuracy or ease of operation. Consequently, many flammability studies and ignition temperature determinations are still based on this technique. Jentzsch (37) in 1924 used a stainless steel crucible situated in an electric furnace and divided into four symmetrically disposed equal pockets. One of these chambers acts as a thermometer pocket, while the other three are used as ignition spaces, each being fed with oxygen from a central channel. The spontaneous ignition temperature is taken as the lowest temperature at which self ignition occurs in the presence of a rich oxygen stream. In 1930 the American Society for Testing Materials (A.S.T.M.) adopted a standard method for measuring ignition temperature, which utilizes a glass conical flask of 160 ml capacity heated in a solder bath over a gas flame- a new version of the crucible method. Scott et al (65) in

1948 modified this procedure by using a quartz flask placed in a electrically heated inconel block.

The bomb method employs high pressures to measure spontaneous ignition temperatures. In the bomb test the temperature is regulated to the desired level; then air is admitted and allowed to reach the temperature of the bomb. Fuel is then injected and the time between admission and explosion is recorded. The temperature at explosion is taken as the spontaneous ignition temperature. Ignition delays of the order of few hundredths of a second are possible with the bomb tester. Experimental apparatus for spontaneous ignition tests, using the bomb method developed by the Bureau of Standards, is described in detail by Bridgeman and Marvin (12). There is a disadvantage in this bomb method; it cannot be used to record the pressure-time and inflammation characteristics of autoigniting mixtures which react too rapidly. In this instance, a more convenient method is to employ a rapid compression technique.

The ignition of flammable mixtures by heated surfaces-such as metal wires, rods, particles, spheres or plane surfaces has been the subject of much experimentation. The primary measurement is the limiting surface temperature above which ignition occurs. These values are generally higher than the corresponding ignition temperatures determined by the heated crucible method.

While considerable data are available on the spontaneous ignition temperatures of organic compounds, there is wide discrepancy between the results of various investigators, and even within the findings of a single investigator. This difficulty is due to the marked sensitivity of the determinations to a large numbers of variables and, accordingly, to even minor variations in equipment or procedure. The major factors recognized as having a significant effect upon the ignition temperature measured are (a) material of the igniting vessel or ignition mechanism, (b) volume of the ignition chamber, (c) concentration of oxygen in the inflammable mixtures, (d) time lag before ignition, (e) pressure and (f) composition of fuel. Hence, the value reported for spontaneous ignition temperature of any substance depends on the specific apparatus and method used. A detailed discussion based on the experimental evidence, as found in the literature, was presented by Bridgeman and Marvin (12) and Sullivan et al (73).

Flammability Limits

Ignition takes place only in the vapor phase for solids and liquids. As defined previously the flammability limits are the minimum and maximum concentrations of the vapor mixture mixed with air for which the presence of a specified source of ignition is enough to sustain a flame. The lower flammability limit of any pure substance or mixture will depend on the vapor pressure of the substance. Goto and

Nikki (31) estimated with fair accuracy the weak flammability limit in air of camphor, naphthalene and phthalic acid anhydride from vapor pressure data and measured flash points in saturated air. Mullins (57) has presented a comprehensive mathematical treatment of flammability limits of petroleum products based on true boiling point distillation data. Affens (2) derived some mathematical equations which describe the interrelationship of flammability limit and other related properties of n-alkanes.

$$1/L = 0.1347\ n + 0.04353 \qquad \text{(II-14)}$$

$$1/U = 0.01337\ n + 0.05151 \qquad \text{(II-15)}$$

$$T_f = 0.6946\ T_b - 73.7 \qquad \text{(II-16)}$$

where

n = number of carbons in molecular structure

L = lower flammability limit

U = upper flammability limit

T_f = flash point temperature in °C

T_b = boiling point temperature in °C

In a later paper, Affens and Mclaren (3) extended these relations to vapor and liquid fuel mixtures. By applying Raoult's and Dalton's laws governing vapor pressure and composition above a solution of two or more liquid hydrocarbons, to LeChatelier's rule governing the flammability limits of vapor mixtures, they derived equations which predict overall flammability properties of mixtures from the properties of mixtures from the properties and proportions of the individual components.

The flammability limits are sensitive to a number of variables as discussed below:

Pressure: The lower limit of flammability decreases with an increase in static pressure above one atmosphere, whereas the upper limit increases or decreases depending on the nature of the particular fuel.

Temperature: The flammability range widens with an increase in the initial temperature as a result of enhanced diffusivity of the ignition source in the flame propagation process. Since the temperature dependency is not large, ordinary variations of laboratory temperature have no appreciable effect on the flammability limits.

Vessel Diameter: Quenching distance is one kind of representation of flammability. Flammability ranges widen as the vessel diameter is made larger.

Turbulence: Mixing between the unburned and burned products will be faster if turbulence exists. However, in the mixing process two opposing effects can be present: (a) either recirculation of hot active radicals and heat energy widen the flammability limits, or (b) quenching at the wall (or other factors) narrow the flammability limits. Which effect predominates depends on the specified system and physical conditions.

Zabetakis and Richmond (86) have described flammability determination that fall into the following four categories:

1. Determination of flammability limits of a fuel as a function of pressure for a fixed temperature and diluting atmosphere.

2. Determination of flammability limits of a fuel as a function of the diluting atmosphere for a fixed temperature and pressure.

3. Determination of flammability limits of a fuel as a function of temperature for a fixed pressure and diluting atmosphere.

4. Determination of the saturated flammability limits of a liquid or solid fuel as a function of pressure for a fixed diluting atmosphere; when the vapor pressure of the fuel as a function of temperature is known, the saturated limits may be expressed in terms of fuel concentration.

Factors Involved in Ignition

Previous studies of various factors influencing the ignitability of a pool of liquid fuel have shown that the ignition behavior is strongly dependent on whether the initial temperature of the fuel is above or below its flash point. A fuel above its flash point is readily ignitable. When the fuel is below its flash point temperature, further heating is necessary; the requirement of heat is in turn dictated by the fluid motion induced by the heating. The fluid motion could be the result of a combination of factors such as surface tension, buoyant forces (or gravity) and heat conduction from the walls of the container. In this section only liquids initially below their flash points will be considered with respect to parameters such as the effect of radiation source and its absorption, effect of container

material, pilot and its position, subsurface hydrodynamics, heat loss from surface, and effective thermal conductivity.

Effect of Radiant Source and Its Absorption

An electric arc, solar furnace, hydrocarbon diffusion flame, laser beam, tungsten lamp or radiation panel is generally used as the heating source in ignition or flame spreading studies. Each of these sources has particular advantages depending on test apparatus, the purpose of the test and the range of variables to be investigated. In any test procedure, however, one cannot ignore the fact that the ignition behavior of flammable materials is most strongly dependent upon the spectral distribution of the incident irradiance and the monochromatic absorptance of the material being irradiated. As Sliepcevich et al (78) demonstrated, white cotton fabric, for example, can be ignited in less than one-third the time with flame radiation as compared to tungsten lamp radiation at identical levels of incident irradiation flux.

The absorption of radiation energy by a hydrocarbon liquid is related to the increment in the energy of vibration or rotation associated with a covalent bond, provided that such an increase results in a change in the dipole moment of the molecules. For normal paraffins, the absorption bands associated with various modes are given in Table 2-1 (25). the band absorption, theoretically, can be calculated by a formula from Siegel and Howell (67):

TABLE 2-1

INFRARED POSITIONS OF VARIOUS BOND VIBRATION
OF NORMAL HYDROCARBONS AND WATER

Bond	Mode	Relative Strength	Wave Length (μ)	Wave Number (1/cm)
C-C	Stretch	m-w	8.3-12.5	800-1200
C-H	Stretch	s	3.0- 3.7	2700-3300
C-H	Stretch (2v)	m	1.6- 1.8	5600-6300
C-H	Stretch (3v)	w	1.1- 1.2	8300-9000
C-H	Stretch (C)	m	2.0- 2.4	4200-5000
C-H	Bend, in-plane	m-s	6.8- 7.7	1300-1500
C-H	Bend, out-of-plane	w	12.0-12.5	800- 830
C-H	Rocking	w	11.1-16.7	600- 900
O-H	Bending	m-w	6.9- 8.3	1200-1500
O-H	Stretch (2v)	s	1.4- 1.5	6700-7100

Approximate only; fundamentals unless noted
s = strong; m = medium; w = weak
(2v) means second harmonic or first overtone, etc.
(C) means combination frequency

(i) $\nu \geq 2$

$$F_{0-\lambda T} = \frac{15}{\pi^4} \sum_{m=1,2,..} \frac{e^{-m\nu}}{m^4} \{[(m\nu + 3)m\nu + 6]m\nu + 6\} \quad \text{(II-17)}$$

(ii) $\nu < 2$

$$F_{0-\lambda T} = 1 - \frac{15}{\pi^4} \nu^3 \left(\frac{1}{3} - \frac{\nu}{8} + \frac{\nu^2}{60} - \frac{\nu^4}{5040} + \frac{\nu^6}{272,160} - \frac{\nu^8}{13,305,600} \cdots\right) \quad \text{(II-18)}$$

where

$\nu = C_2/\lambda T$: is a parameter

T = absolute temperature

C_2 = Planck's constant

λ = wavelength

$F_{0-\lambda T}$ = fraction of black body emission power in spectral region $0-\lambda T$

The fraction absorbed (α') is

$$\alpha' = \sum_{\substack{\text{absorbing} \\ \text{bands}}} \left[F_{0-(\lambda T_s)_{\text{upper}}} - F_{0-(\lambda T_s)_{\text{lower}}}\right] \text{band} \quad \text{(II-19)}$$

As mentioned previously, ignition occurs in the gas phase near the surface of the combustible solid or liquid when the conditions of a flammable gas composition and temperature are satisfied. Heat transfer to the gas phase is by (1) convection-conduction from the heated surface, and (2) absorption of the incident radiation. In general, the first process has been considered as the principal mechanism. Very little information is available, however, on the fraction of radiation absorbed by gas phase between the radiation

source and the surface of the combustible solid or liquid. Recently, Kashiwagi (40) has applied a carbon dioxide laser beam to heat and ignite the condensed fuels of polymethylmethacrylate (PMMA) and red wood. The emission from his laser is monochromatic, having a wavelength of 10.6 μm, which is much longer than the emission from tungsten filament lamps or flames. He observed a strong attenuation of the incident laser radiation by the plume of thermal decomposition products in the gas phase above the surface of the combustible and a subsequent ignition on the surface of the red wood or in the plumes above the heated PMMA and red wood.

Effect of Material of Construction of Container

Ignition temperature is not a true physical property of a substance since its value is dependent on the testing conditions as well as the chemical or physical properties of the substance itself. For example, it is well known that the construction material of the container--particularly its thermal conductivity--and its surface characteristics--roughness and catalytic capability--affects the values measured for ignition temperature and flame spreading.

Thompson (74) has shown, in his study of auto-ignition temperatures of the flammable liquids, that there is a decided advantage in using glass rather than metal as the ignition surface, not only from the standpoint of the ignition values obtained but also on account of the greater facility with which results are secured. For example, the ability to

duplicate results in most pronounced when using glasses. Chromium is also quite satisfactory, steel is somewhat less desirable, and copper--in some cases--was definitely unacceptable.

Sortman et al (71), in spontaneous ignition studies of liquid fuels, used a stainless steel crucible, rather than to follow the A.S.T.M. specification (designation D-286-30) of a glass crucible (flask). They concluded that the steel surface gave good reproducibility, without requiring any unusual care in cleaning. Normally, stainless steel containers give higher ignition temperature than glass containers, but the difference is not relatively important.

Frank and Blackham (27), in their studies on ignition of hydrocarbons, used two metal blocks (one stainless steel and one copper) and concluded that a change in the metal surface had no substantial effect on the spontaneous ignition temperature measurements of most compounds which undergo spontaneous ignition below 290°C. However, for compounds with high spontaneous ignition temperature values, the catalytic effect of the metal surface becomes pronounced. The difference in ignition temperature obtained by using a heavily oxidized, compared to a bright metal, surface can amount to well over 50°C. In that case the copper block was not suitable for use at the high temperatures because of the rapid formation of a heavy copper-oxide layer under these conditions.

Mackinven et al (53) observed that the flame spreading rate is, in all cases, faster in glass lined trays than in unlined aluminum trays. A glass liner can be considered as a good insulator for heat transfer in that solution.

Pilot and Its Position

Piloted ignition tests require an external energy source to trigger ignitions. An electric spark, naked flame, hot gases, shock wave, hot surface and many other forms can be used as pilots. Two excellent discussions on the subject are Lewis and von Elbe (52) and NACA report 1300 (10). In the conventional fire or flash point testers, Pennsky-Martens and Cleveland open cup, a jet with diameter of 5/16 inch and a flame size of a bead is inserted about 1 1/4 inches above the liquid surface.

In the liquid propagation study by Glassman et al (28, 29, 53), three methods were employed to light a small section of the fuel at one end of the tray: a (Bernz-O-Matic) propane torch, hexane/spark and asbestos wick.

Wesson (79) has given a detailed discussion and tabulation of the effects of size and positions of pilot flames in his study of iginition of solid materials.

Subsurface Hydrodynamics

This topic is of interest mainly in the study of flame spreading over a liquid surface. Two factors, surface tension forces induced by the temperature difference in the liquid surfaces ahead and behind the flame front and the buoyant

force have been found to effect the flame spread by many investigations.

Burgoyne et al (14) presented flow patterns, two convective cells, within the liquid near the wick during the induction period of flame propagation. Torrance (75, 76) studied this problem from the point of veiw of mathematics only. The velocity distributions or stream functions have been plotted as functions of bed thickness, Reynolds number, Grashof number and Prandtl number.

Glassman and Hansel (28) showed that increasing the viscosity (by adding Vistanex, a polyisobutylene of molecular weight≈2,000,000) to the fuel, lowered the rate of flame propagation and burning, but increased its ignitability.

Murad et al (58) presented streak photographs of the steady state motion induced in n-decane by a heated wire in his analysis of the effect of igniter power on ignition delay. The delay seemed to be sensitive to small amounts of additives which alter the physical properties of the liquid. Generally, when the fuel is thickened, there is less convective motion, more heat is retained at the source and ignition occurs with a simple pilot flame. Again one can actually observe the slower surface currents in the thickened liquids. The thickened fuels then act very much like thick wick. Also the addition of 1.5 percent of a surfactant (test sample by 3M Company, # FC-176) decreases the surface tension on temperature in the range of interest; the net effect of the

surfactant is a significant decrease in the ignition delay at a given igniter power. The effect is more dramatic when 1.5 percent of the viscosity enhancer, Vistanex is added to n-decane. The fuel viscosity is increased by a factor of approximately 50, and its ignition delay is sharply decreased, particularly for low ignitor power. The combination of viscosity enhancer and surfactant decreases the ignition delay still further.

Yumoto, Takahashi and Handa (83) present a burning rate study of hexane in small pyrex glass vessels. The particle streak photographs which were taken in the earlier stage of combustion, showing subsurface convection in the liquid are included in this paper. Radiation from the flame and the wall heating effect are two major reasons for the convection loops.

Surface Heat Transfers

Heat transfer to and from the combustible sample can affect the results of flammability measurements significantly. Hottel (34) explained the experimental data of Blinov and Khudiahov on the variation in burning rate with pool diameter by means of the equation

$$\frac{q}{\P d^2/4} = \frac{4k(T_f - T_b)}{d} + h(T_f - T_b) + \sigma F[1 - \exp(-\kappa d)] (T_f^4 - T_b^4) \qquad \text{(II-20)}$$

which simply states that the heat flux to the liquid per unit surface area is equal to the heat gained from the pan rim, the convection from the flame and the radiation from the

flame, respectively: where k is the thermal conductivity; h is the convective heat transfer coefficient; F is the view factor; d is the pan diameter and κ is the extinction coefficient; all other physical parameters are assumed constant. For small diameters, the first term on the right side is the only one of importance. At large diameters the first term is negligible, the second term is constant, and the third term will dominate being practically constant because "d" is so large. Thus, the observed effect of diameter on burning rate is simply a heat transfer effect. Corlett and Fu (21) conducted similar studies on liquid pool fires.

Alvares et al (8) in their studies on the vertical ignition of cellulose by thermal radiation showed that for a vertical wall whose surface temperature is kept constant, the heat transfer by free convection is given by

$$Nu_x = hx/k_g = 0.378\ Gr_x^{0.25} \text{ for a vertical wall} \qquad \text{(II-21)}$$

where

Nu_x = the Nusselt number at x

h = the convective heat transfer coefficient

x = the characteristic length

k_g = the conductivity coefficient of gas or vapor

Gr = the Grashof number ($Gr = gx^3\Delta T/\nu^2$)

g = gravity acceleration

β = expansion coefficient

ΔT = temperature difference

ν = kinematic viscosity

Burgoyne et al (15) found that fuel bed thickness and diameter of vessel can effect the hydrodynamics in the liquid, and consequently the heat transfer processes. For example, for a liquid depth less than 0.12 cm they concluded that circulation of liquid due to natural convection has virtually ceased. Thus, the liquid behaves as a thin film, heated at one surface and in contact with a heat sink at the other surface. They relate to the heat transfer conditions, across a fluid layer between two surfaces within the fluid, to the product of the dimensionless Grashof and Prandtl numbers by,

1. $PrGr < 10^3$; $Nu = 1$ heat transfer is by conduction alone
2. $10^3 \leq PrGr < 10^6$; $Nu = 0.15(PrGr)^{0.25}$ so that $h \propto L^{-0.25}$
3. $10^6 \leq PrGr$; $Nu = (PrGr)^{0.33}$ so that $h \neq f(L)$ and heat transfer by convection only

where

L = the depth of the liquid fuel bed, in centimeters

$GrPr = 10^6 * L^3$

Effective Thermal Conductivity

The absorption of radiant energy as it passes through a liquid is given by Lambert-Beer's law;

$$\ln (I/I_o) = - kbc \quad \text{or} \quad \log_{10}(I_o/I) = A = abc \qquad \text{(II-22)}$$

where

I_o = the initial intensity of source

I = the intensity at length b

k = proportional constant

c = concentration

A = absorbance

a = constant of proportionality

b = path length

The restriction to isothermal homogeneous medium made the above law limited in its application to a small range. The penetrating incident radiant energy flux at the surface can be deduced from Hottel's pool energy equation (9);

$$I_o = \sigma F(T_f^4 - T_b^4)(1 - r)[1 - \exp(-\kappa d)] \qquad \text{(II-23)}$$

where

r = surface reflectivity of the fuel ($r = \left(\frac{n - 1}{n + 1}\right)^2$)

n = index of reflectivity

σ = Stefan-Boltzmann constant

F = view factor

κ = extinction coefficient

T_f = flame temperature

T_b = bulk temperature of liquid

For large size and relatively low bulk temperature, above equation can be simplified as $I_o = \sigma F T_f^4$; because of the penetration of radiant energy into the liquid, along with other possible influencing factors such as surface tension, buoyancy force (gravity) and wall heating effect, the mechanism of heat transfer in the liquid is very complicated. There are many convective cells observed under liquid surface. It will be a mistake if only thermal conduction mechanism is considered in treatment of heat transfer in liquid phase.

Considering the fuel bed as transparent, the radiative rays will penetrate into the medium in the preheating period. The energy absorption takes place not only on the surface of liquid, but also along the light path in the medium and also absorbed on the surface of the vessel, especially if the vessel is made up of metals. The latter absorption is the main reason to induce the heat conduction through pan rim in Hottel's pool energy equation. Rosseland approximation has been applied by many investigators (77, 59) to simplify the expression for radiation flux in the energy equation. For a system close to thermodynamic equilibrium, optically thick medium and intense absorption, the radiant-energy flux vector can be approximately expressed as follows:

$$E(r,t) = -\frac{1}{3\kappa}\nabla(4n^2\sigma T^4) = -\frac{16}{3\kappa}n^2\sigma T^3\nabla T \qquad \text{(II-24)}$$

where

∇ = vector operator used for the gradient of a scalar

E = radiant energy flux vector

r = position vector

t = time

T = temperature

n = index of refraction

κ = absorption (or extinction) coefficient

σ = Stefan-Boltzmann constant

This relation has been applied by Viskanta and Grosh (77), Noble (59) and others. The effective thermal conductivity (k_{eff}) of fluid can then be expressed as follows:

$$k_{eff} = k + k_r \simeq k + 16n^2\sigma T^3_{avg}/3K \qquad \text{(II-25)}$$

where

k = pure thermal conductivity coefficient

k_r = the radiative conductivity coefficient

Burgoyne et al (15) have calculated the effective thermal conductivities in the directions along the surface, assigned as x direction, and the depth, assigned as the z direction, together with values of F_x and F_z, the ratio of the appropriate effective thermal conductivities to the actual thermal conductivities of the liquids. The magnitudes of F_x and F_z are approximately two thousand and twenty, respectively. Murad et al (58) noted that there exists (in the steady state) a balance between the shear stress due to the surface tension gradient at the free surface and viscous shear within the liquid. This yields an order of magnitude expression for the characteristic liquid velocity at the surface. The ratio of the heat convected to the heat conducted parallel to the surface is, in general a Peclet number, but in the case of a velocity driven by a surface tension gradient it becomes a Marangoni number (Ma)

$$Ma = \left(\frac{\sigma_T/\rho}{\nu\alpha}\right) L\Delta T \qquad \text{(II-26)}$$

where

σ_T = change of surface tension per degree of temperature

ρ = density

ν = kinematic viscosity

α = thermal diffusivity

ΔT = temperature difference over the span

L = characteristic length

In the case of flow driven by the temperature-induced buoyancy, the relevant dimensionless group is the Rayleigh number (Ra)

$$Ra = \left(\frac{\beta g}{\nu \alpha}\right) L^3 \Delta T \qquad \text{(II-27)}$$

where

β = thermal expansion coefficient

g = acceleration due to gravity

Marangoni number measures the effectiveness of the induced motion in cooling off the liquid region adjacent to the ignition heat source and thereby delaying the occurrence of ignition. Rayleigh number depends on the physical properties of the fuel, on the imposed temperature difference and on the size of the flow field effected. As viscosity is thickened, Rayleigh number becomes smaller, and indicates shorter ignition delay. The heating effect from the walls of container to the fluid adjacent to it has been noticed by many investigators (4, 83). One of the most thoughtful work was done by Akita and Yumoto (4). They have concluded that the burning rate of liquid methanol is much greater at the vessel rims (next to flame base) than near the vessel center, and that the total burning rate in the compartments of a concentric vessel is equal to that in a single vessel of the same size. Wall heating effect, besides the convective effect above the rims, is seriously counted on in this instance.

Surface Temperature Computation

Many studies have been devoted to techniques for calculating the surface temperature at ignition since it cannot be measured reliably. Some of the most profound analyses have been related to models for the ignition of solid propellants under constant radiant flux. In these papers (30, 39, 41, 42, 43, 48, 49) the detailed mechanisms such as gasification, oxidation, ignition in the gas phase, regression rate of the solid surface, in-depth radiation absorption, and heat conduction in the solid phase are considered. Because of the complexity of the phenomena, a number of assumptions are generally made to arrive at a tractable model.

1. One dimensional analysis is adequate.

2. The ratio of activation energy to surface temperature is large compared with unity. (The need for this assumption was proposed some 20 years earlier by Chambre, as mentioned previously in this chapter.)

3. The density is constant.

4. A stream function "Ψ" is employed in the gas phase to account for variable gas density ρ_g.

5. The solid-gas interface remain fixed at $x = 0$. The solid occupies the region $x > 0$, and the gas $x < 0$. Then, the energy equation for a solid fuel under radiative flux can be written as follows:

Solid Phase

$$\rho c \frac{\partial T}{\partial t} + \rho v c \frac{\partial T}{\partial x} = \frac{\partial}{\partial x}(k \frac{\partial T}{\partial x}) + \dot{q}\mu \exp(-\mu x) \qquad \text{(II-28)}$$

Gas Phase

$$c_g \frac{\partial T_g}{\partial t} + \rho v c_g \frac{\partial T_g}{\partial \Psi} = \frac{\partial}{\partial \Psi}(\rho_g k_g \frac{\partial T_g}{\partial \Psi}) - \frac{W_f Q}{\rho_g} \qquad \text{(II-29)}$$

Initial conditions

$$T(0,x) = T(0,\Psi) = T_o$$

Boundary conditions

$$T(t,\infty) = T_g(t,-\infty) = T_o$$

$$T(t,0) = T_g(t,0)$$

$$-k(\partial T/\partial x)_s + \rho_g k_g (\partial T_g/\partial \Psi)_s - \rho v L = 0 \quad \text{at } x = 0$$

$$(\partial T/\partial x)_{x=0} = 0$$

where

$v = -B \exp(-E/RT_s)$ regression rate

$\Psi = \int_0^x \rho_g \, dx$ mass coordinate

k, k_g = thermal conductivity of liquid, gas

$\dot{q}$ = flux of external heat at the surface

ρ, ρ_g = density of liquid, gas

Q = heat of combustion per gram of fuel consumed

B = overall frequency factor for vaporization

v = liquid surface regression rate

L = latent heat of gasification

E = activation energy

R = universal gas constant

c = heat capacity of liquid

c_g = heat capacity of gas

μ = absorption coefficient

W_f = rate of production of fuel

T_s = surface temperature

The results of the numerical analysis and asymptotic analysis have been presented in the forms of diagrams in the above identified references. Since some of the criteria used are hard to define and difficult to measure, there are no experimental results available that can be used to check the model, but in a logical sense the results seem plausible.

For an inert sample undergoing no decomposition, the previous equation can be simplified as follows:

$$\rho c \frac{\partial T}{\partial t} = k \frac{\partial^2 T}{\partial x^2} \qquad \text{(II-30)}$$

If the front surface boundary condition is taken as $-k(\partial T/\partial x) = H_i$ and the rear surface boundary condition is $\partial T/\partial x = 0$ at $x = L$, the analytical solution can be found from Carslaw and Jaeger (18) in non-dimensional form

$$\frac{\Delta T_s \rho c L}{H_i t} = 1 + \frac{1}{F}\left(\frac{1}{3} - \frac{2}{\pi^2} \sum_{n=1}^{\infty} \frac{1}{n^2} e^{-n^2 \pi^2 F}\right) \qquad \text{(II-31)}$$

where

ΔT_s = surface temperature rise at ignition

F = Fourier number $\alpha t/L^2$

α = thermal diffusivity $k/\rho c$

H_i = heat incident on the surface

t = time

ρ = density

c = heat capacity

L = thickness of the fuel bed

k = thermal conductivity

Simms (51) included convective cooling losses at the front surface in the boundary equation. Thus at the exposed surface of the sample

$$-k(\partial T/\partial x) = H_i - h(T - T_\infty)$$

The analytical solution of the previous equation corresponding to this boundary condition was given by Simms as:

$$\frac{H_i \sqrt{t}}{\Delta T_s \sqrt{k\rho c}} = \frac{\beta}{1 - \text{erfc}\beta \exp\beta^2} \qquad \text{(II-32)}$$

where

$$\beta = (h^2 t/k\rho c)^{0.5}$$

$$\text{erfc } x = 1 - \text{erf } x = (2/\P^{0.5}) \int_x^\infty \exp(-\xi^2)\, d\xi$$

β is called the cooling modulus and ΔT_s is the surface temperature rise. If β^2 is small, the surface heat loss may also be neglected. The energy modulus therefore would be constant if the thermal properties and heat transfer coefficient are constant. Simms then plotted the energy modulus versus the cooling modulus, $h\sqrt{t}/\sqrt{k\rho c}$, and applied a constant ignition temperature such that the theoretical curve gave the best fit through the experimental data (within 30 percent). Simms concluded that a fixed surface temperature is a reasonable criterion for the attainment of ignition. It has been deduced by several investigators that the convective motion is so significant in the determination of the heat transfer mechanism

in the liquid, when radiation energy is applied on its surface, that an effective heat transfer coefficient should be used, in the above two analytical solutions of the temperature distribution. Thus, instead of k, k_{eff} should be inserted. With this consideration the theoretically computed ignition surface temperature should approach the measured values even more closely. However, no matter how much it could be improved, such agreement is probably fortuitous because of the presence of the large number of physical parameters, which are treated as arbitrary constant terms.

Magnus (11), in the combustion rate studies of gasoline and ethanol, used an array of thermocouples in series to measure the temperature profiles in the flame and beneath the surface of the burning liquid.

CHAPTER III

EXPERIMENTAL APPARATUS AND PROCEDURE

In this work, flammability studies of liquid fuels were performed in a horizontal ignition test cabinet specially fabricated for this purpose. The details of the sample dish, the pilot flame, venting system and experimental procedure are described in this chapter. An overall view of the cabinet and a closeup of the sample dishes are photographically shown in Figure 3-1.

Apparatus

The overall dimension of the cabinet is a three-foot cubic structure. It is elevated three feet from the ground by a steel frame. An observation window installed on the front of cabinet is made of Herculite, tempered safety glass. The rest of the cabinet walls are lined with asbestos cement or transite board. Tungsten lamps are connected to an elevating screw which is operated manually to adjust the lamp height. A blower is used to remove the hot exhaust vapors from the cabinet after each run. A honeycomb screen in the base of the cabinet is used to provide uniform flow of air upward through the cabinet.

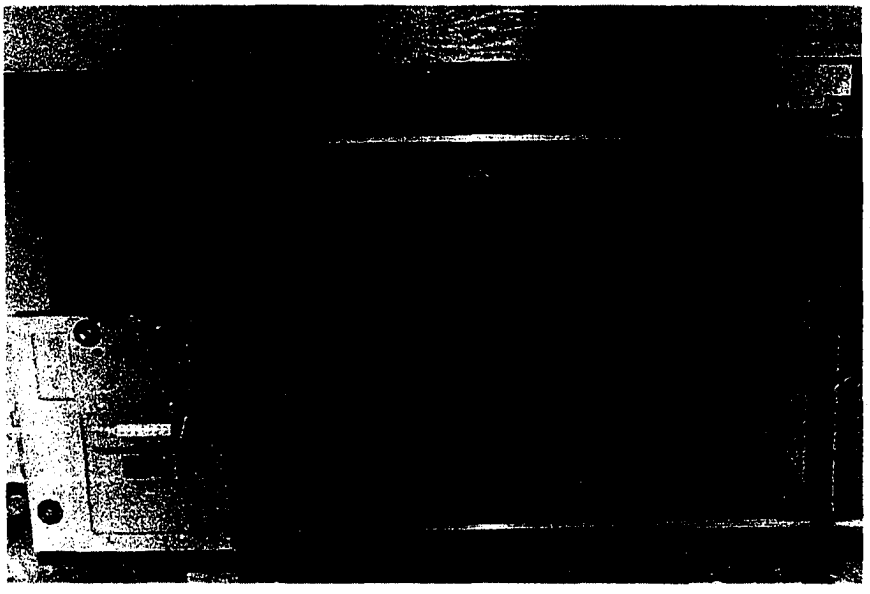

(a) Flammability Cabinet

(b) Closeup of Liquid Sample Dish for Radiometer Measurements

Figure 3-1. Basic Flammability Apparatus

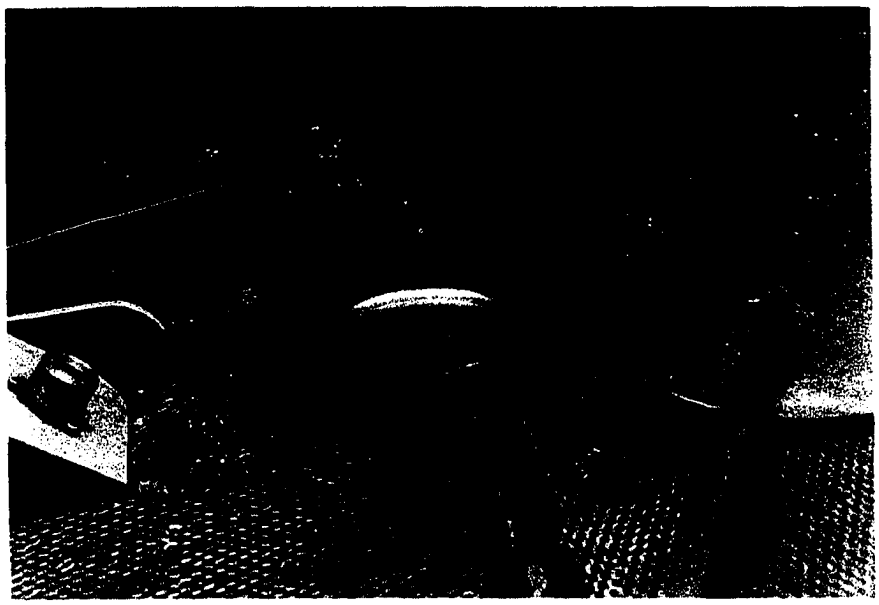

(c) Closeup of Liquid Sample Dish for Thermocouple Measurements

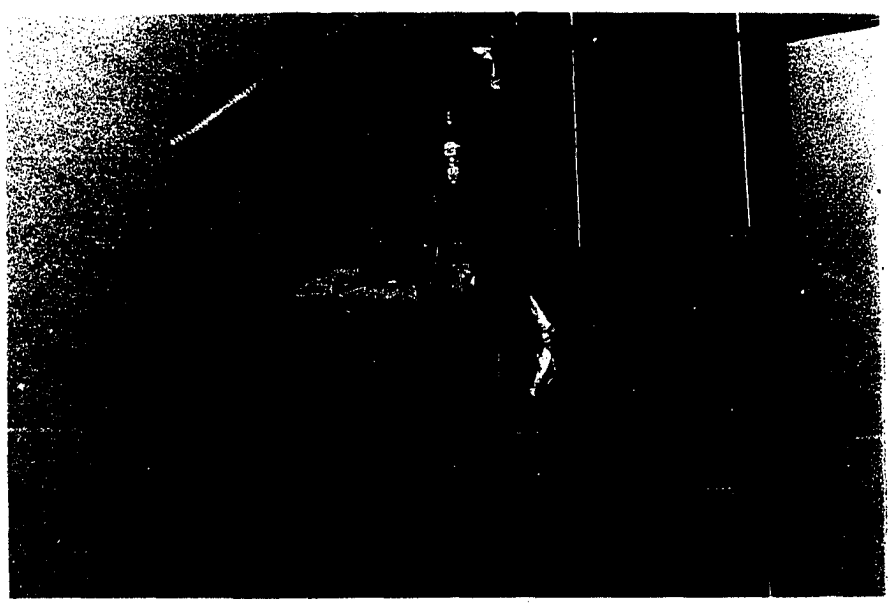

(d) Closeup of Tungsten Lamps

Figure 3-1. Basic Flammability Apparatus

Tungsten Lamp System

The tungsten lamps used as the thermal radiation source consisted of a bank of six, 2000-watt tube lamps mounted opposite a reflector. The incident irradiance at the surface of the liquid sample was controlled by varying the height of the lamp assembly above the liquid surface. Power to the lamps was supplied by a 240 volt AC supply. The lamp reflector was cooled by a bank of S-bend shaped copper tubes of 1/8 inch diameter, using tap water as the coolant. The lamp ends and power leads were cooled by a low velocity nitrogen flow, which was controlled by a needle valve. Plastic fittings were used for the nitrogen line above the lamp to prevent short circuiting.

Radiometer and Thermocouples

A leak-proof, water-cooled radiometer was used to determine the incident irradiance at the liquid surface and below the liquid surface. The radiometer was placed at the center of the sample holder dish. The irradiance level of each test was determined by recording the millivolt output and converting it to irradiance flux with the factory-calibrated, characteristic chart of the radiometer. The typical recorder output in millivolt versus time scale is shown in Figure 3-2. Although the lamp remained at a fixed height during a run, its irradiance reading from the recorder was not constant because the tungsten filament temperature increased slightly with time. The average irradiant flux for an

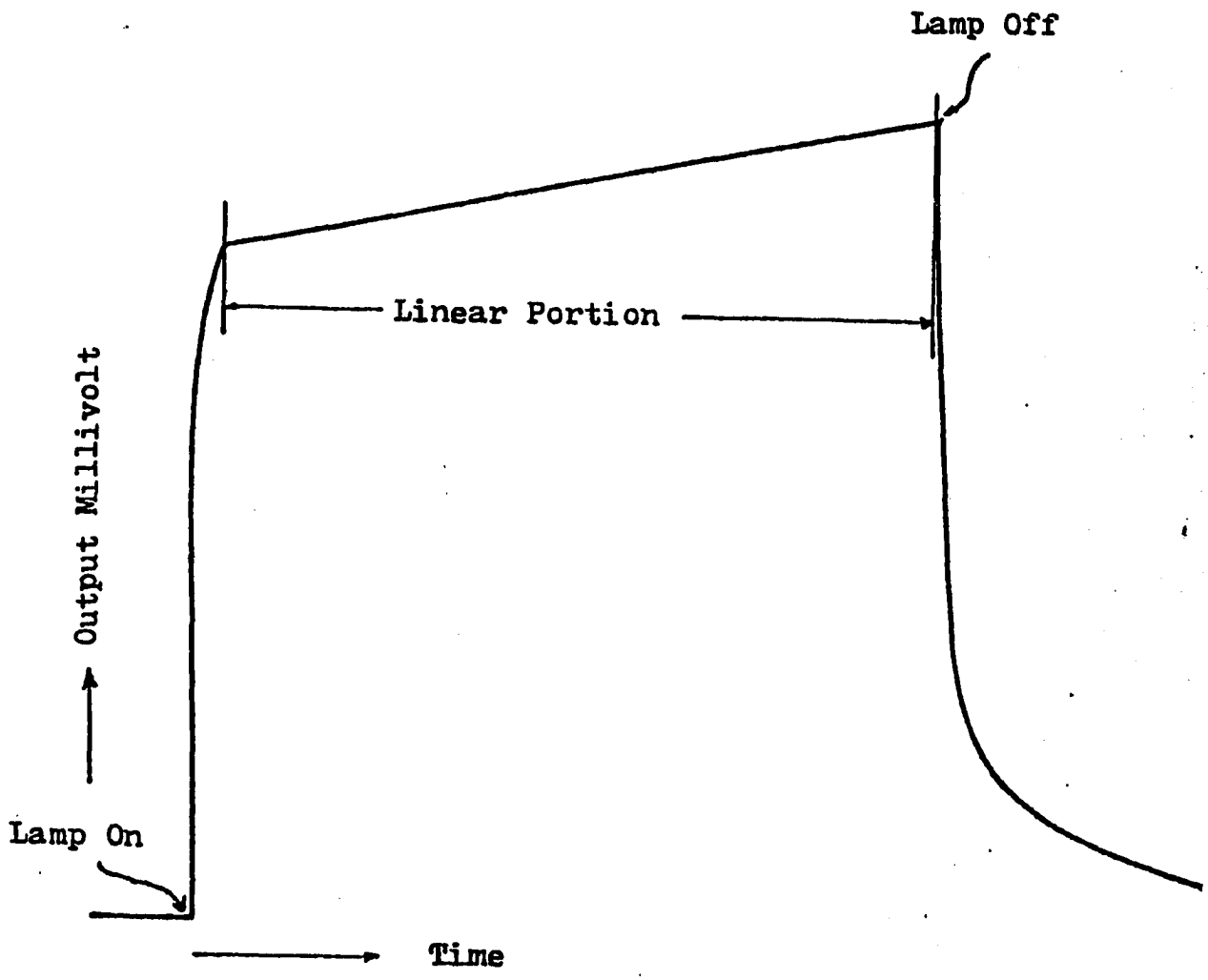

Figure 3-2. Typical Recorder Output for Radiometer

individual test was determined by averaging the area under the millivolt versus time curve traced by the recorder.

Two liquid sample dishes identical in shape and size but differing in the design of the base, as shown in Figure 3-3 and 3-4, were adopted for measuring the intensity of irradiation and the temperature of the liquid surface; preliminary experimentation revealed that both the radiometer and thermocouples could not be accommodated simultaneously in one sample dish without sacrificing accuracy in the readings. Although three thermocouples located at different positions were used, the reading from the center one was used as the ignition surface temperature.

Sample Dishes and Pilot Light Assembly

The sample dish assembly for the thermocouples was made from stainless steel with dimensions of 4 7/8 inches in diameter and 1 1/4 inches in height. Three thermocouple leads were soldered on the outside of the base of the dish. They are lined up together in a straight line, one is in the center of the pan, the other two are 7/32 inch and 17/32 inch from the center point as shown in Figure 3-3. Three half-cut 1/16 inch unions, two stainless steel and one brass, were welded on the base from underneath; they were used as the leads of the thermocouple probes. Plastic ferrules were used in the assembly to set the position of the thermocouple probes at any desired height.

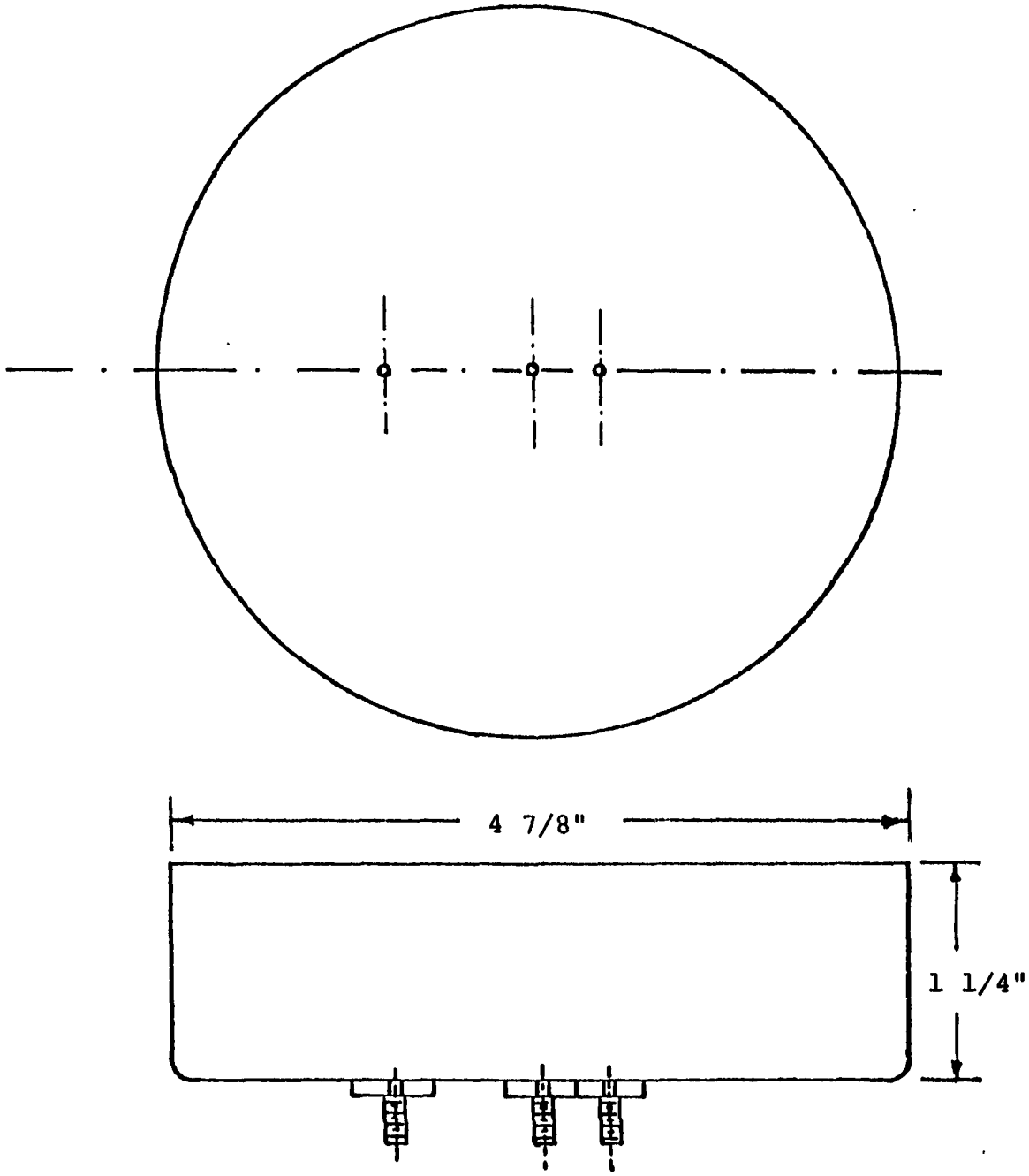

Figure 3-3. Liquid Sample Dish for Thermocouple Measurements

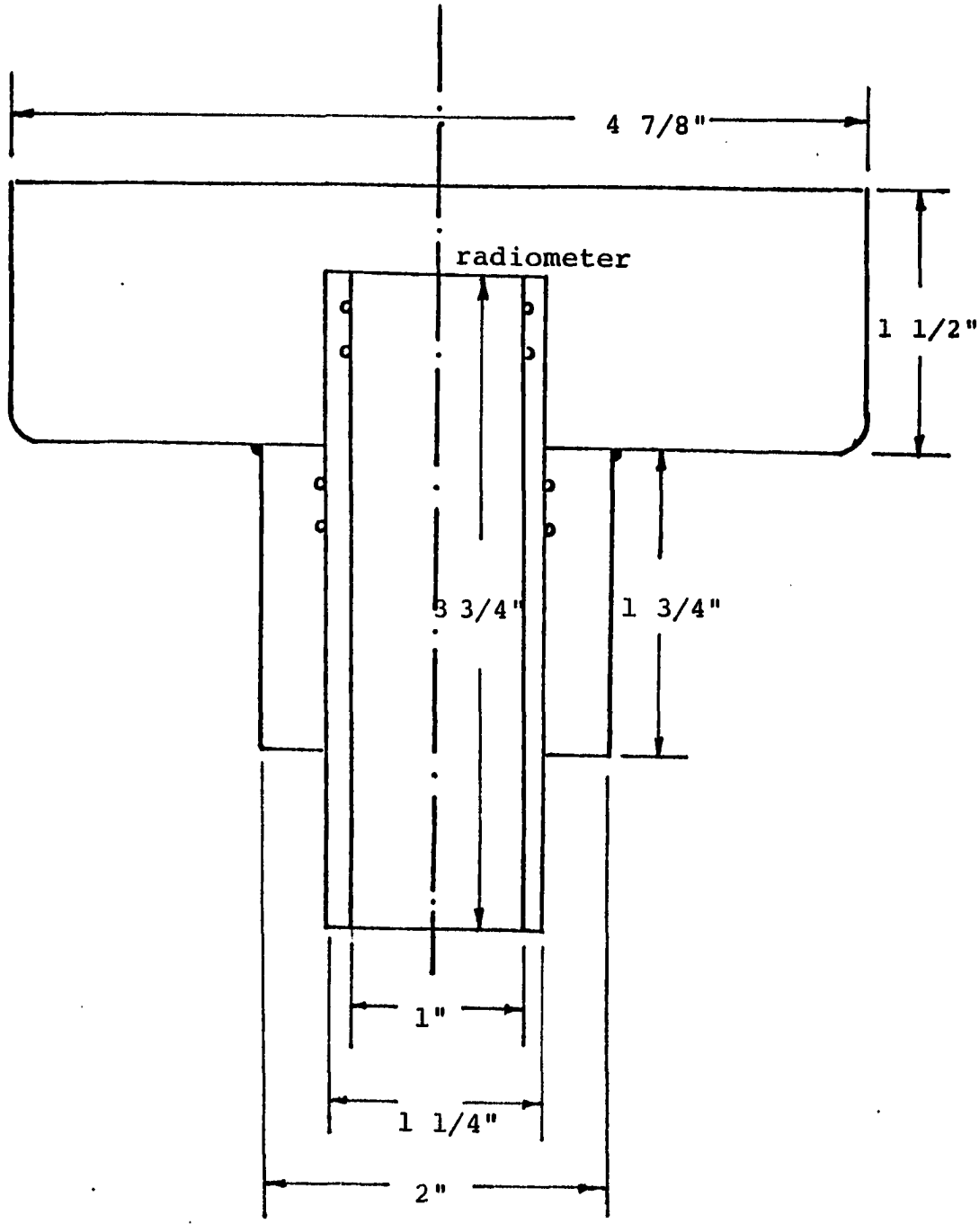

Figure 3-4. Liquid Sample Dish for Radiometer Measurement

The sample dish assembly for the radiometer, Figure 3-4, was also made from stainless steel with dimensions of 4 7/8 inches in diameter and 1 1/2 inches in height. A 1 1/4 inches diameter hole was cut in the bottom of the dish. A stainless steel pipe nipple, 1 3/4 inches long, 2 inches in outside diameter and walls 3/8 inch thick, was welded to the bottom of the dish. The radiometer was inserted into a sleeve made from a stainless steel tube, 3 3/4 inches in length, 1 1/4 inches in diameter and walls 1/8 inch thick. The radiometer-sleeve assembly was inserted in the two-inches diameter tube welded to the dish. O-rings were provided to prevent leakage. This arrangement enabled the radiometer to be moved up and down to the desired position.

The jet for the pilot flame burner was fabricated from 1/16 inch stainless steel tubing. The burner section of the pilot flame was connected to a propane gas supply by flexible plastic tubing. One diaphragm control valve and three needle valves were used to monitor the propane gas supply and flame size. The burner of the pilot flame was mounted on a horizontally movable hinge so that the pilot could be swept over approximately one-third of the surface area of the sample dish.

Liquid Removal System

After each test, excess hot liquid fuel was removed from the sample holder dish by means of a liquid suction system schematically shown in Figure 3-5. The 1000 ml conical flask was partially immersed in a water bath. The hot excess

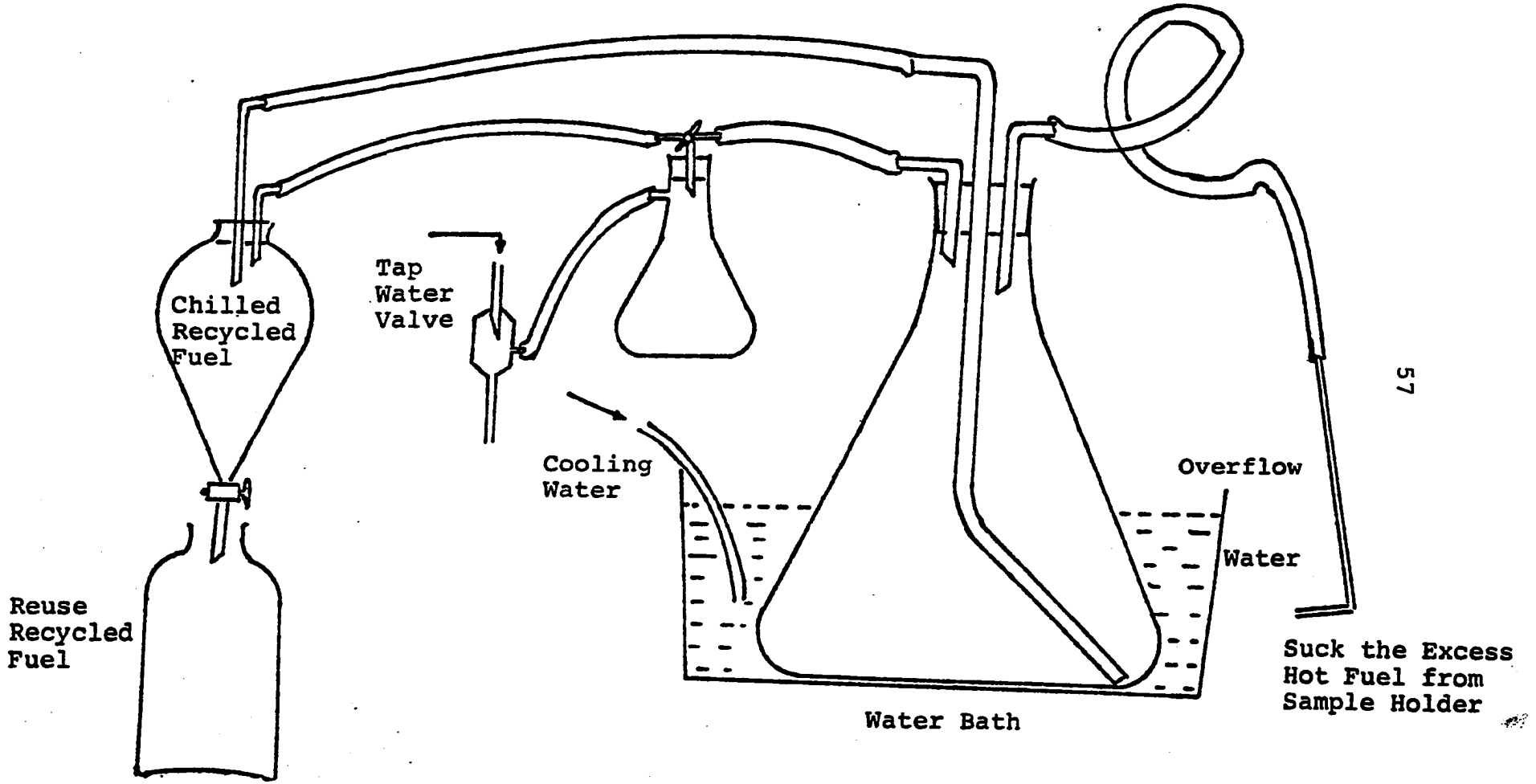

Figure 3-5. Liquid Removal System

liquid fuel from the sample dish was transferred into the flask by applying suction from a laboratory water jet aspirator. The cooled liquid fuel was transferred to a separation funnel using the same suction system as shown in Figure 3-5. The recovered excess fuel might be recycled for subsequent tests if the fuel was pure n-tetradecane or n-tridecane.

Analysis of the Fuel

The hydrocarbon fuel used in the tests was analyzed for composition by a gas-liquid Chromatograph.

Procedure

Before starting the experiment the following items were checked or activated:

1. Connect main electrical supply.
2. Activate the nitrogen and cooling water through radiometer and cooling coils.
3. Check ice level in the thermo-cup since ice point of water was used as the reference junction for thermocouples.
4. Light the pilot flame (this step not needed for unpiloted ignition tests).
5. Clean the window of the radiometer if it is necessary.
6. Set recorder for appropriate chart scale and pen speed.
7. Check the output of the temperature reading of thermocouple and set the base line (for each test it was

arbitrarily set at 40°C).

8. Pour predetermined quantity of the testing fuel into the sample dish. Close the front window and switch off the air blower.

The procedure for each run was:

1. Turn on the recorder.

2. Turn on the radiation lamp and start the stop watch simultaneously.

3. Swing the pilot light handle manually. (This step is not necessary for unpiloted ignition test.)

4. Observe the progress of the test.

5. Once ignition is observed, stop timing and turn off the lamp and recorder.

6. Move the extinguishing cover on the sample dish to suffocate the fire.

7. Turn on the exhaust blower to remove the gas products of the combustion and other vapors inside the cabinet.

8. Open the safety windows and remove the extinguishing cover.

9. Suck the excess unburned hot fuel from the sample dish.

10. Allow the radiation lamps and the sample dish to cool down.

11. Change the lamp height to the desired position, if necessary, and repeat the above precedure for the next test. For the unpiloted ignition tests, in addition to the steps

listed above, an additional step has to be included. When the radiation lamp is turned on start two stop watches (instead of one mentioned before) and record the elapsed time starting from the turning-on of the lamp to the first pop sound heard, which indicates flashing at the radiation lamps. Allow the other stop watch to clock until ignition occurs.

In order to obtain the radiative absorption of liquid fuel, the sample dish as in Figure 3-4 was used. The radiometer was set flush with the rim's edge first. After recording the radiative flux from the lamp for a period of thirty seconds or one minute, the radiometer was adjusted to another desired height by simply pulling the sleeve of radiometer down from underneath. The procedure was repeated for the emptied sample dish and when it was full of the testing liquid.

CHAPTER IV

EXPERIMENTAL RESULTS AND DISCUSSIONS

This chapter summarizes the experimental results for both piloted and unpiloted ignition tests of six different compositions of saturated hydrocarbon fuels. Their major components are n-dodecane (n-$C_{12}H_{26}$), n-tridecane (n-$C_{13}H_{28}$), n-tetradecane (n-$C_{14}H_{30}$), n-pentadecane (n-$C_{15}H_{32}$), and traces of other saturated and unsaturated, including aromatic organic, compounds. A chronology of modifications in the experimental equipment and techniques, the distribution of incident irradiance and the compositions of each fuel are presented in the appendix section.

Ignition Data and Analysis

Six different compositions of normal hydrocarbon fuels were used. Their ignition times, for various liquid volumes in the sample dish and for different irradiation fluxes, were obtained and are tabulated in Tables 4-1-A1, 4-1-A2, 4-1-B, 4-1-C, 4-1-D, 4-1-E and 4-1-F. Figures 4-1-A1, 4-1-A2 and 4-1-B summarize the results for Fuel A (either with the radiometer protruding one inch from the base of the dish into the liquid or with the radiometer flush with the bottom and for

TABLE 4-1-A1

EXPERIMENTAL RESULTS FOR PILOTED IGNITION TESTS FOR VARIOUS LIQUID VOLUMES AND INCIDENT IRRADIANCES

(Radiometer protrudes one inch from the base into the liquid at the center of the holder)

Volume (ml)	T_i* or I	Distance** (inch)				
		4	6	8	10	12
50	T_i/I	28.6/1.08	46.8/0.708	71.4/0.507	103.7/0.374	152.9/0.296
75	T_i/I	30.3/1.10	49.5/0.719	79.3/0.515	115.4/0.377	163.8/0.304
100	T_i/I	32.9/1.13	51.3/0.73	80.8/0.524	122.7/0.377	174.2/0.309
125	T_i/I	31.3/1.19	52.6/0.77	80.0/0.543	124.3/0.374	187.0/0.32
150	T_i/I	31.5/1.24	50.1/0.808	83.2/0.561	124.8/0.374	188.5/0.328
175	T_i/I	33.3/1.242	51.5/0.811	82.6/0.564	126.8/0.374	190.1/0.328
200	T_i/I	30.0/1.237	51.6/0.811	83.6/0.57	128.3/0.374	188.5/0.328
250	T_i/I				128.3/-	

*The T_i value shown in this table and later on are average values.

**Distance between the top edge of the liquid fuel holder and the lamp.

Units T_i = (sec); I = (cal/cm^2-sec).

TABLE 4-1-A2

EXPERIMENTAL IGNITION DATA OF FUEL A

(Radiometer Flush with the Sample Dish Bottom)

Distance	Volume (ml)							
	Piloted				Unpiloted			
	50	100	150	200	50		100	
	Ignition, T_i, T_f, or I							
	T_i/I	T_i/I	T_i/I	T_i/I	T_f/I	T_i/I	T_f/I	T_i/I
12	118.2/.282	133.4/2.96	137.0/.321	137.2/.323	--	--	--	--
10	85.8/.363	97.1/.381	98.8/.412	100.8/.415	--	--	--	--
9	--	--	--	--	110.9/.436	--	131.7/.459	--
8	62.6/.499	67.0/.513	69.8/.548	69.6/.557	93.2/.522	--	104.5/.543	--
7	--	--	--	--	71.3/.604	118.4/.644	79.0/.632	131.6/.672
6	41.4/.703	45.5/.724	46.6/.801	43.3/.796	62.5/.726	84.8/.754	63.6/.747	84.5/.771
5	--	--	--	--	53.2/.897	63.4/.914	51.8/.930	68.6/.956
4	25.7/1.07	28.7/1.13	28.1/1.23	28.5/1.23	43.7/1.10	49.9/1.12	46.1/1.17	51.4/1.18
3	--	--	--	--	38.0/1.51	38.2/1.51	38.6/1.56	39.9/1.57

Distance in inches

T_i or T_f in seconds

I in cal/cm^2-second

TABLE 4-1-B

EXPERIMENTAL IGNITION DATA OF FUEL B

(Radiometer Flush with the Sample Dish Bottom)

Distance	Volume (ml)							
	Piloted				Unpiloted			
	50	100	150	200	50		100	
	Ignition, T_i, T_f, or I							
	T_i/I	T_i/I	T_i/I	T_i/I	T_f/I	T_i/I	T_f/I	T_i/I
12	103.8/.28	117.8/.29	128.7/.32	126.6/.32	--	--	--	--
10	74.7/.36	86.9/.37	91.4/.41	92.4/.41	--	--	--	--
9	--	--	--	--	102.3/.431	--	119.8/.455	--
8	55.2/.49	64.5/.52	66.3/.55	64.8/.54	84.2/.501	156.3/.555	91.7/.532	163.1/.569
7	--	--	--	--	73.3/.583	111.1/.642	74.1/.628	124.7/.665
6	38.2/.70	42.8/.72	41.0/.79	42.3/.80	58.8/.721	79.3/.75	59.5/.745	85.6/.775
5	--	--	--	--	49.3/.89	65.8/.914	52.1/.928	68.0/.956
4	22.5/1.06	27.0/1.12	26.1/1.23	23.2/1.22	43.4/1.10	43.6/1.10	43.7/1.16	46.4/1.16
3	18.0/1.45	18.8/1.50	19.5/1.59	18.8/1.57	38.2/1.51	38.4/1.51	37.7/1.56	38.1/1.56

Distance in inches

T_i or T_f in seconds

I in cal/cm^2-second

TABLE 4-1-C

EXPERIMENTAL IGNITION DATA OF FUEL C

(Radiometer Flush with the Sample Dish Bottom)

Distance	Volume (ml)											
	Piloted				Unpiloted							
	50		100		50				100			
	Ignition, T_i, T_f, or I											
	T_i	I	T_i	I	T_f	I	T_i	I	T_f	I	T_i	I
12	103.3	.278	118.5	.293	--	--	--	--	--	--	--	--
10	77.9	.36	86.3	.357	--	--	--	--	--	--	--	--
9	--	--	--	--	97.0	.428	--	--	109.1	.452	--	--
8	55.9	.483	58.9	.504	83.5	.513	160.5	.55	88.2	.532	161.7	.565
7	--	--	--	--	70.9	.602	113.7	.639	75.1	.63	110.8	.658
6	36.8	.693	39.6	.719	60.3	.724	85.3	.754	61.6	.745	84.9	.752
5	--	--	--	--	50.3	.895	58.7	.909	53.4	.932	59.8	.942
4	22.	1.06	26.2	1.12	45.4	1.11	47.5	1.11	46.5	1.16	49.1	1.17
3	17.7	1.45	18.7	1.5	40.1	1.51	40.1	1.51	39.7	1.56	39.7	1.56

Distance in inches

T_i or T_f in seconds

I in cal/cm^2-second

TABLE 4-1-D

EXPERIMENTAL IGNITION DATA ON FUEL D

(Radiometer flush with the Sample Dish Bottom)

Dis-tance	Volume (ml)											
	Piloted											
	50		100		50			100				
	Ignition, T_i, T_f, or I											
	T_i	I	T_i	I	T_f	I	T_i	I	T_f	I	T_i	I
12	102.6	.277	109.5	.291	--	--	--	--	--	--	--	--
10	76.4	.358	82.5	.375	--	--	--	--	--	--	--	--
9	--	--	--	--	104.9	.43	--	--	115.4	.454	--	--
8	54.5	.492	61.4	.508	85.7	.515	138.7	.543	93.	.534	153.3	.569
7	--	--	--	--	68.2	.600	99.9	.628	73.3	.625	107.7	.656
6	38.2	.696	40.1	.719	61.0	.726	81.2	.75	60.1	.743	87.7	.775
5	30.9	.862	32.6	.895	52.5	.897	61.7	.911	51.0	.925	65.8	.953
4	24.5	1.07	24.8	1.12	43.7	1.11	44.0	1.11	46.	1.17	49.4	1.17
3	18.3	1.45	18.4	1.5	40.4	1.51	40.4	1.51	39.8	1.56	39.8	1.56

Distance in inches

T_i or T_f in seconds

I in cal/cm^2-second

TABLE 4-1-E

EXPERIMENTAL IGNITION DATA ON FUEL E

(Radiometer Flush with the Sample Dish Bottom)

Distance	Volume (ml)											
	Piloted				Unpiloted							
	50		100		50				100			
	Ignition, T_i, T_f, or I											
	T_i	I	T_i	I	T_f	I	T_i	I	T_f	I	T_i	I
12	94.7	.275	98.	.285	--	--	--	--	--	--	--	--
10	66.8	.351	69.9	.364	--	--	--	--	--	--	--	--
9	--	--	--	--	101.0	.429	--	--	110.2	.45	--	--
8	47.5	.487	52.0	.499	70.3	.504	140.5	.543	86.0	.527	136.6	.557
7	--	--	--	--	66.1	.6	101.5	.628	73.6	.625	105.9	.656
6	33.4	.698	35.9	.714	58.9	.724	76.6	.745	58.	.745	78.5	.766
5	--	--	--	--	47.7	.89	58.3	.909	49.4	.925	61.3	.944
4	20.3	1.06	21.	1.11	44.0	1.11	45.7	1.11	43.8	1.16	46.8	1.17
3	15.2	1.44	15.4	1.49	39.3	1.52	39.3	1.52	40.1	1.53	40.1	1.57

Distance in inches

T_i or T_f in seconds

I in cal/cm^2-second

TABLE 4-1-F

EXPERIMENTAL IGNITION DATA OF FUEL F

(Radiometer Flush with the Sample Dish Bottom)

Distance	Volume (ml)											
	Piloted				Unpiloted							
	50		100		50				100			
	Ignition, T_i, T_f, or I											
	T_i	I	T_i	I	T_f	I	T_i	I	T_f	I	T_i	I
12	106.6	.278	121.1	.292	--	--	--	--	--	--	--	--
10	74.1	.356	86.2	.375	--	--	--	--	--	--	--	--
9	--	--	--	--	100.7	.429	--	--	121.9	.455	--	--
8	54.7	.492	60.8	.506	94.5	.522	160.4	.553	101.2	.548	164.8	.565
7	--	--	--	--	77.7	.607	116.9	.642	79.9	.632	111.8	.661
6	34.7	.656	40.2	.721	62.4	.726	87.7	.759	62.1	.747	84.5	.771
5	--	--	--	--	54.7	.899	64.0	.918	55.2	.937	64.5	.951
4	23.6	1.07	23.9	1.12	45.8	1.11	48.0	1.12	46.0	1.16	49.5	1.17
3	18.8	1.45	18.8	1.50	41.4	1.52	41.4	1.52	40.7	1.57	40.7	1.57

Distance in inches

T_i or T_f in seconds

I in cal/cm^2-second

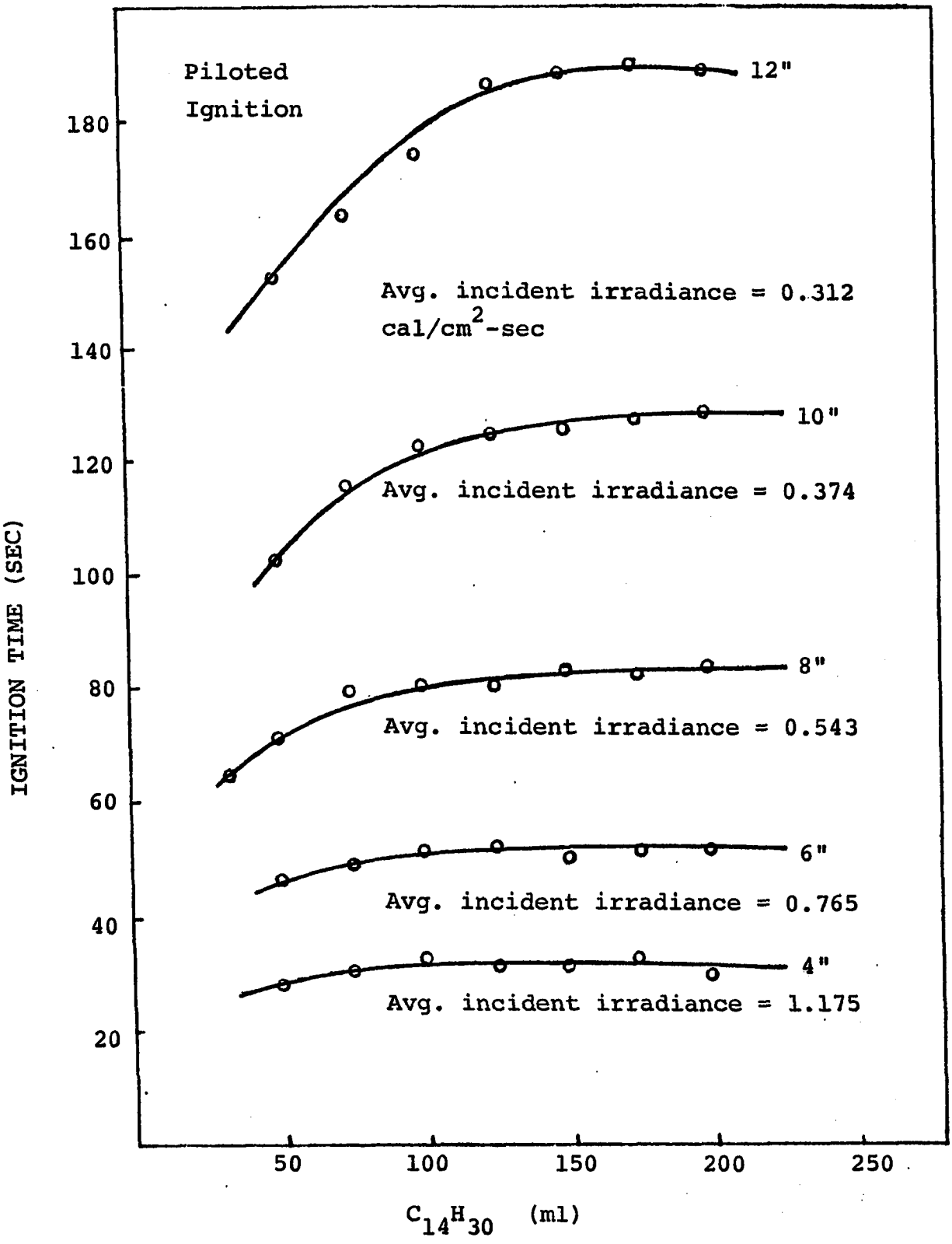

Figure 4-1-A1. Relationship Between Liquid Volume and Ignition Time at Various Incident Irradiances for Fuel A (Recycled)

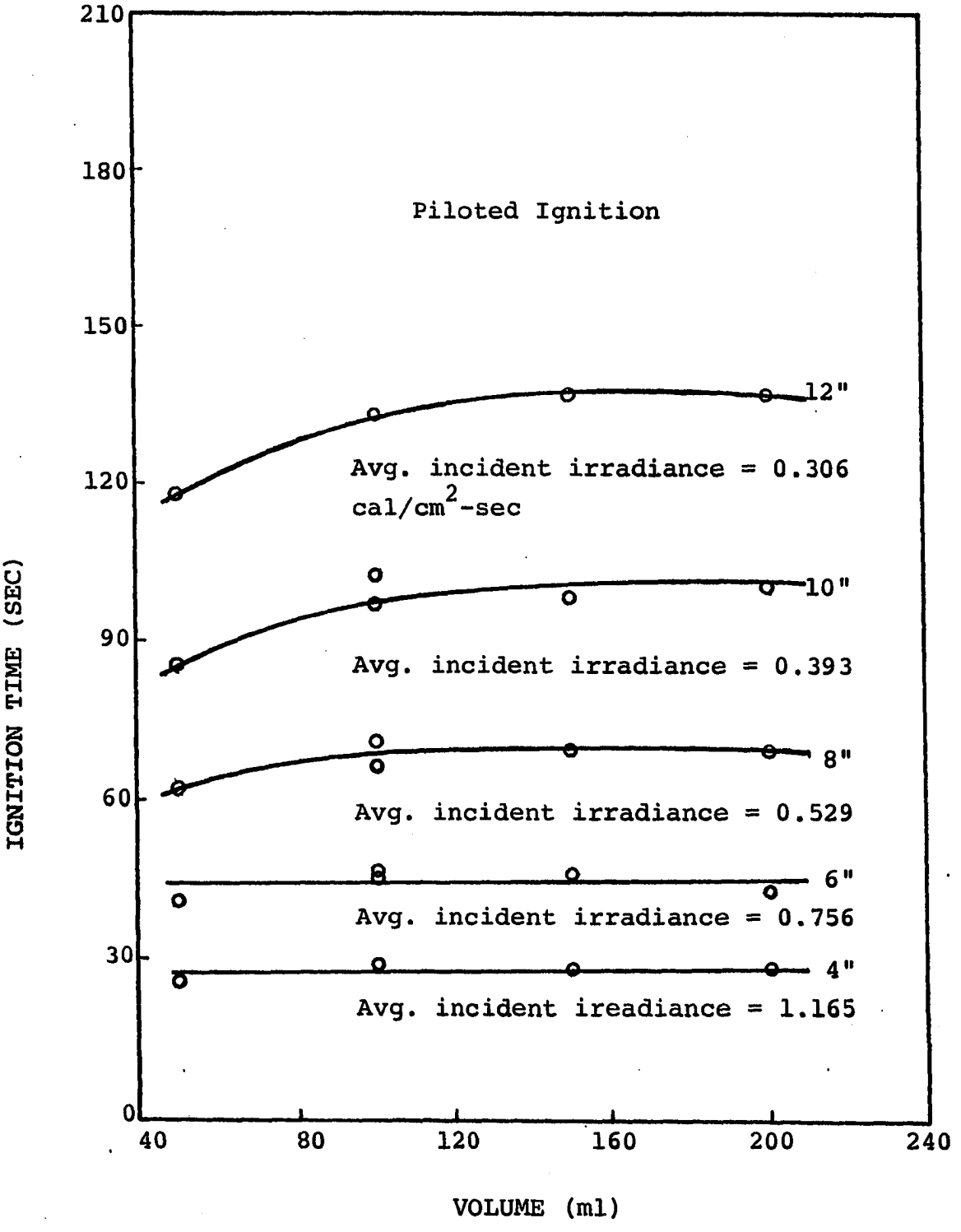

Figure 4-1-A2. Relationship Between Liquid Volume and Ignition Time at Various Incident Irradiances for Fuel A (Fresh)

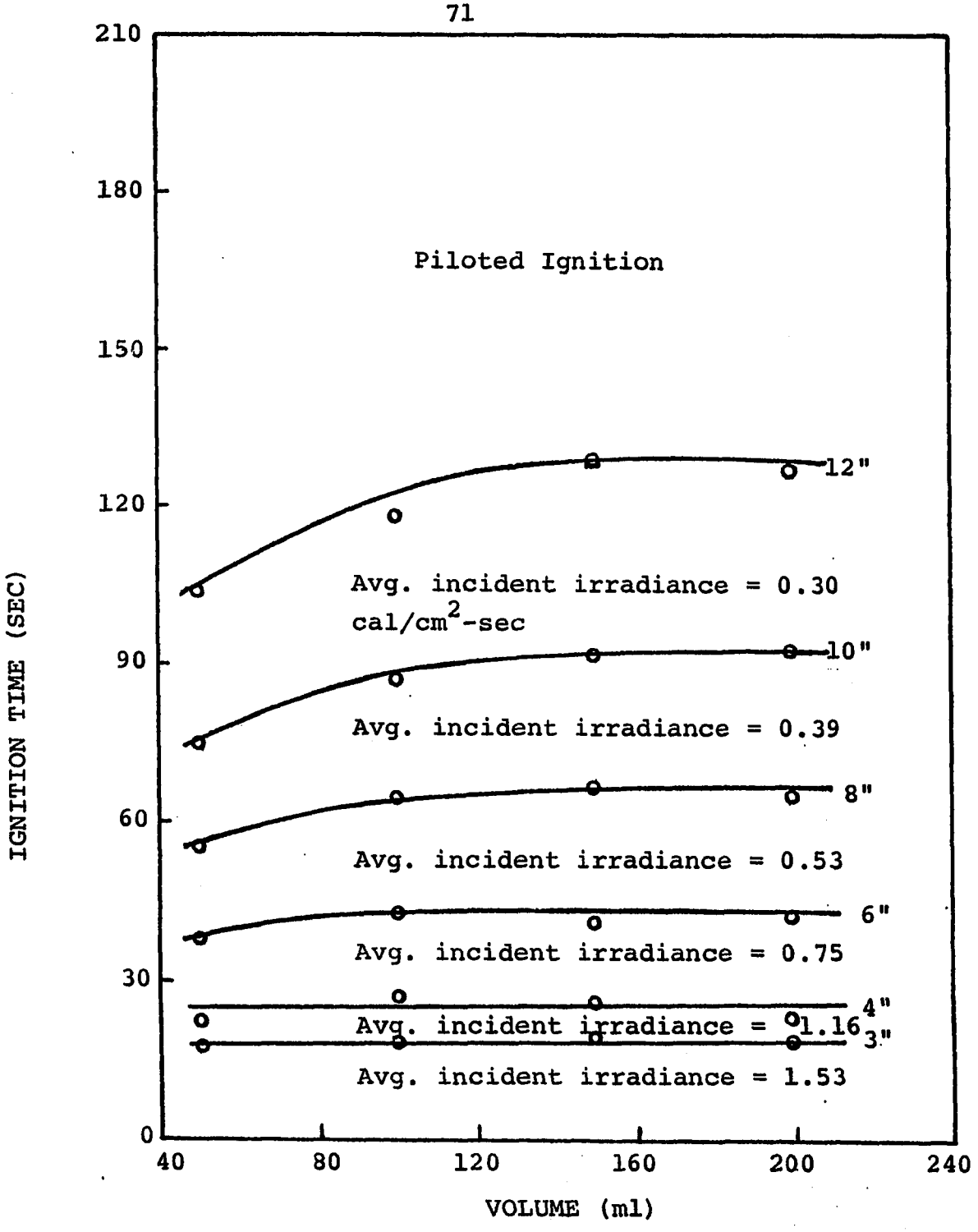

Figure 4-1-B. Relationship Between Liquid Volume and Ignition time at Various Incident Irradiances for Fuel B (Fresh)

Fuel B (radiometer always flush with the bottom of the dish) in graphical forms and indicate that for higher radiative flux the ignition time remains almost constant. However, as the radiation flux is decreased, an increase in ignition times was observed for increased liquid sample volumes. (This phenomenon was observed in spite of the fact that as the liquid sample volume was increased the irradiant flux increased slightly due to the decreased distance between the lamp and the liquid surface level.) At lowest irradiant fluxes the fraction of the rate of heat loss from the surface to the surroundings and to the bulk of the liquid is relatively higher compared to the heat input in irradiation at the surface. As a consequence a longer time is required to attain the ignition temperature. Figures 4-2-A and 4-2-B show the variation of piloted ignition time with irradiant flux for all six species of fuels at volumes of 50 ml and 100 ml respectively. These figures illustrate that as the radiative flux is increased the ignition time decreases but at a progressively slower rate as expected. Conversely, as the irradiant flux is decreased, the rate of increase in the ignition time rises rapidly and appears to approach, asymptotically, an incident irradiance below which ignition will not occur in infinite time. Lighter (more volatile) composition fuels have shorter ignition times for designated incident radiative fluxes; Fuel E (with 71.6 percent n-$C_{12}H_{26}$) is an example.

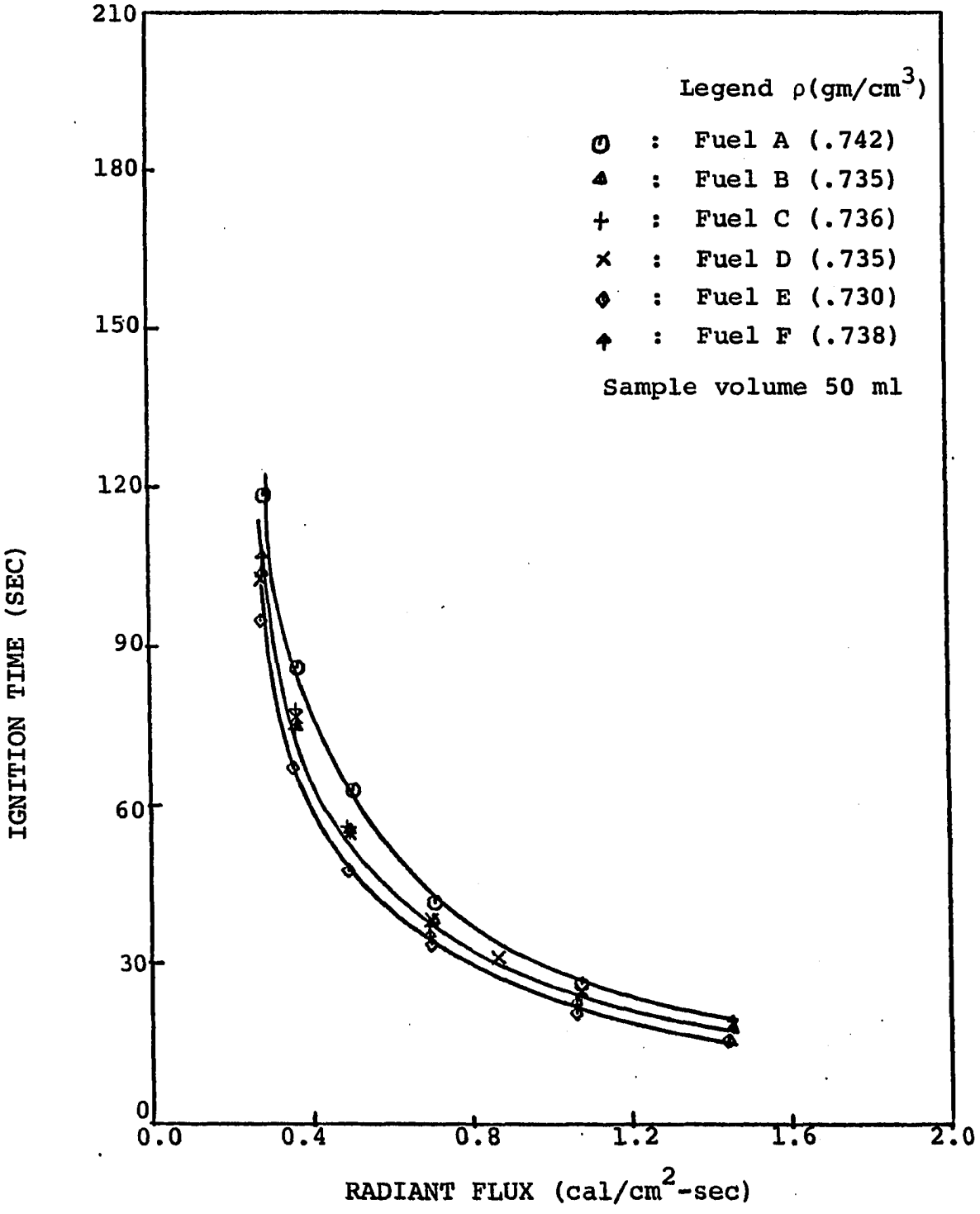

Figure 4-2-A. Variation of Piloted Ignition Time with Raidant Flux for Sample Volume of 50 ml

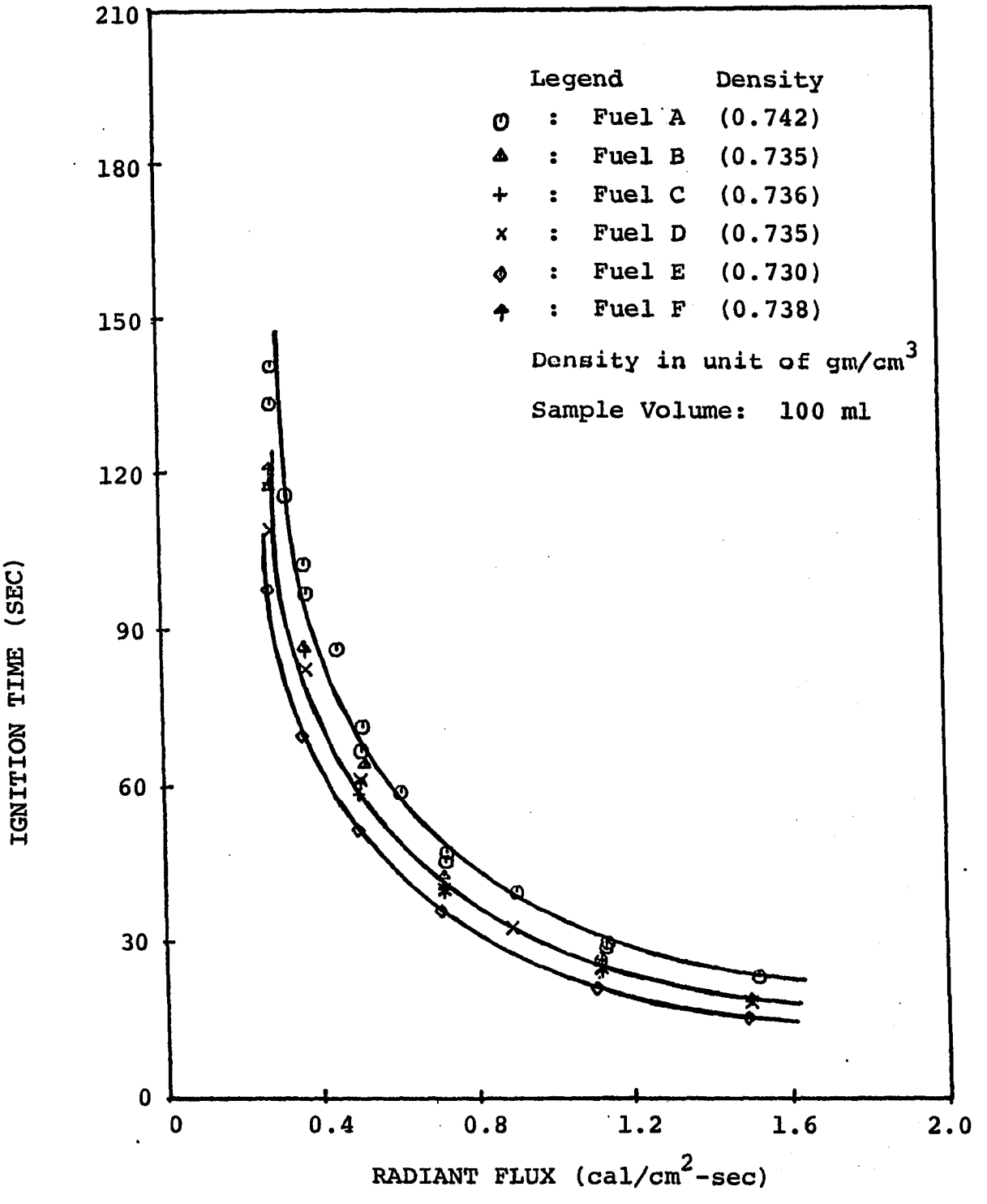

Figure 4-2-B. Variation of Piloted Ignition Time with Radiant Flux for Sample Volume of 100 ml

Figures 4-3-A and 4-3-B summarize the results of the unpiloted ignition time with irradiative flux for all six fuel samples at volumes of 50 ml and 100 ml respectively. Conclusions similar to those given above for ignitions apply.

Figures 4-4-A and 4-4-B show the linear relationship between the ignition time and incident irradiance on a log-log scale for Fuel A and Fuel B, respectively. In each figure, volume is a parameter, which includes 50 ml, 100 ml, 150 ml and 200 ml. It is evident that for a volume of 50 ml the ignition time is the fastest. There also is an indication that at 100 ml the ignition times are faster than for 150 and 200 ml. However, within the limits of experimental precision as revealed by the scatter in the data, it appears that for samples of 100 ml and larger, volume becomes an insensitive parameter, which indicates that the wall effect, or contribution of heat input by the metal vessel walls to the sample becomes relatively smaller as sample volume increases. Similar plots for all six fuel samples at values of 50 ml and 100 ml are given in Figures 4-5-A and 4-5-B. These plots demonstrate that fuel E which has the lowest density and also the highest concentration of the most volatile component, dodecane, (see Table A-2, Appendix) has the fastest ignition time while fuel A which has the highest density and the least volatiles has the slowest ignition time. The fact that the linear, logarithmic relationship holds for all fuels and

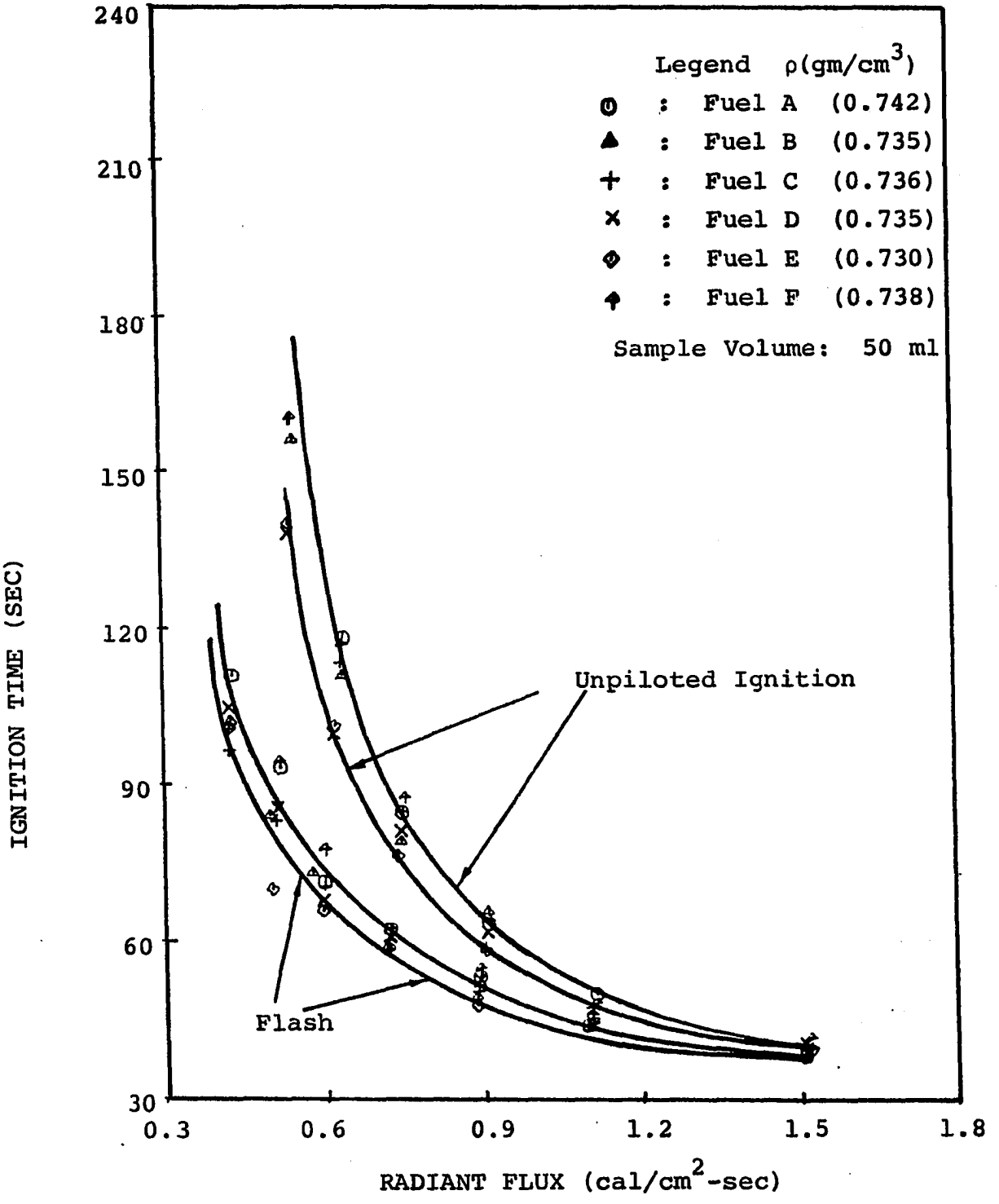

Figure 4-3-A. Variation of Unpiloted Ignition Time with Raidant Flux for Sample Volume of 50 ml

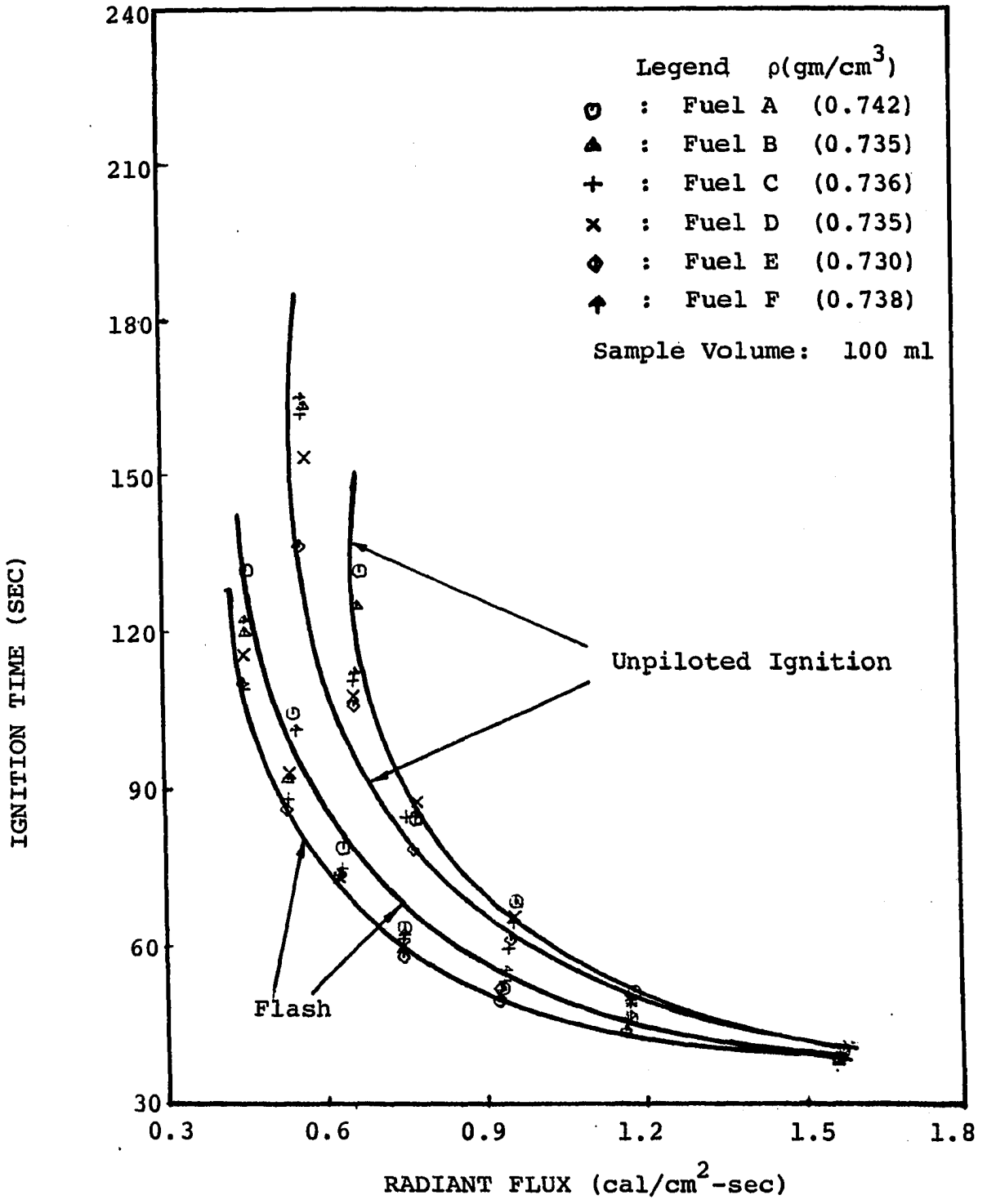

Figure 4-3-B. Variation of Unpiloted Ignition Time with Radiant Flux for Sample Volume of 100 ml

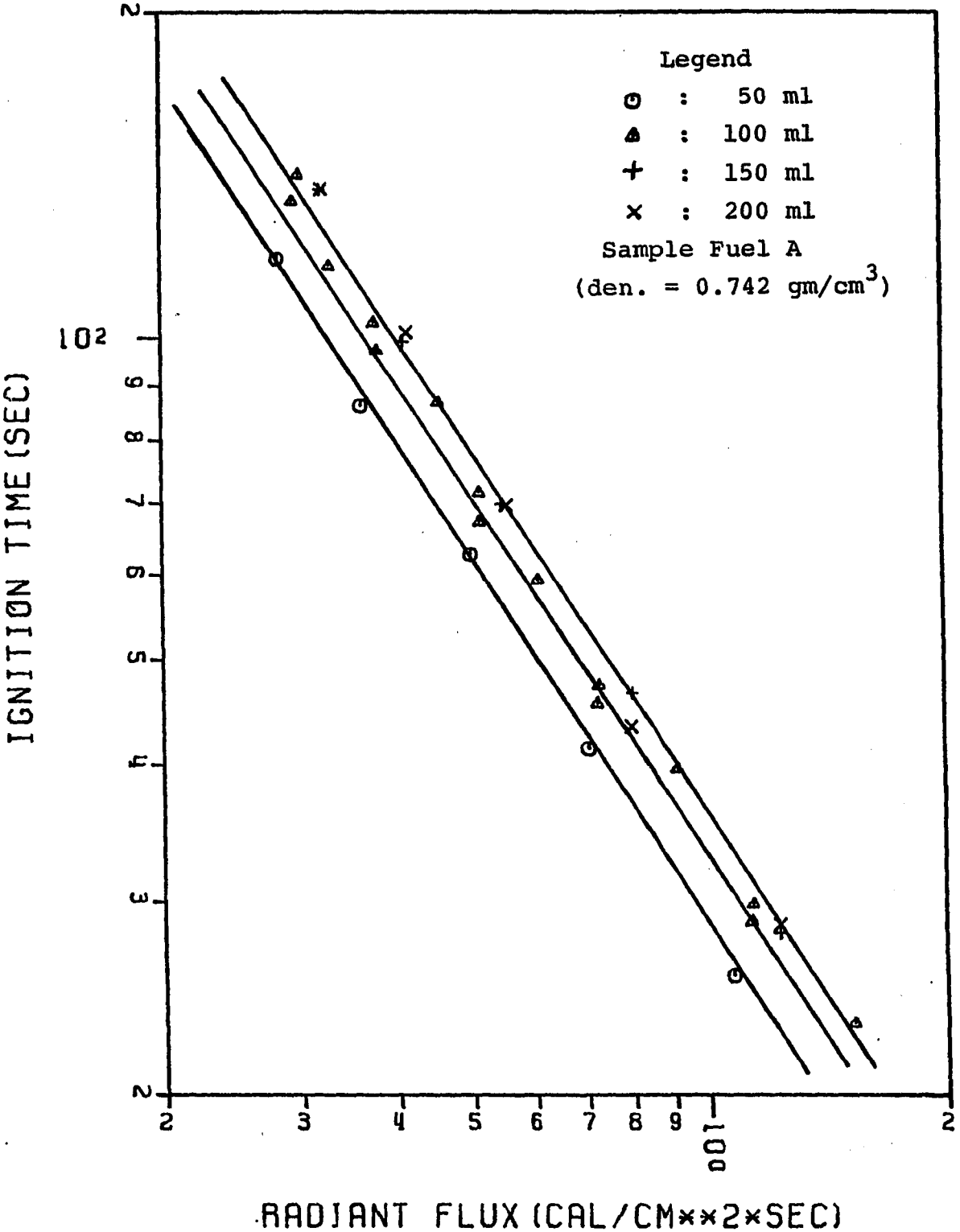

Figure 4-4-A. Logarithmic Relationship between Radiant Flux and Piloted Ignition Time for Fuel A.

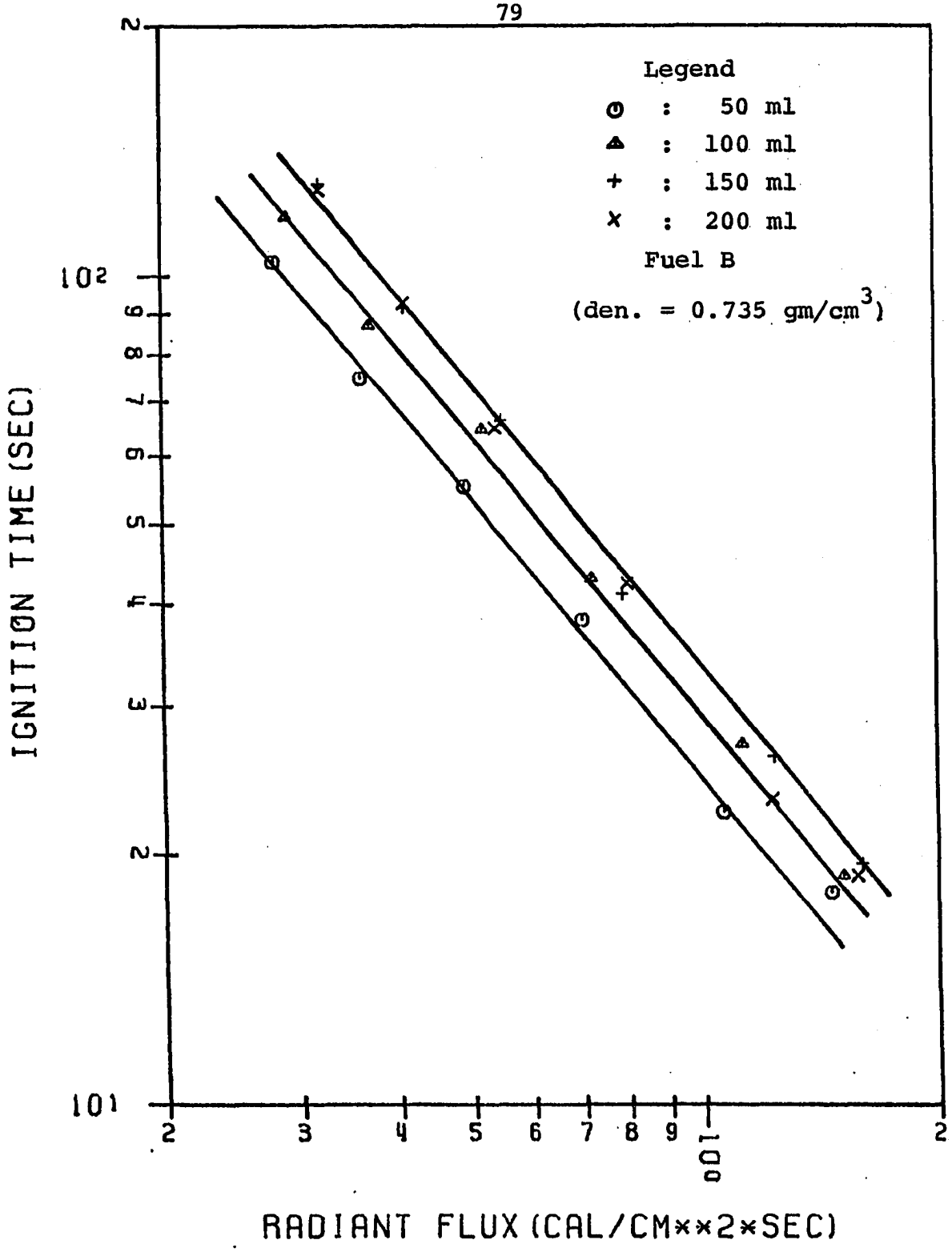

Figure 4-4-B. Logarithmic Relationship Between Radiant Flux and Piloted Ignition Time for Fuel B

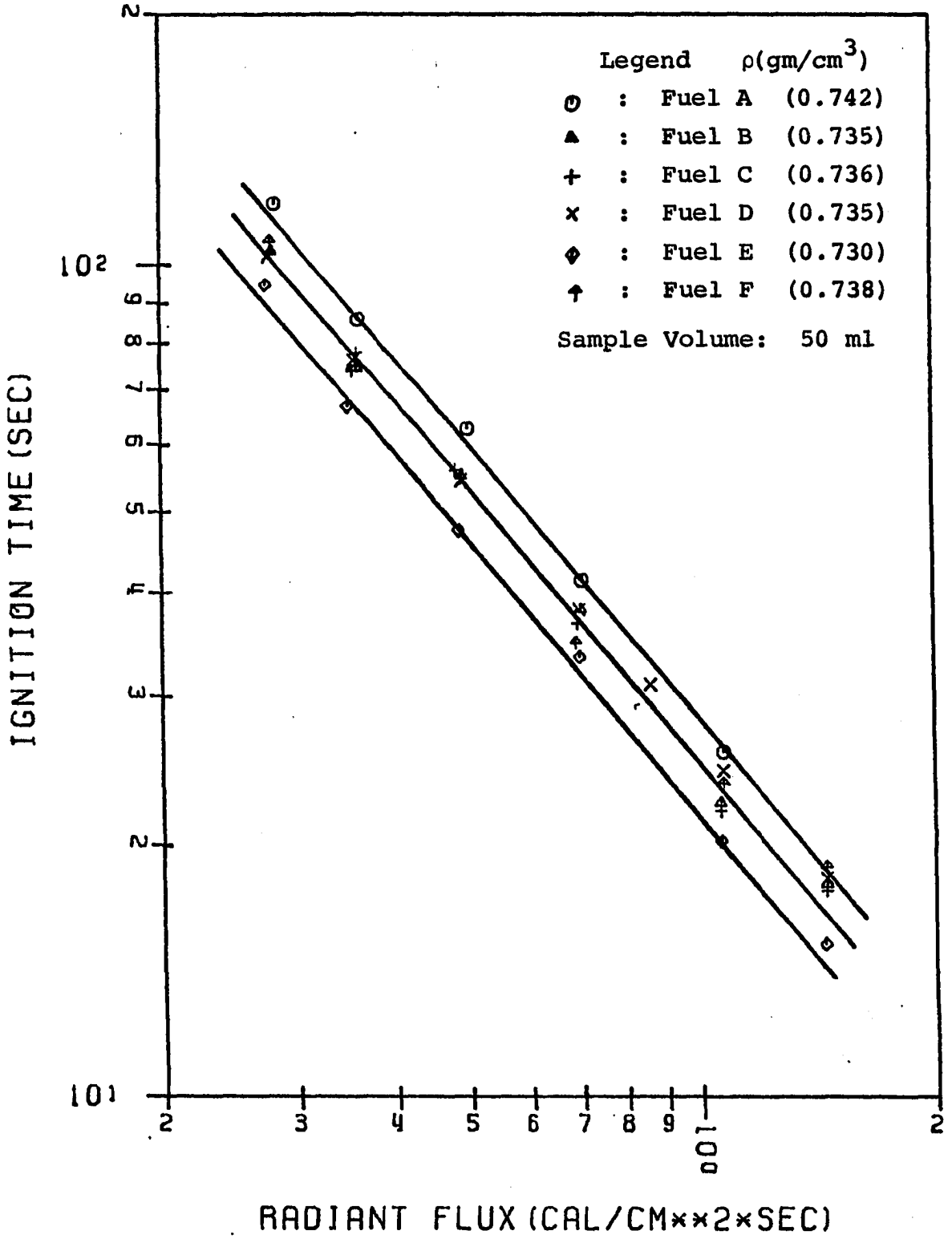

Figure 4-5-A. Logarithmic Relationship Between Radiant Flux and Piloted Ignition Time for Sample Volume of 50 ml

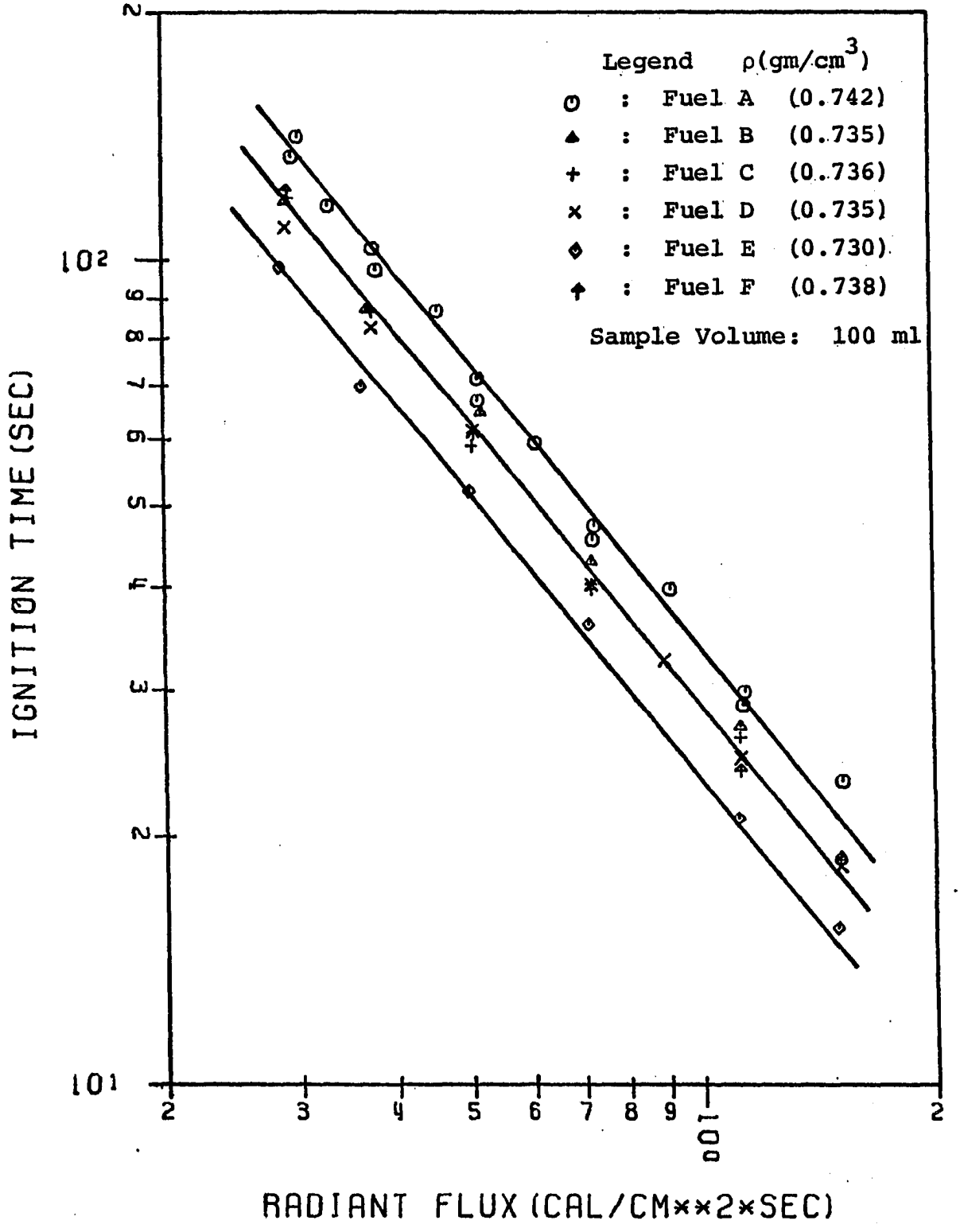

Figure 4-5-B. Logarithmic Relationship Between Radiant Flux and Piloted Ignition Time for Sample Volume of 100 ml

that the lines are parallel indicates that the four components and their mixtures have similar ignition characteristics. At 50 ml, the slope of the lines is about -1.3 whereas at 100 ml it is about -1.2.

Typical log-log plots of unpiloted ignition time versus radiant flux for Fuel B at volumes of 50 ml and 100 ml are shown in Figure 4-6 for both the initial flash (due to presence of heating lamp in evolved vapors) and auto-ignition conditions. For both cases the linear behavior which was observed in piloted ignition over the range of incident fluxes used (up to about 1.5 cal/cm^2-sec) breaks down at about 0.75 cal/cm^2-sec. The principal similarity between piloted and unpiloted ignition is that a sample of 50 ml volume has a shorter ingition time than a volume of 100 ml sample at the same incident irradiance.

When the incident irradiant flux is plotted against the reciprocal of the piloted ignition time, a linear relation is obtained as shown in Figures 4-7-A, 4-7-B, 4-7-C, 4-7-D, 4-7-E and 4-7-F for the representative six fuel samples. (A similar linear behavior has been previously observed for ignition of solids, such as pine wood). When the straight line is extrapolated to the ordinate, infinite time, a "minimum" incident irradiance of 0.078 cal/cm^2-sec was obtained for Fuel A and 0.06 cal/cm^2-sec for the rest of the fuel samples from the present experimental results.

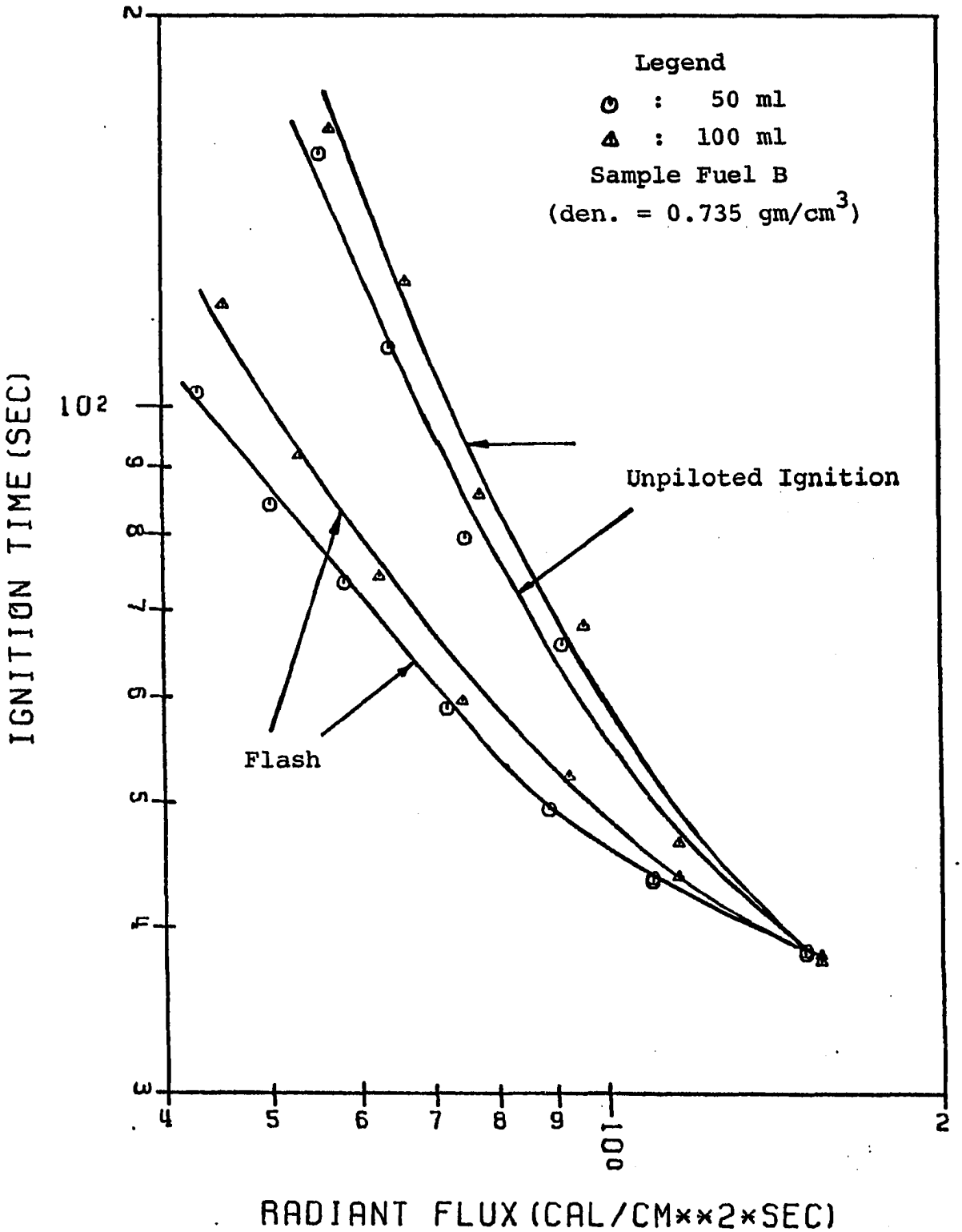

Figure 4-6. Logarithmic Relationship Between Radiant Flux and Unpiloted Ignition Time for Fuel B

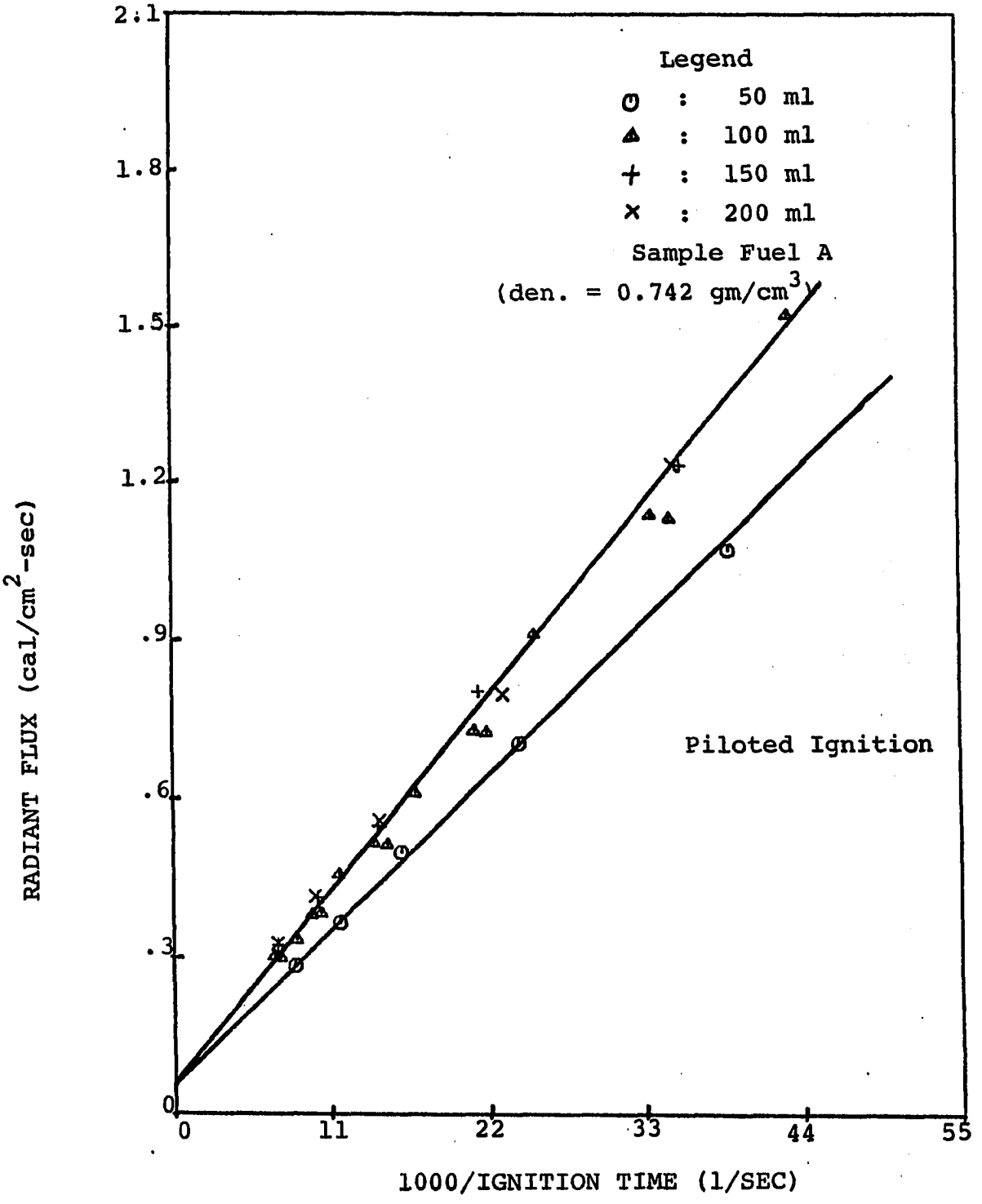

Figure 4-7-A. Relationship Between Radiant Flux and Reciprocal Ignition Time for Fuel A

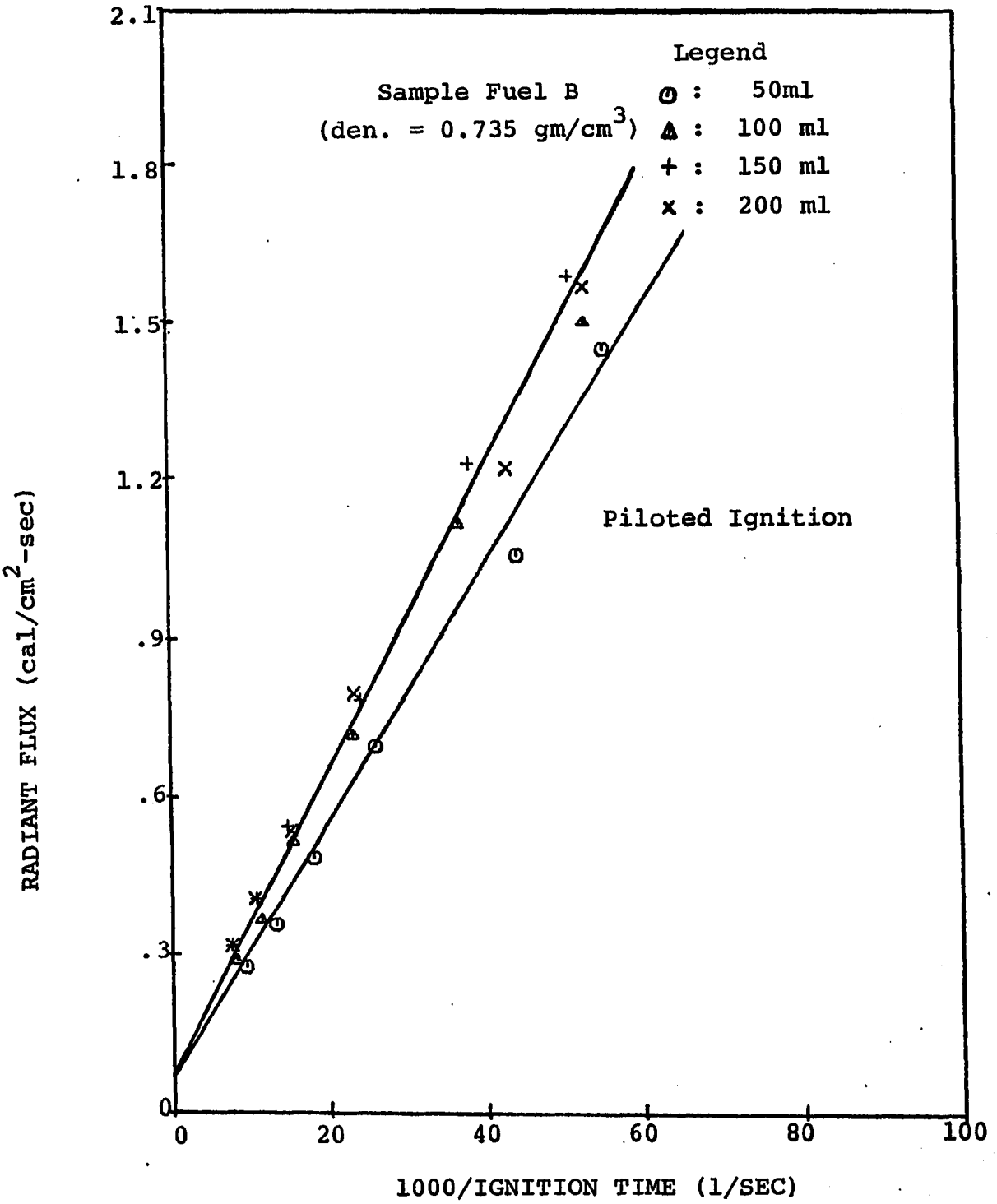

Figure 4-7-B. Relationship Between Radiant Flux and Reciprocal Ignition Time for Fuel B

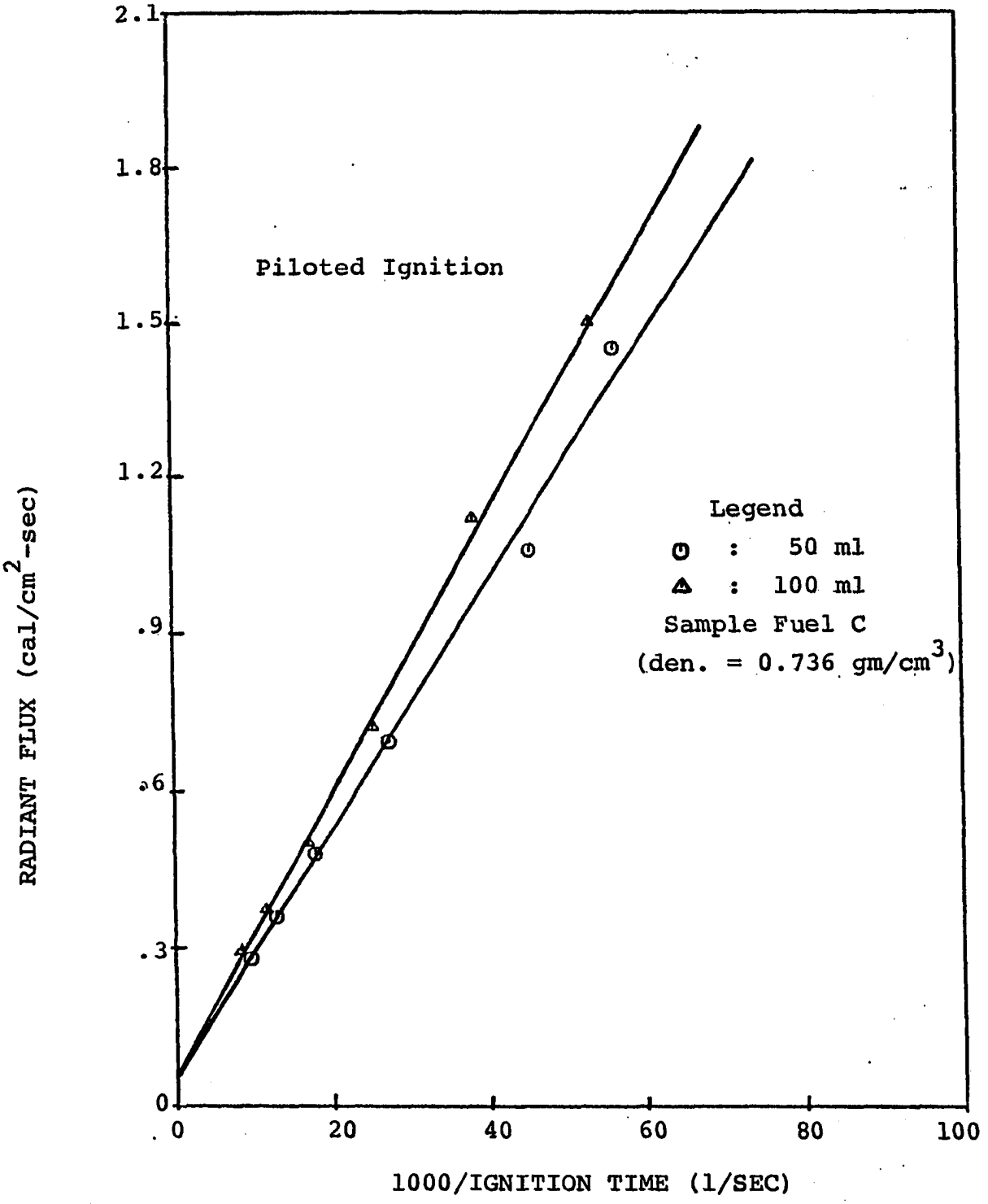

Figure 4-7-C. Relationship Between Radiant Flux and Reciprocal Ignition Time for Fuel C

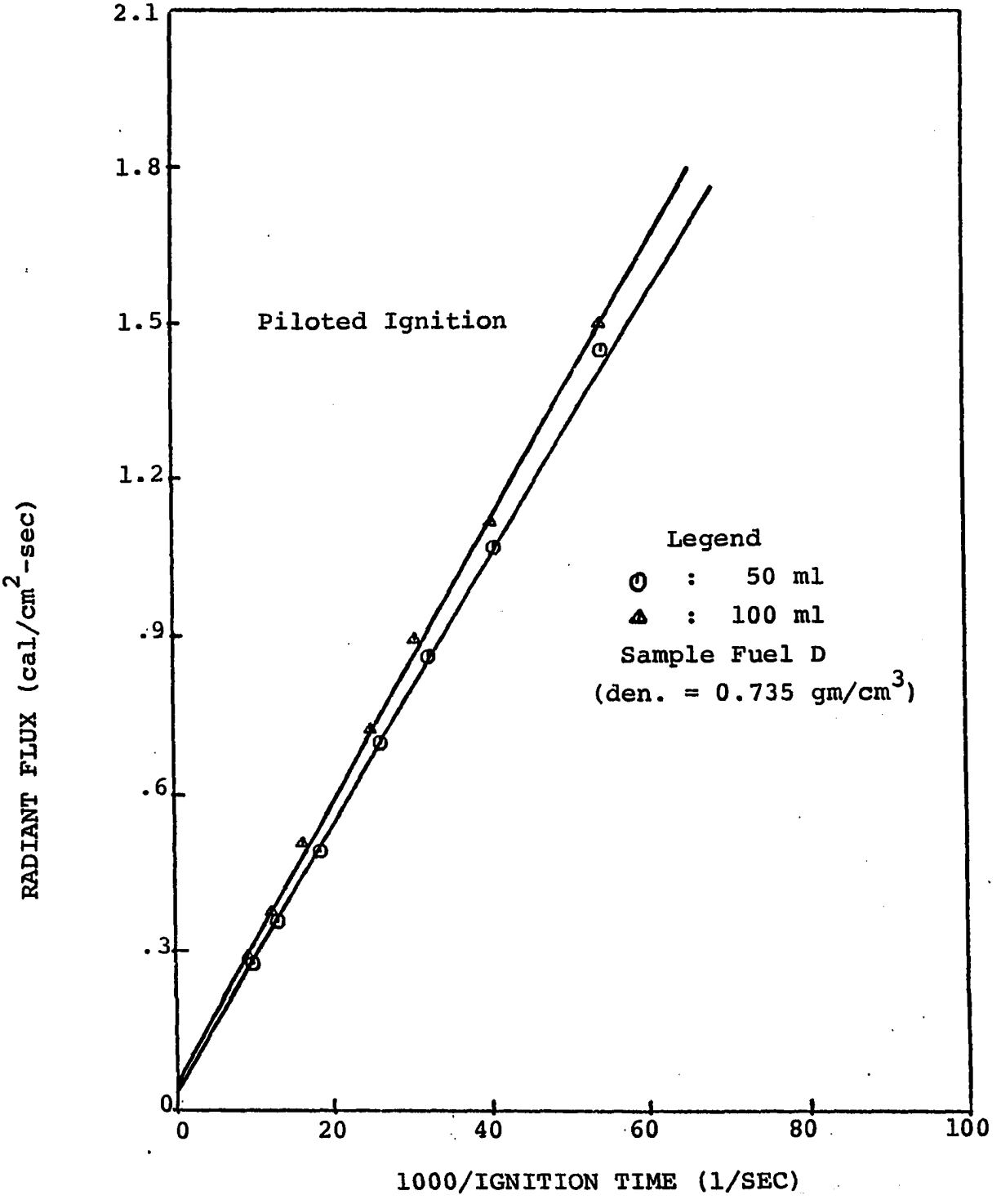

Figure 4-7-D. Relationship Between Radiant Flux and Reciprocal Ignition Time for Fuel D

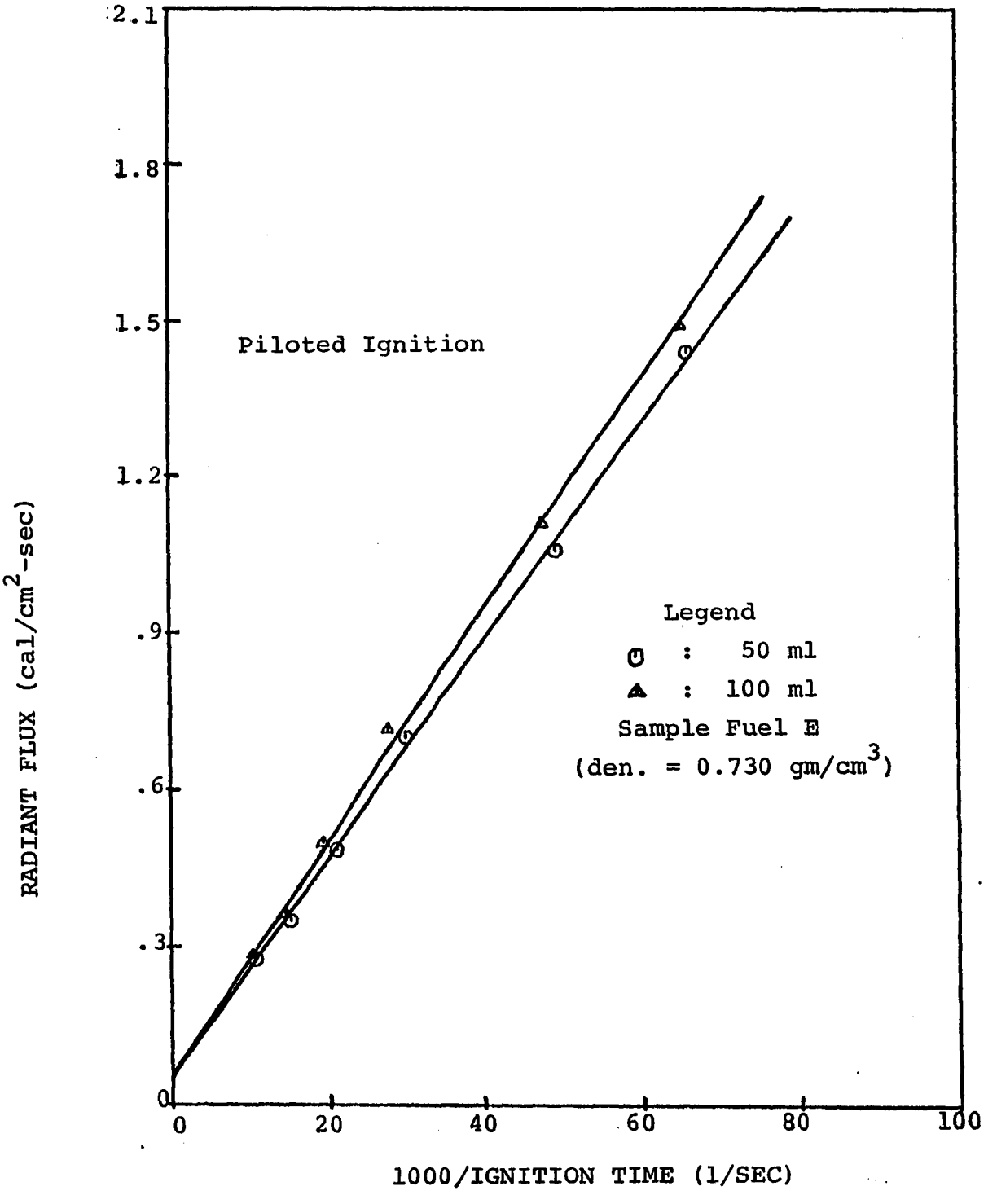

Figure 4-7-E. Relationship Between Radiant Flux and Reciprocal Ignition Time for Fuel E

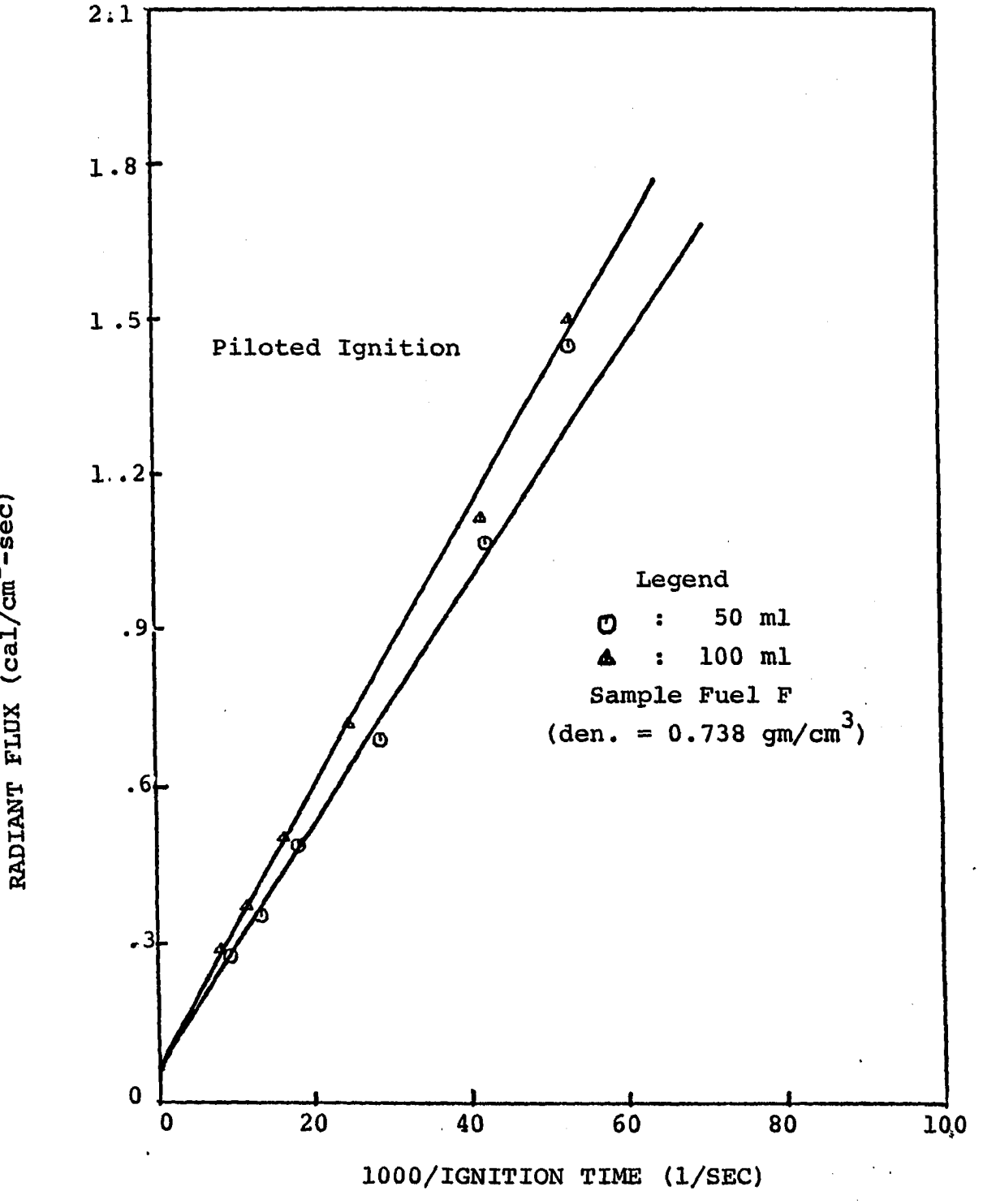

Figure 4-7-F. Relationship Between Radiant Flux and Reciprocal Ignition Time for Fuel F

From the apparent linearity shown both on Figures 4-5 and 4-7,

$$\ln t = A \ln H + \ln B \quad \text{for Figures 4-5}$$

and

$$H = C/t + D \quad \text{for Figures 4-7}$$

where

t = measured ignition time

H = incident irradiance

A, B, C, and D are constants determined by inserting the measured t and H value

The correspondence between these two sets of plots can be seen from the following:

$$\ln H = \ln C - \ln t + \ln D$$

$$\ln t = - \ln H + \ln (CD)$$

Figures 4-5 and 4-7 are consistent only if the slope A in Figures 4-5 is equal to "-1". The actually measured slopes of the lines in Figure 4-5 range from -1.2 to -1.3; the variation is probably caused by the inherent scatter in the data. Furthermore, the intercept B (at H = 1) in Figures 4-5 should equal product of C and D in Figures 4-7. Using Figure 4-7-A, 50 ml of Fuel A, as the example

$$C = \frac{1.2}{45} \times 1000 = 26.67$$

$$D = 0.078$$

and $$C \times D = 2.07$$

which is very comparable to the B value of "2.1" (at H = 1) from Figure 4-5-A

For unpiloted ignition, there is no such linear relationship between the incident flux and the reciprocal of the ignition time or flash time. Figures 4-8-A and 4-8-B are two typical representatives for unpiloted ignition of Fuel A and Fuel B, each includes the volume of 50 ml and 100 ml. However no minimum incident irradiance could be obtained from these two figures because of the increasing rate of curvature of the curves at long times precludes reliable extrapolation. Piloted ignition gives shorter ignition times than the unpiloted ignition. Table 4-2 and Figure 4-9 show the typical results obtained for piloted as well as unpiloted ignitions of Fuel A at volume of 50 ml. Results for other fuels were previously tabulated in Tables 4-1-A2, 4-1-B, 4-1-C, 4-1-D, 4-1-E and 4-1-F. In the case of unpiloted ignition the ignition was observed to take place at the radiating lamps and to propagate quickly to the liquid surface. The elapsed time for the flame to reach the liquid surface from the lamp varies, depending on the distance between the lamp and the liquid surface. In this case the lamp served as both pilot and ignition source. Figures 4-10-A, 4-10-B, 4-10-C, 4-10-D, 4-10-E and 4-10-F show the relationships between the distance from the ignition source to the liquid surface and the elapsed time for the flame to reach the liquid surface for all six fuel

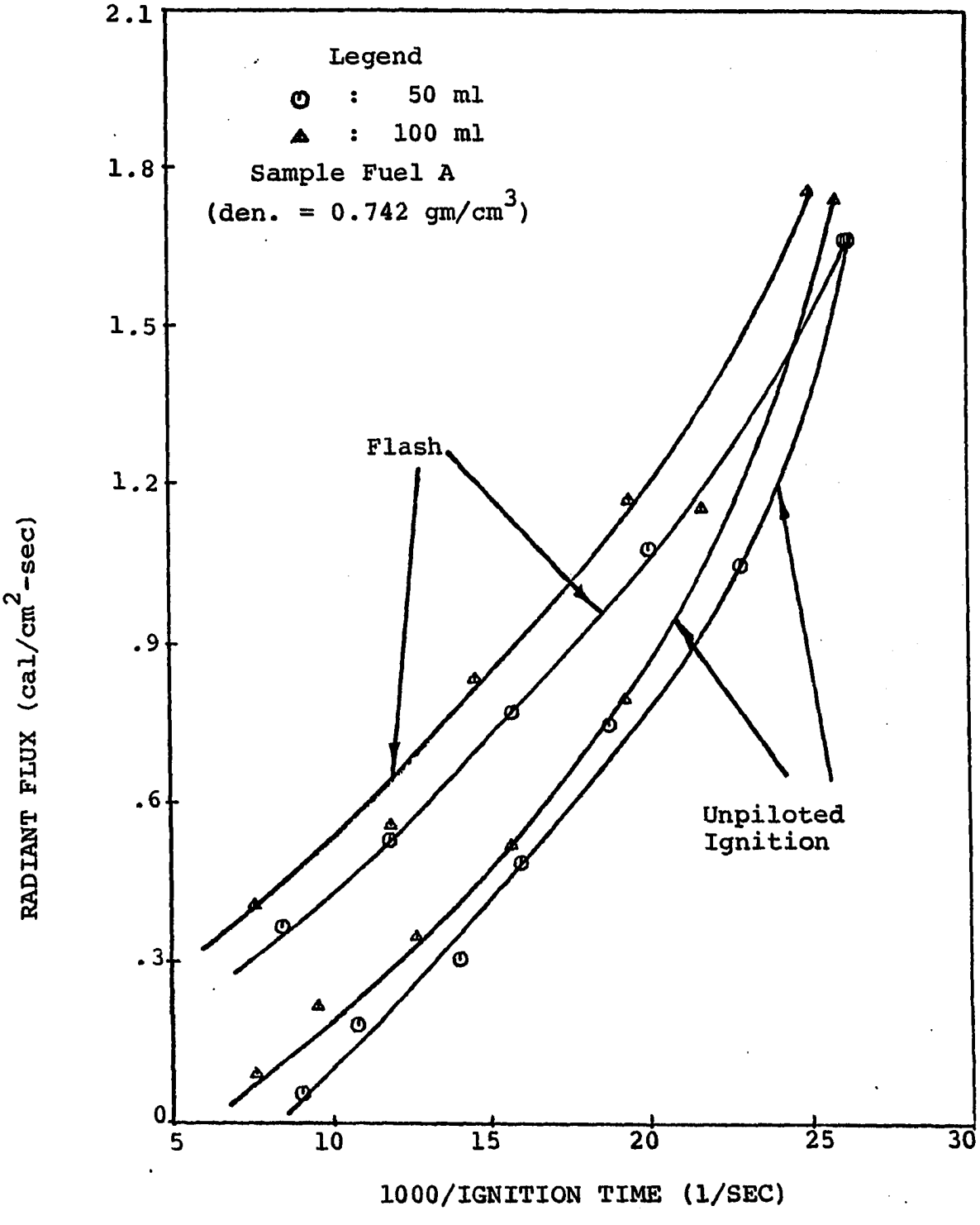

Figure 4-8-A. Relationship Between Radiant Flux and Reciprocal Unpiloted Ignition Time for Fuel A

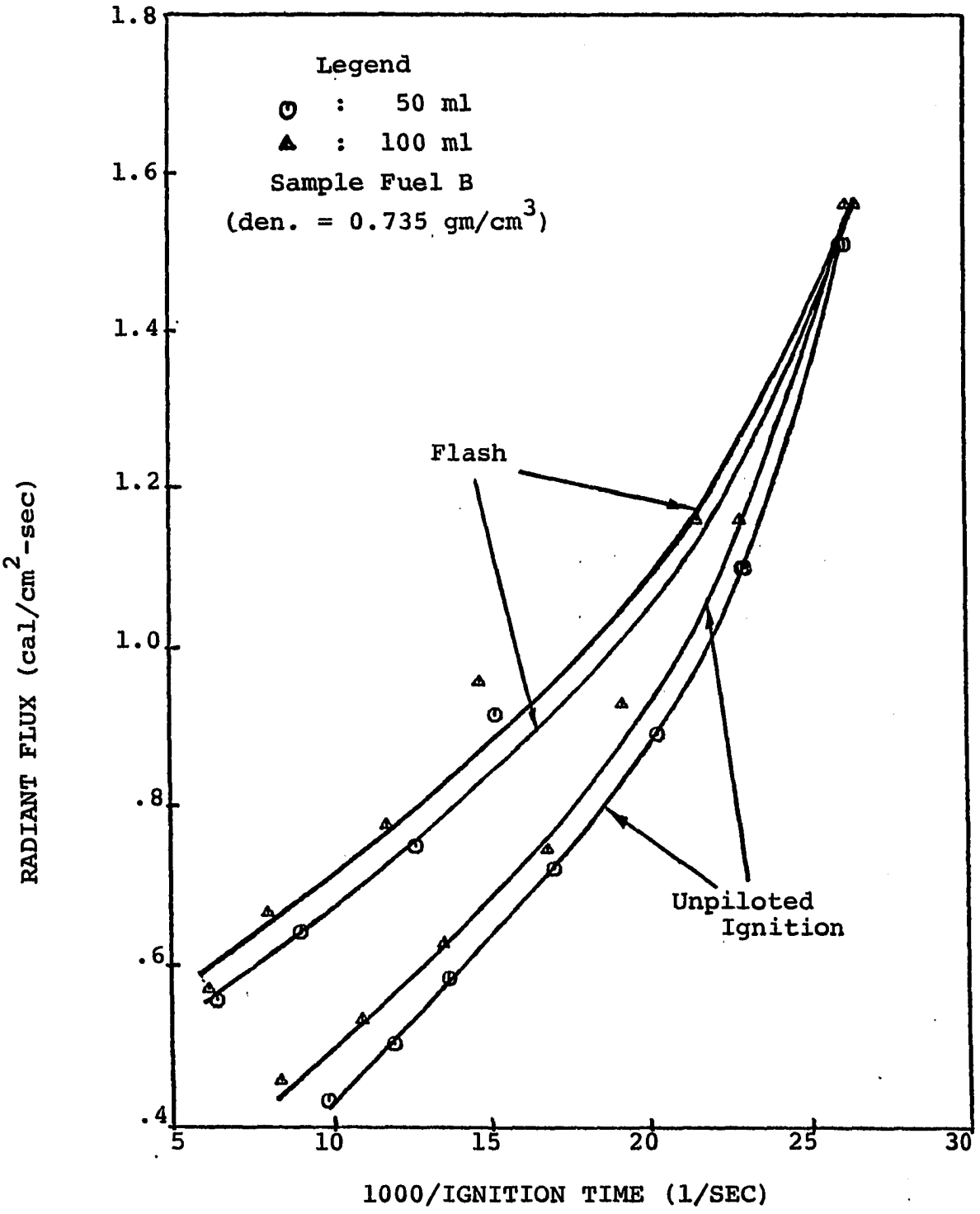

Figure 4-8-B. Relationship Between Radiant Flux and Reciprocal Unpiloted Ignition Time for Fuel B

TABLE 4-2

PILOT AND UN-PILOTED IGNITION OF $C_{14}H_{30}$ WHEN FUEL VOLUME IS 50 ML

(Center Radiometer Height ≈ 5/32 Inches)

Ignition	Distance, Inches									
Time (sec)	3	4	5	6	7	8	9	10	11	12
T_i (Piloted)	22.0	28.2	37.8	47.2	55.4	70.8	82.5	100.7	115.1	147.5
I	5.40	3.96	3.20	2.60	2.16	1.85	1.54	1.36	1.20	1.07
T_i (Non-Piloted)	38.5	46.	64.9	94.4	142.7					
I	5.71	4.8	3.37	2.82	2.42					
T_f (Non-Piloted	38.2	43.9	53.0	67.9	83.9	105.7				
I	5.70	4.06	3.31	2.69	2.26	1.96				

All above data are shown in Figure 10.

T_f represents the elapsed time between the initiation of heating and the first flash or sound from lamp.

T_i represents the elapsed time between the initiation of heating and the moment when a self-sustaining flame is observed on the liquid surface.

I Incident irradiance (Btu/ft^2-sec).

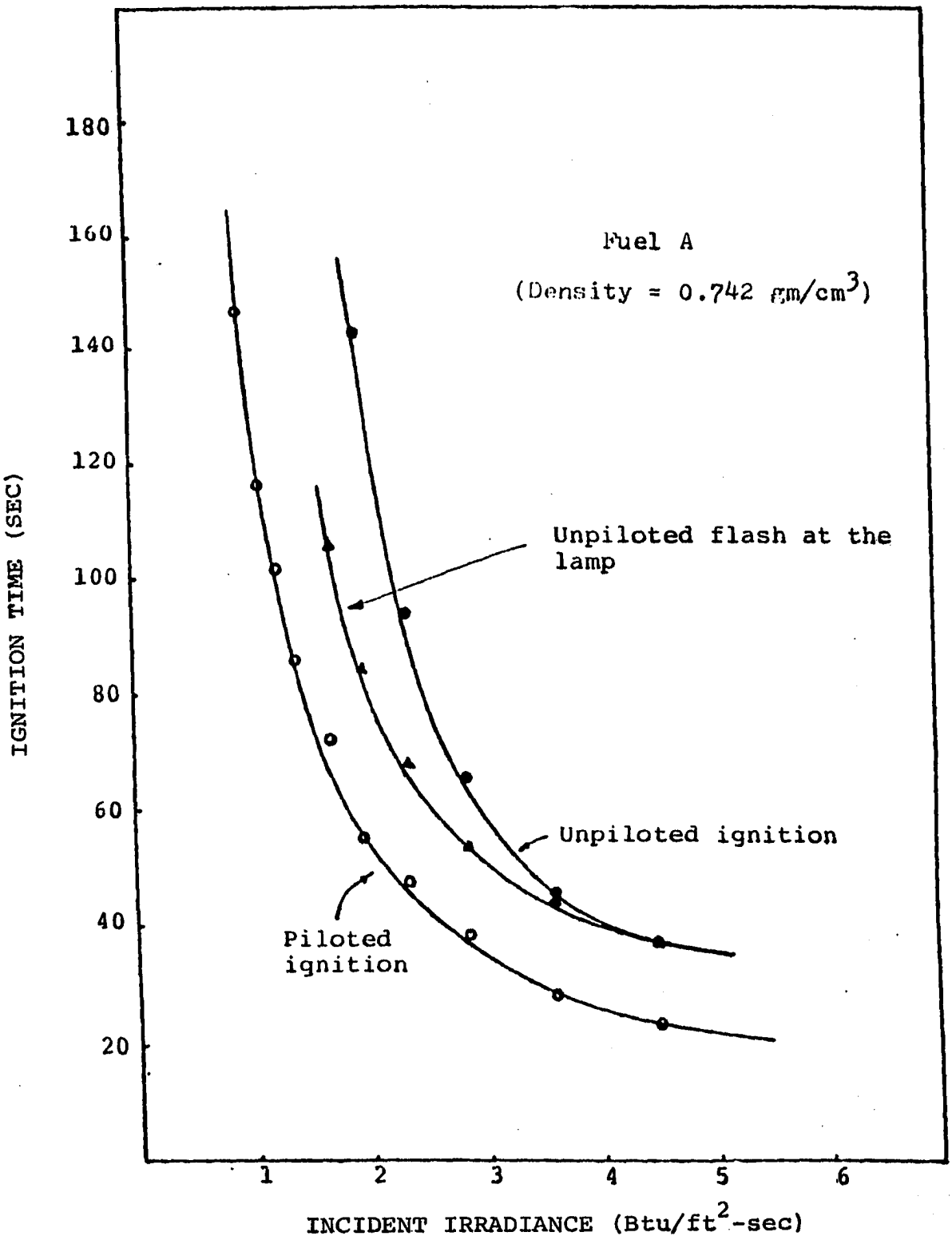

Figure 4-9 Relationship Between Incident Irradiance and Ignition Time for Both Piloted and Unpiloted Ignition for Fuel A

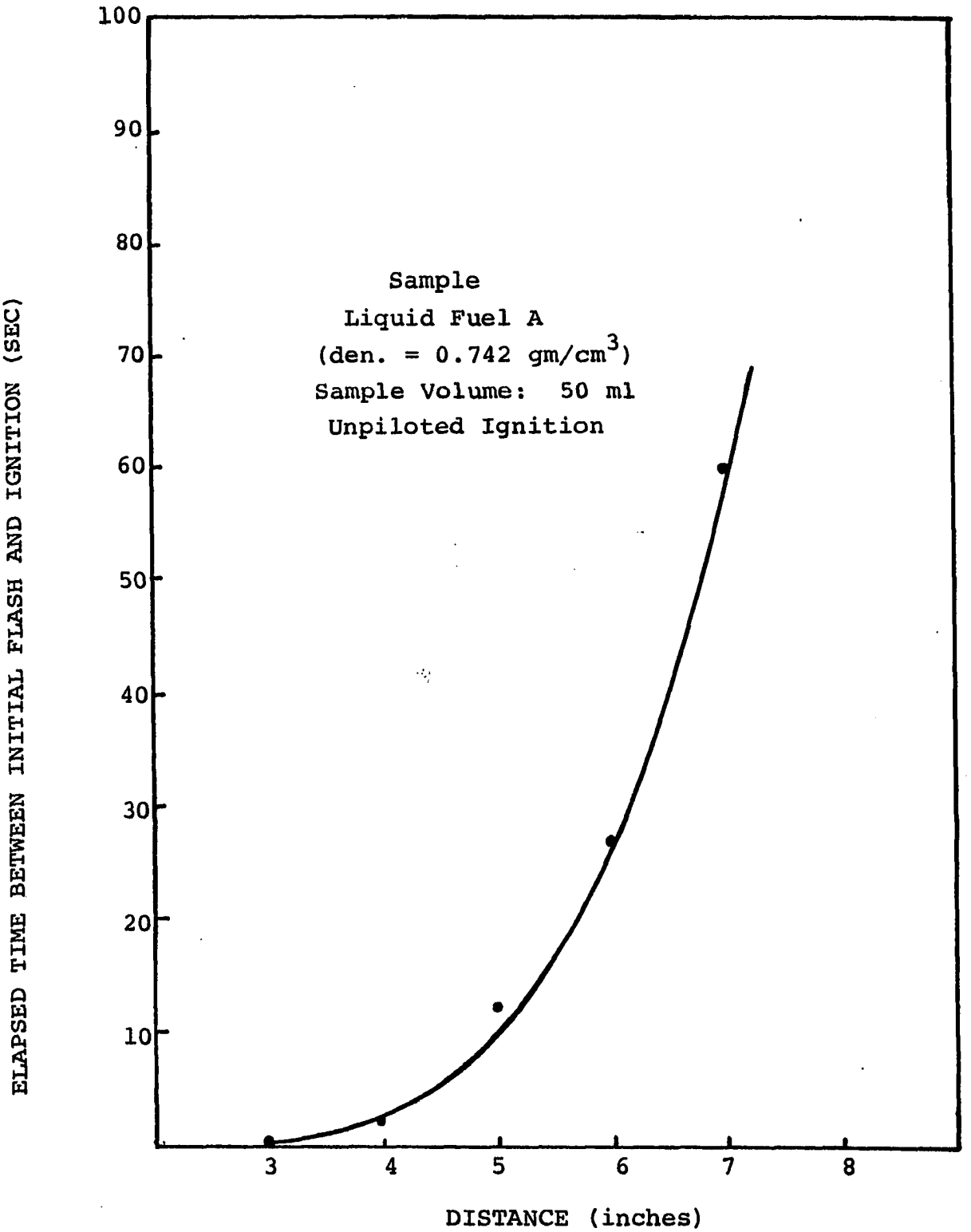

Figure 4-10-A. Relationship Between the Ignition Source Distance and Elapsed Time for the Liquid Surface to Ignite for Fuel A

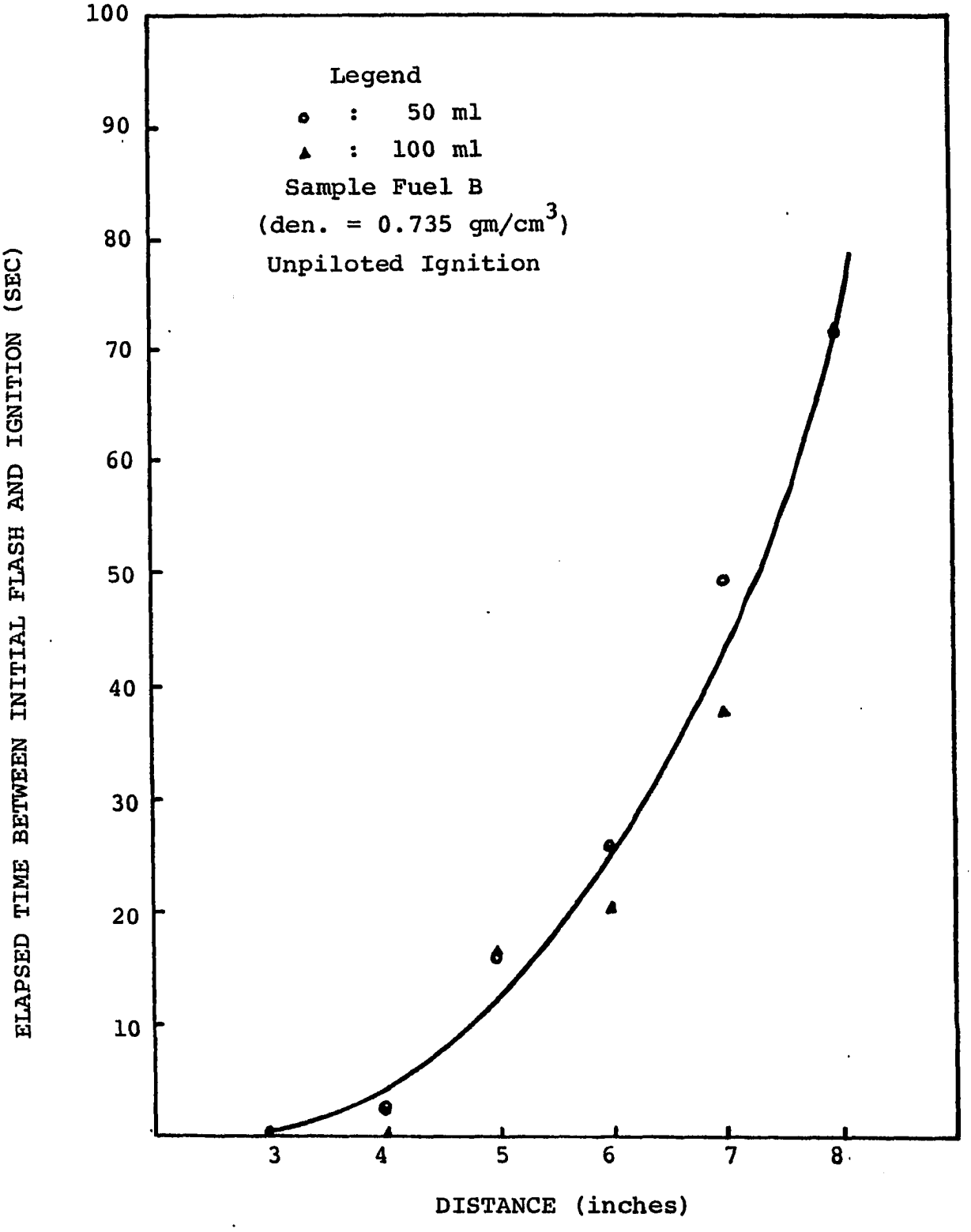

Figure 4-10-B. Relationship Between the Ignition Source Distance and Elapsed Time for the Liquid Surface to Ignite for Fuel B

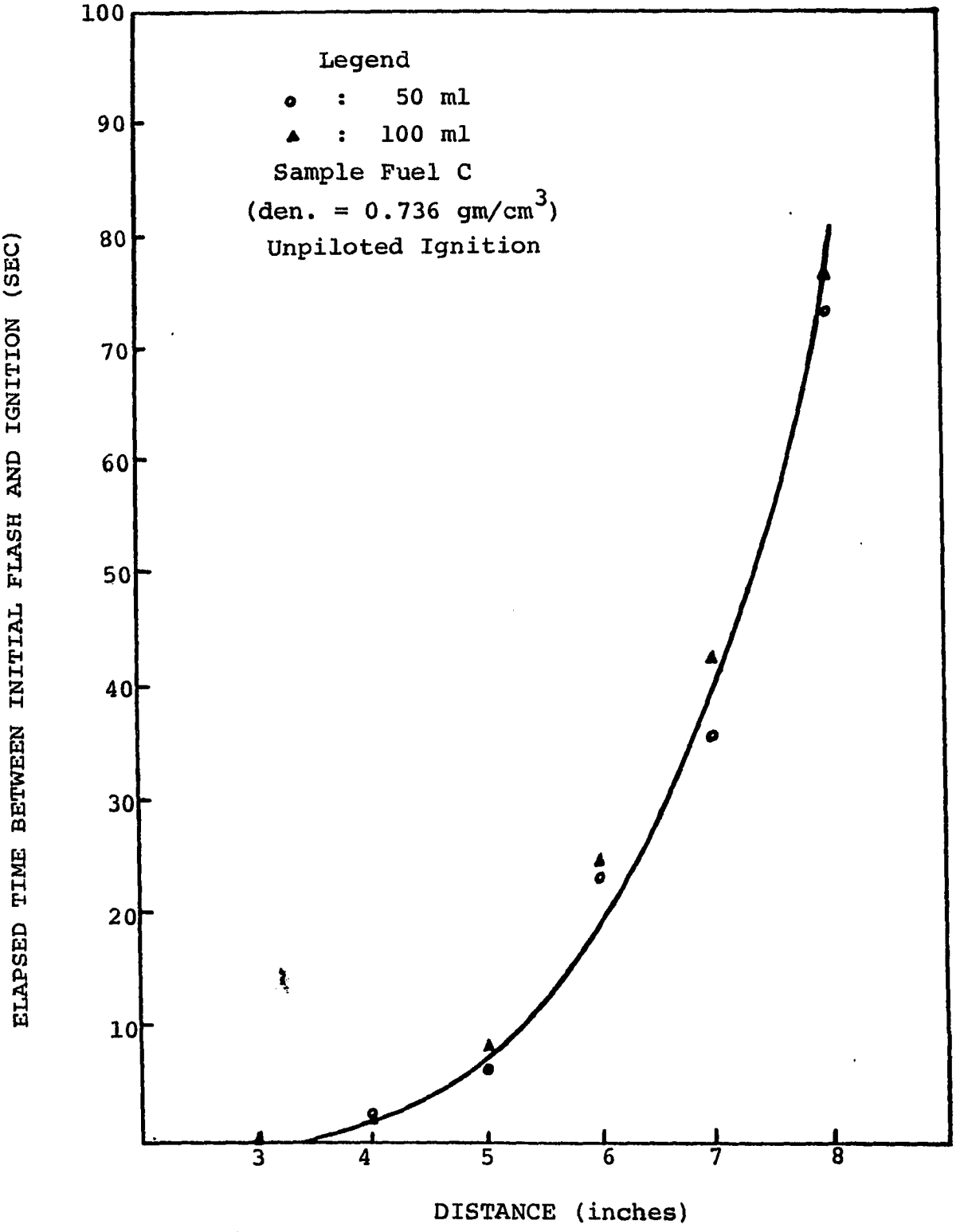

Figure 4-10-C. Relationship Between the Ignition Source Distance and Elapsed Time for the Liquid Surface to Ignite for Fuel C

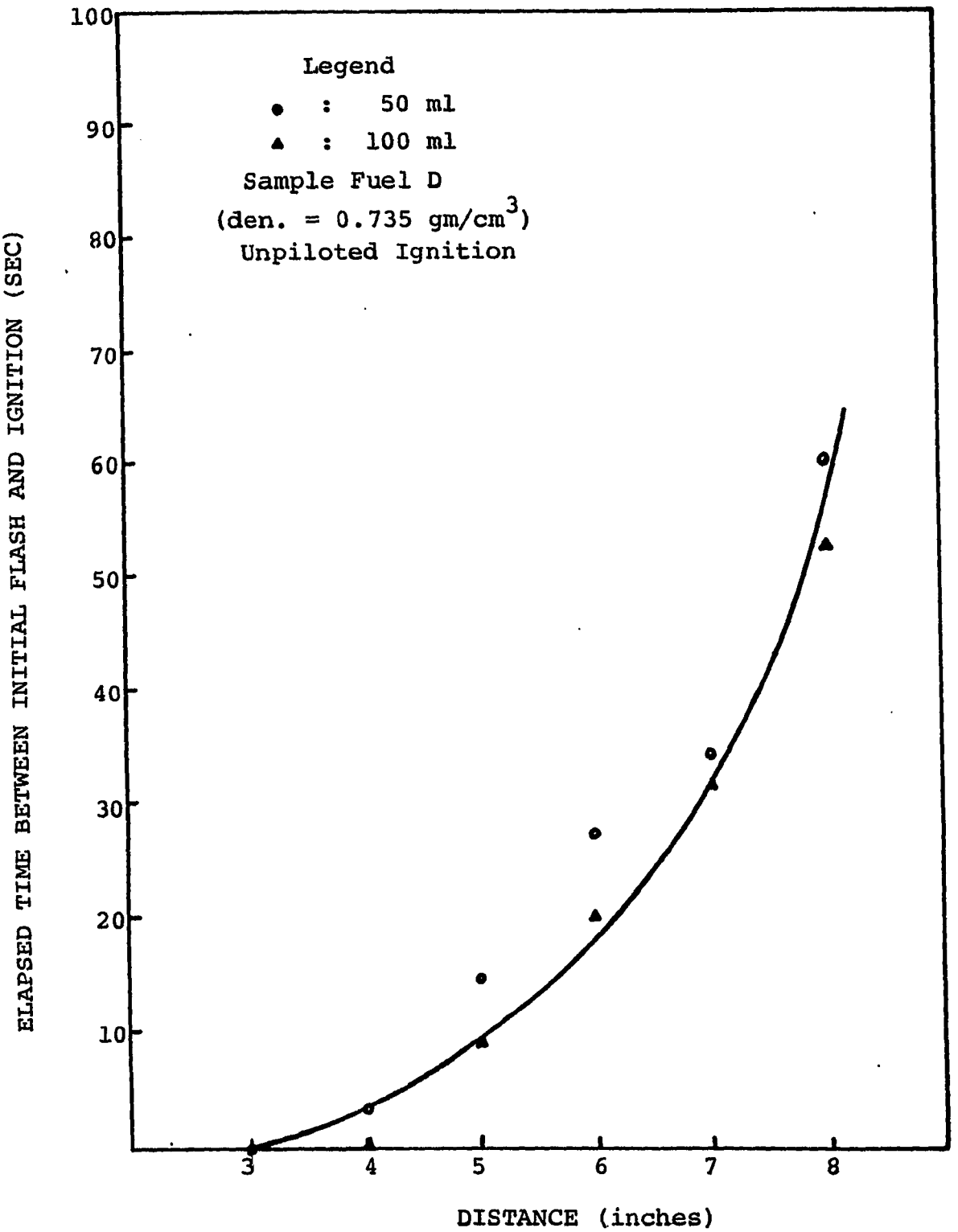

Figure 4-10-D. Relationship Between the Ignition Source Distance and Elapsed Time for the Liquid Surface to Ignite for Fuel D

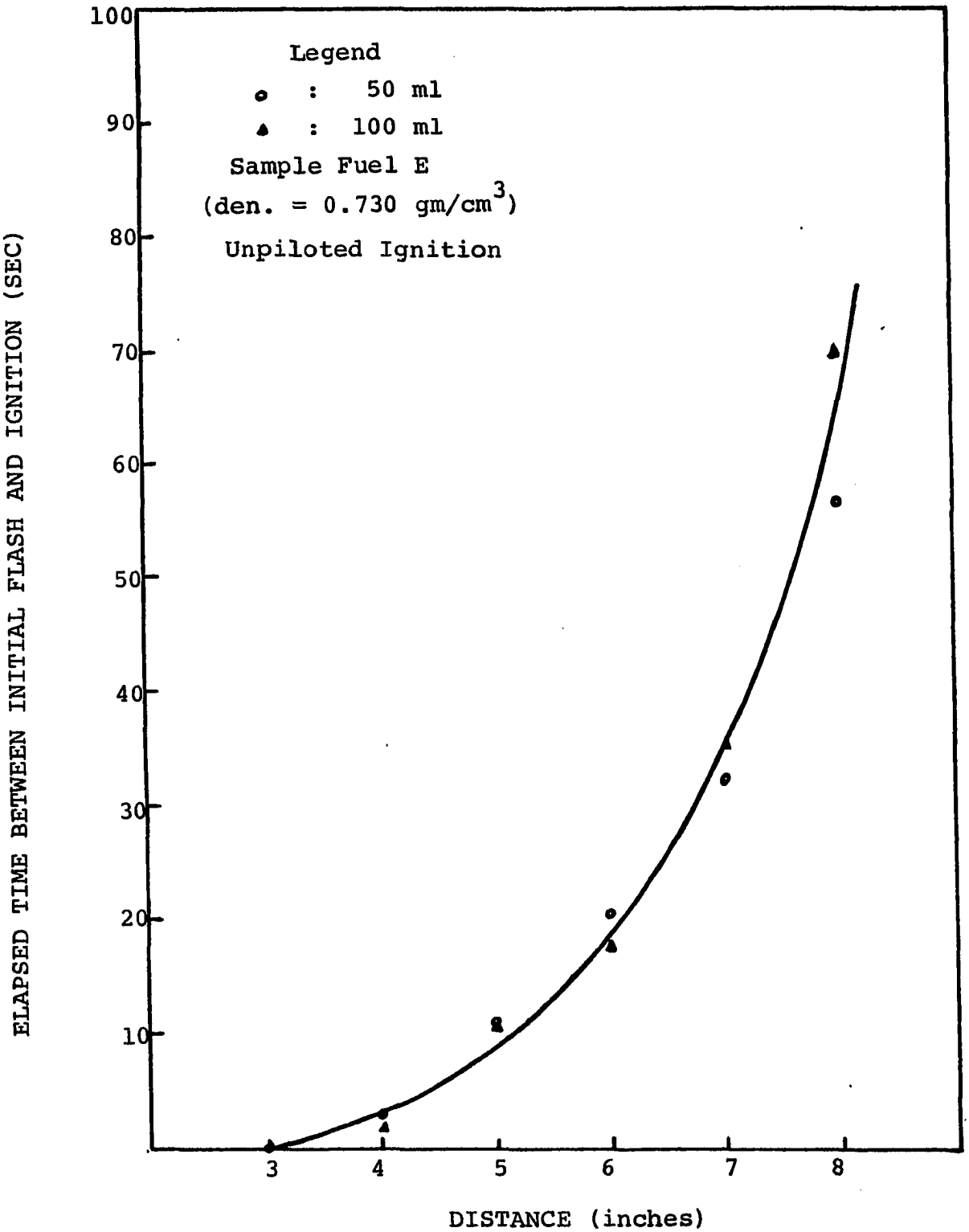

Figure 4-10-E. Relationship Between the Ignition Source Distance and Elapsed Time for the Liquid Surface to Ignite for Fuel E

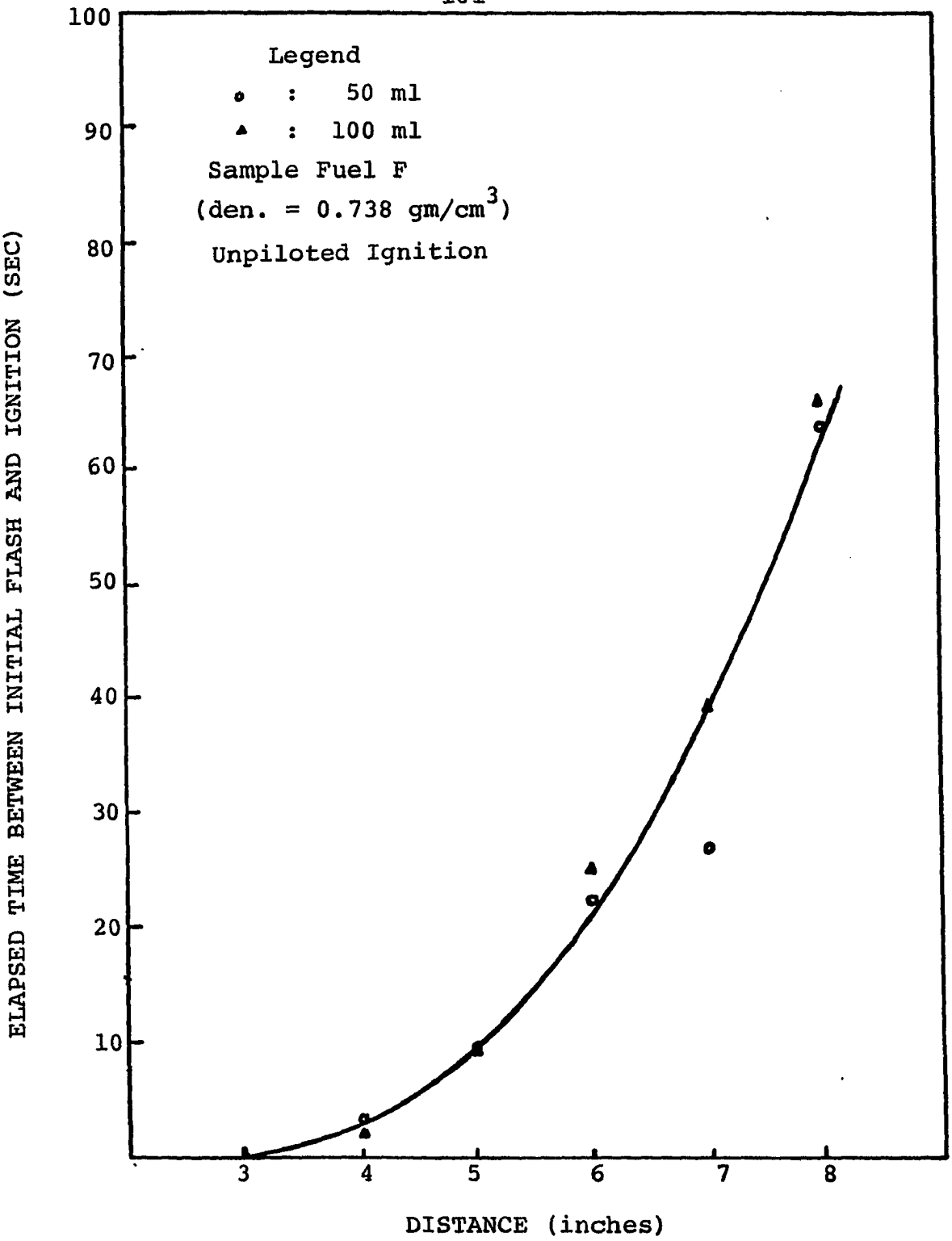

Figure 4-10-F. Relationship Between the Ignition Source Distance and Elapsed Time for the Liquid Surface to Ignite for Fuel F

samples. For distances shorter than three inches (1.62 cm), the propagation seems to be instantaneous. Based on this finding, the propane pilot flame was set at about one inch to 1.5 inches above the liquid surface in piloted ignition tests.

It was observed that the placement of the radiometer in the liquid sample dish affects the ignition time as shown in Table 4-3 and Figure 4-11. The ignition times were longer when the radiometer was protruding into the liquid sample than when it was mounted flush with the bottom of the liquid sample dish. One explanation is that since the radiometer was water cooled, it abstracted heat from the liquid sample via the wetted walls of the radiometer. For this reason, the surface of the radiometer was set flush with the bottom of the sample dish during the ignition measurements. However, for calibration purposes the radiometer was raised (and lowered) in the empty sample dish to simulate various levels of liquid fuel.

Experimental Surface Ignition Temperature

To verify the premise that even though the ignition times vary appreciably with irradiant fluxes, the surface temperature of the liquid at the moment of ignition remains essentially constant, experiments were conducted at different irradiance levels while monitoring the temperature. It was found that the temperature at the surface of the fuel for

TABLE 4-3

COMPARISON OF THE PILOTED IGNITION TIME FOR 100 ML OF TETRADECANE WITH DIFFERENT HEIGHTS OF THE CENTER RADIOMETER

Time or Intensity	Distance of Lamp from Liquid Sample Holder, Inches									
	3	4	5	6	7	8	9	10	11	12
t_i (sec)										
h* = 1"		32.9		51.3		80.8		122.7		174.2
t_i										
h = 11/32	23.9	33.5	42.5	53.7	66.9	80.8	97.4	118.2	140.7	180.7
I	5.60	4.19	3.37	2.70	2.28	1.93	1.62	1.39	1.25	1.13
t_i										
h = 0	23.2	29.8	39.6	47.3	59.2	71.4	86.4	103.0	116.1	141.0
I	5.60	4.19	3.35	2.68	2.25	1.90	1.68	1.39	1.22	1.11

*h represents the height of center radiometer above the bottom of the liquid fuel holder.

I is incident irradiance in Btu/ft^2-sec.

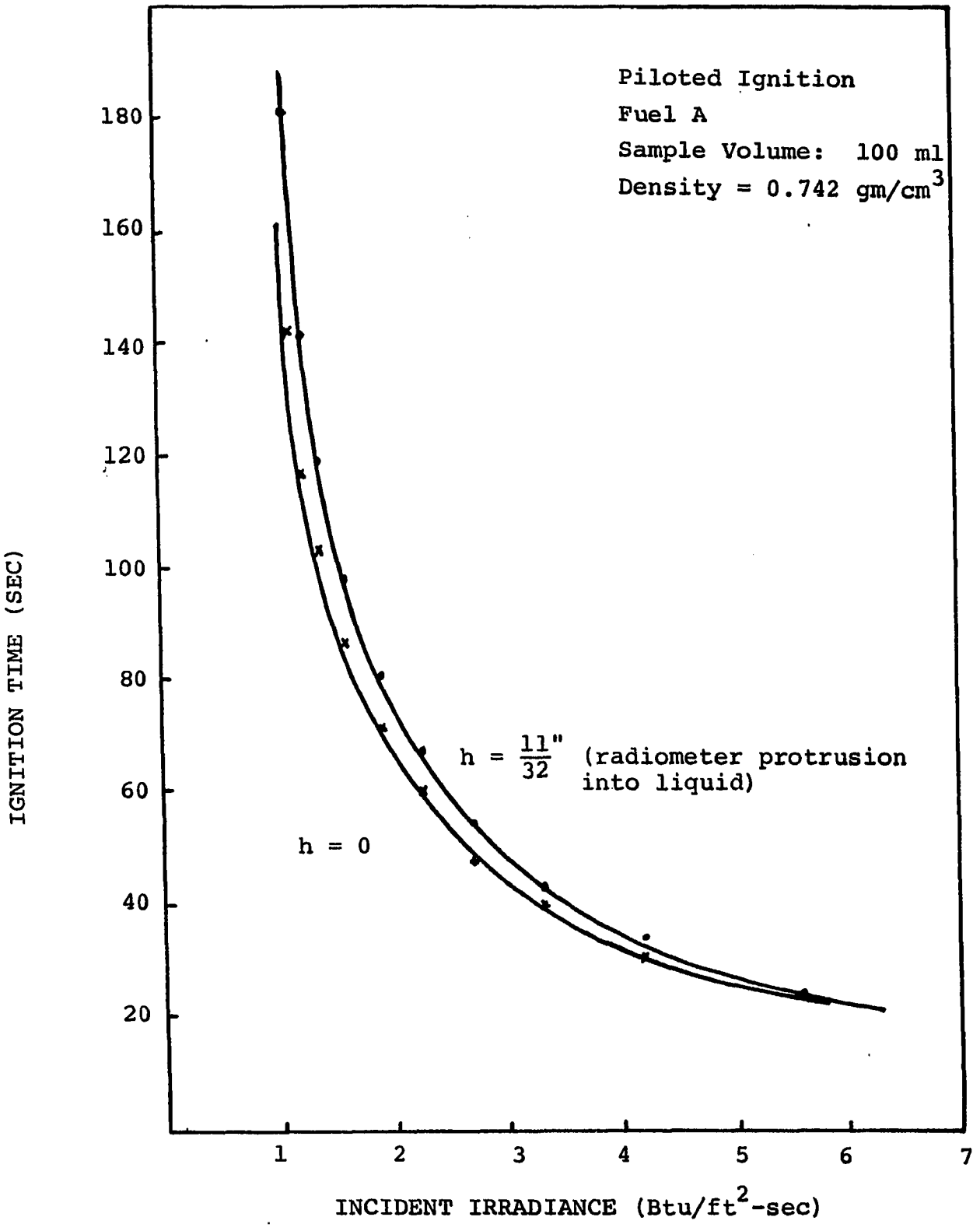

Figure 4-11. Influence of Presence of Radiometer Inside the Liquid on Ignition Time for Fuel A

piloted ignition remained almost constant under various intensities of incident radiant fluxes. On the contrary, in the standard procedure for determining flash points or fire points (ASTM open or closed cups) the flash point temperature represents a bulk average since the fuel sample is stirred. It has been reported that this bulk average is quite sensitive to the rate of heating and consequently the flash point temperature varies accordingly. In this study the surface temperature of the center-positioned radiometer for Fuel A ($n\text{-}C_{14}H_{30}$) was 210°F, compared to the published flash point temperature of 212°F for $n\text{-}C_{14}H_{30}$ {at least from two sources (47, 62)}. The experimental ignition for all fuels are:

Fuel	Observed Ignition Temperature °F
A	210
B	200
C	198
D	199
E	190
F	200

Complete data for the ignition temperature measurements are listed in Tables 4-4-A, 4-4-B, 4-4-C, 4-4-D, 4-4-E and 4-4-F respectively. For the mixtures (Fuel C, D, E and F), the experimental surface ignition temperatures, at the center point of the liquid surface in the sample dish, are close to their individual components, which might be

TABLE 4-4-A

EXPERIMENTAL IGNITION TEMPERATURE OF FUEL A

Volume (ml)	Radiation Flux (cal/cm^2-sec)	Ignition Time (sec)	Ignition Temperature (°F)		
			Center	A	B
		Piloted			
50	--	39.9	211.5	--	--
100	0.34	103.6	213.0	--	--
100	0.46	69.7	207.0	--	--
100	0.518	74.3	218.5	206.5	204.3
100	0.614	60.0	216.5	203.5	201.0
100	0.64	43.9	198.3	--	--
100	0.726	49.0	215.5	202.0	198.0
100	1.01	29.7	206.5	--	--
150	--	48.0	209.0	--	--
		Unpiloted			
50	--	38.9	315.0	--	--
50	--	48.2	311.7	--	--
50	--	56.4	311.7	--	--
50	--	85.1	336.0	--	--
50	--	128.0	390.5	--	--
100	0.71	92.3	334.3	--	--
100	0.785	96.6	328.0	310.5	309.0
100	0.956	68.8	305.0	286.0	282.0
100	1.18	51.8	292.0	269.0	268.5
100	1.56	37.3	281.5	256.5	257.5
150	0.96	71.9	300.5	274.5	273.0
150	1.17	49.2	282.0	248.3	252.3
150	1.57	39.6	286.5	253.0	252.3
200	0.785	96.8	315.5	291.0	276.5
200	0.951	66.8	297.0	268.0	251.3
200	1.17	47.1	279.0	250.5	238.0
200	1.56	36.7	285.0	252.5	235.0

A----0--------B

1.03 2.14

(cm) (cm)

TABLE 4-4-B

EXPERIMENTAL IGNITION TEMPERATURE OF FUEL B

Volume (ml)	Radiation Flux (cal/cm^2-sec)	Ignition Time (sec)	Ignition Temperature (°F)		
			Center	A	B
		Piloted			
50	0.492	57.2	208.0	--	--
100	0.506	61.1	203.5	--	--
100	0.508	62.4	198.5	187.0	186.0
100	0.602	49.1	200.0	--	--
100	0.604	54.4	202.5	190.5	189.0
100	0.717	39.3	197.0	--	--
100	0.721	42.9	200.0	180.0	184.5
100	0.895	32.8	199.0	--	--
150	0.548	70.6	203.0	--	--
150	0.649	56.3	198.5	--	--
150	0.801	46.4	200.5	--	--
150	0.988	36.2	200.0	--	--
200	0.55	59.7	197.5	--	--
200	0.658	53.2	201.5	--	--
200	0.801	44.4	204.0	--	--
		Unpiloted			
100	0.672	137.7	348.5	335.0	335.5
100	0.778	91.2	312.0	297.7	297.3
100	0.944	62.7	289.5	272.0	271.7
100	0.949	64.7	291.0	--	--
100	1.17	49.8	295.0	--	--
100	1.18	51.8	291.5	271.7	270.5
100	1.56	38.4	279.0	256.5	255.7
100	1.56	38.6	294.0	--	--
150	1.04	63.0	291.0	--	--
150	1.27	48.0	279.5	--	--
150	1.62	38.0	284.5	--	--
200	0.848	80.8	289.5	--	--
200	1.03	64.3	292.0	--	--
200	1.27	46.9	280.5	--	--
200	1.64	37.7	283.0	--	--

A----0--------B

1.03 2.14

(cm) (cm)

TABLE 4-4-C

EXPERIMENTAL IGNITION TEMPERATURE OF FUEL C

Volume (ml)	Radiation Flux (cal/cm^2-sec)	Ignition Time (sec)	Ignition Temperature (°F)		
			Center	A	B
		Piloted			
100	0.600	50.5	195.7	182.3	180.5
100	0.724	43.6	201.7	187.0	186.3
100	0.892	34.1	198.0	182.3	182.0
		Unpiloted			
100	0.773	86.4	301.0	283.5	278.5
100	0.949	64.2	288.3	269.5	267.0
100	1.17	48.4	283.5	262.0	260.0
100	1.56	37.9	284.3	259.7	260.5

TABLE 4-4-D

EXPERIMENTAL IGNITION TEMPERATURE OF FUEL D

Volume (ml)	Radition Flux (cal/cm^2-sec)	Ignition Time (sec)	Ignition Temperature (°F)		
			Center	A	B
		Piloted			
100	0.597	56.1	203.0	190.0	191.5
100	0.731	45.0	200.0	186.0	187.0
100	0.909	34.7	196.3	181.5	183.0
100	1.12	26.7	196.3	180.0	182.0
		Unpiloted			
100	0.787	99.7	324.7	312.0	305.0
100	0.958	69.0	297.0	278.5	276.5
100	1.18	51.7	287.0	266.5	265.0
100	1.56	39.2	285.0	259.3	255.7

A----0--------B
1.03 2.14
(cm) (cm)

TABLE 4-4-E

EXPERIMENTAL IGNITION TEMPERATURE OF FUEL E

Volume (ml)	Radiation Flux (cal/cm^2-sec)	Ignition Time (sec)	Ignition Temperature (°F)		
			Center	A	B
		Piloted			
100	0.625	50.3	192.7	179.3	179.7
100	0.721	40.4	192.0	177.0	178.5
100	0.895	30.2	186.0	170.7	170.7
100	1.12	24.8	191.5	174.0	175.5
		Unpiloted			
100	0.785	93.7	314.0	296.5	295.5
100	0.949	62.0	279.0	260.0	259.0
100	1.18	50.7	288.7	267.7	265.0
100	1.56	39.0	283.0	258.5	257.0

TABLE 4-4-F

EXPERIMENTAL IGNITION TEMPERATURE OF FUEL F

Volume (ml)	Radiation Flux (cal/cm^2-sec)	Ignition Time (sec)	Ignition Temperature (°F)		
			Center	A	B
		Piloted			
100	0.597	56.1	204.0	188.7	189.7
100	0.726	44.0	197.5	184.0	183.3
100	0.904	34.9	199.0	185.0	184.5
100	1.12	29.0	202.0	185.0	185.5
		Unpiloted			
100	0.775	87.9	299.0	282.6	280.5
100	0.960	69.4	293.7	276.5	275.3
100	1.18	52.3	287.5	267.7	266.5
100	1.57	40.1	278.5	256.5	257.5

A----0--------B
1.03 2.14
(cm) (cm)

expected considering their closeness in chemical and physical properties. In spontaneous ignition studies of organic compounds by Frank and Blackham (27), they indicated that the spontaneous ignition temperatures of n-decane, n-dodecane, n-tetradecane, n-hexadecane and n-octadecane are 234 $\pm$ 2°F. The ignition temperatures observed in this study ranged from 190°F for Fuel E to 210°F for Fuel A. Fuel E has a higher fraction of volatile components (71.6% of n-dodecane) than other fuel samples, so it has the lowest experimental ignition temperature. At the other extreme Fuel F has the highest ignition temperature since it has the highest fraction of lower volatiles among the four fuel samples which are mixtures of components.

For unpiloted ignition, the ignition temperatures were not only much higher (approximately more than 100°F), than the piloted ignitions, but they also varied considerably with distance between the lamp and liquid surface. (As mentioned earlier the lamp acted as an ignition source in the case of unpiloted ignition, causing the flame to propagate back to the liquid surface.)

In Tables 4-4-A through 4-4-F, the variation in the center are shown. All three thermocouples were always just below the liquid surface. Positon A is 1.03 cm away from the center, and position B is 2.14 cm on the other side of the center. They are located in a straight line which is parallel to the colinear with the long-axis of the lamp. Two conclusions are drawn:

1. The lamp's radiation is not uniform; furthermore the heat loss rate is higher in the zones near the edges of the dish. Consequently, the center position always gives highest temperature readings.

2. The temperature readings from position A and position B indicate that in some cases position A gives higher readings than position B, and in other cases the reverse is true. The readings at A and B are affected by complex wall heating effects and preheating times such that it is difficult to anticipate which reading will be higher.

Irradiant Absorption of Liquids

To determine the amount of radiation absorbed by the liquid as a function of depth experiments were conducted in which the height of the liquid level above the radiometer was varied. Three fuel samples, fresh Fuel A, recycled Fuel A (with a little yellowish color) and fresh Fuel B were used. The results are tabulated in Tables 4-5 and are plotted in Figures 4-12-A, 4-12-B, 4-12-C and 4-12-D. All three fuels give similar results. For example, the amount of radiative energy absorbed by the liquid increases rapidly with increased depth of penetration into the liquid up to the first 3/8 inch (1 cm) but thereafter levels off. At a depth of 3/4 inch the amount of radiation that has been absorbed is almost identical to the one-inch depth. The fractions of incident energy absorbed as a function of distance between the liquid surface and the radiation lamp in inches (depth of

TABLE 4-5

RADIATION ABSORPTION BY LIQUID FUEL A AND FUEL B

Height (cm)	Species: $n\text{-}C_{14}H_{30}$ (Fresh)				Species: $n\text{-}C_{14}H_{30}$ (Recycled)				Species: $n\text{-}C_{13}H_{28}$ (Fresh)			
	Categories											
	B.T.	Filled	A.A.	F.A.	B.T.	Filled	A.A.	F.A.	B.T.	Filled	A.A.	F.A.
0.080	.809	.663	.146	.180	.974	.831	.143	.147	.809	.629	.180	.222
0.159	.806	.571	.235	.292	.967	.658	.309	.320	.806	.583	.223	.279
0.318	.802	.534	.265	.330	.964	.596	.368	.382	.802	.547	.225	.318
0.476	.792	.474	.318	.402	.957	.544	.413	.432	.792	.493	.299	.378
0.635	.789	.433	.356	.451	.950	.516	.434	.457	.789	.456	.333	.422
0.794	.787	.405	.382	.485	.936	.480	.456	.487	.787	.427	.360	.457
0.953	.777	.374	.403	.519	.924	.447	.477	.516	.777	.401	.376	.484
1.111	.773	.355	.418	.541	.915	.423	.492	.538	.773	.376	.397	.514
1.429	.767	.330	.437	.570	.907	.392	.510	.562	.767	.343	.424	.553
2.064	.743	.291	.452	.608	.869	.345	.524	.603	.743	.302	.441	.594
2.699	.721	.260	.461	.639	.839	.309	.530	.630	.721	.272	.449	.623
3.493	.699	.235	.464	.664	--	--	--	--	.699	.241	.458	.655

B.T. Blank Test (Btu/ft^2-sec). A.A. Amount Absorbed (Btu/ft^2-sec).
F.A. Fraction Absorbed.
Filled Filled with Liquid Fuel to the Rim's Absorption (Btu/ft^2-sec).
Height Distance Between the Liquid Surface and the Radiometer (cm).

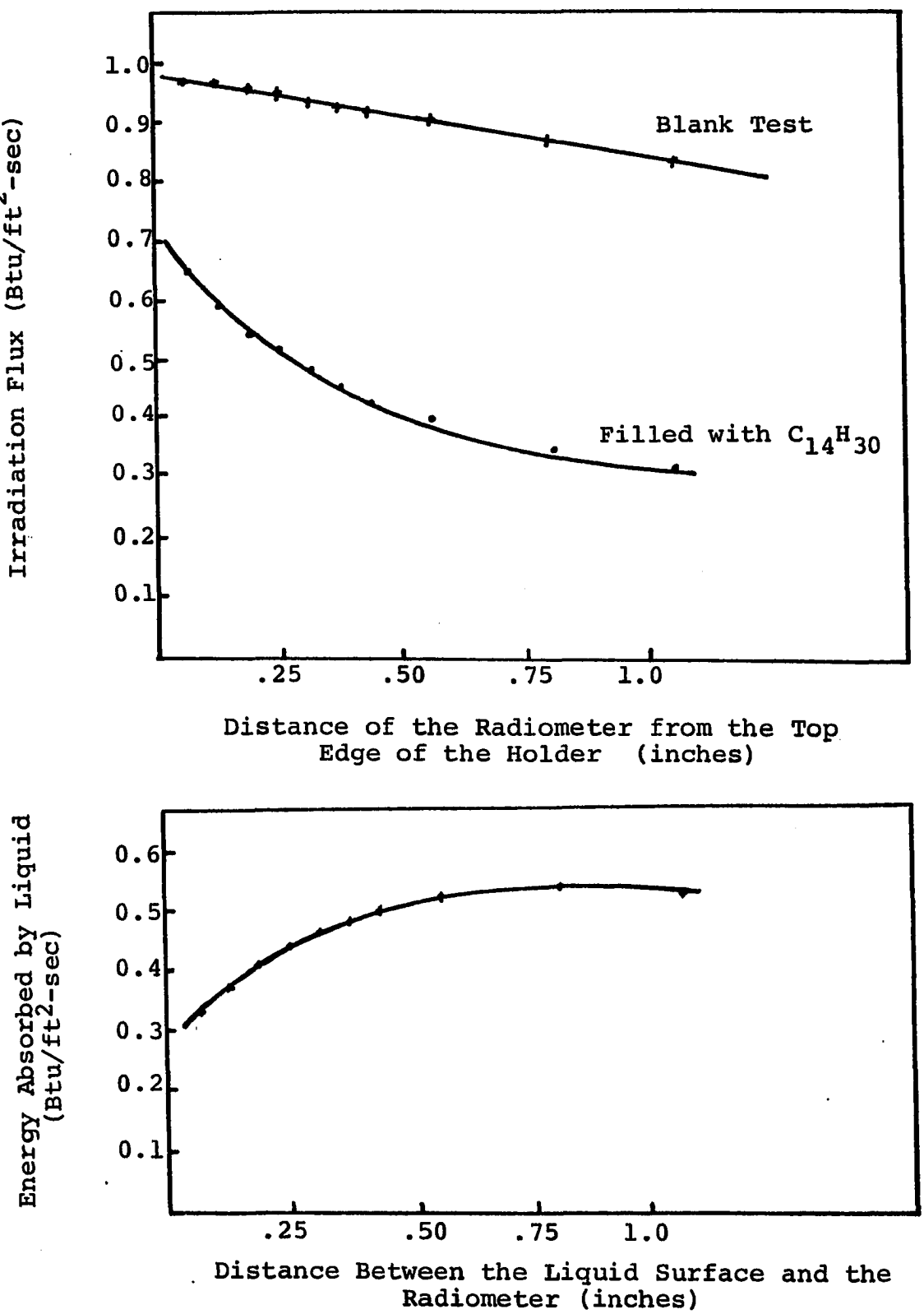

Figure 4-12-A. The Variation of Radiation Absorbed by Fuel A (Recycled) with Liquid Depth

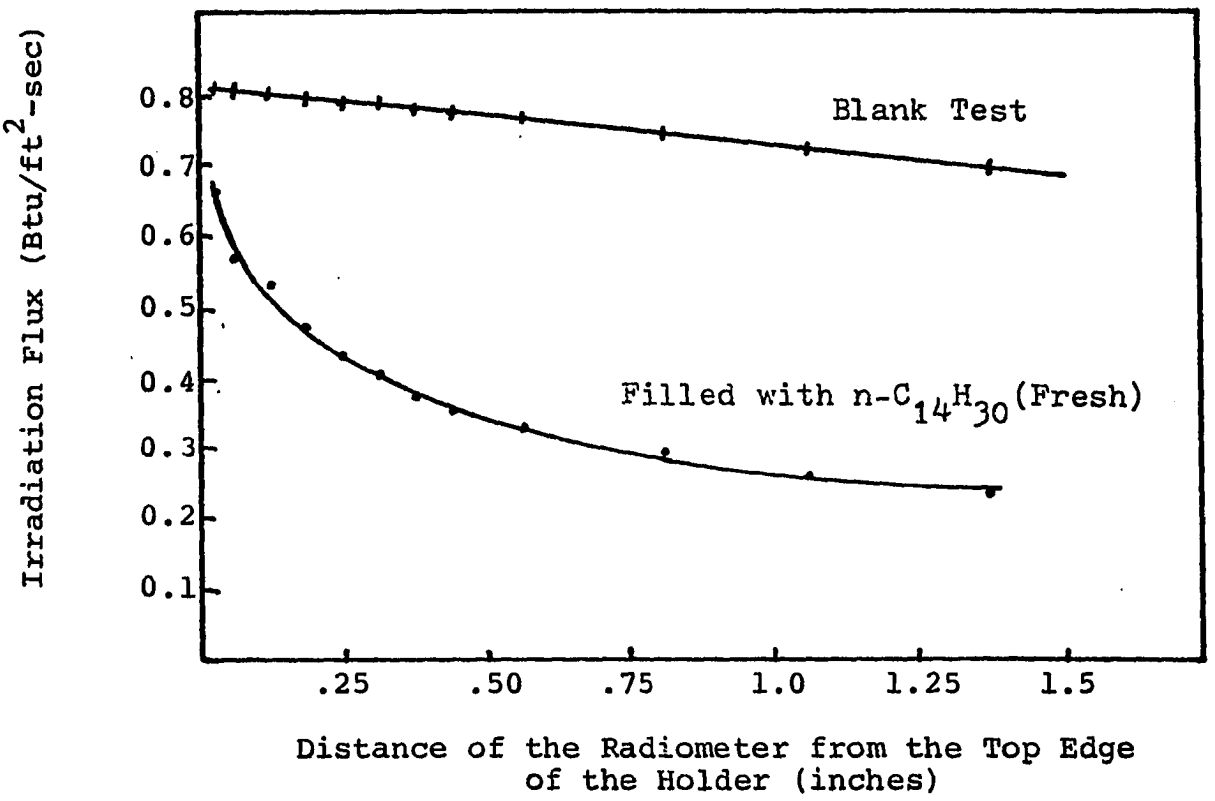

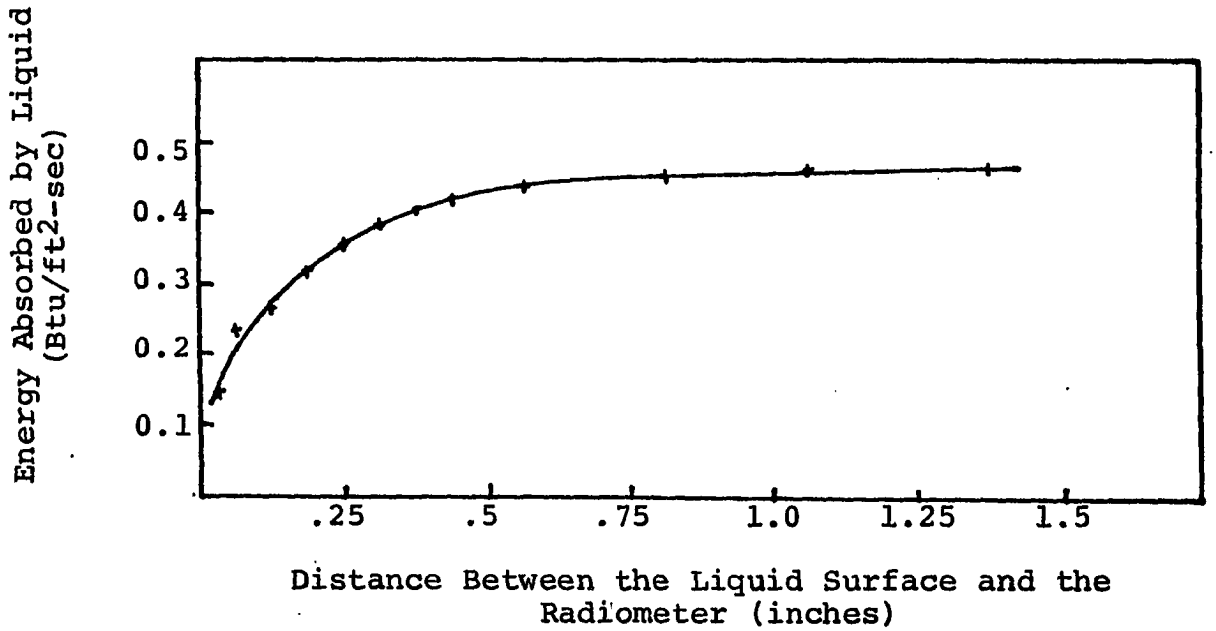

Figure 4-12-B. The Variation of Radiation Absorbed by Fuel A (Fresh) with Liquid Depth

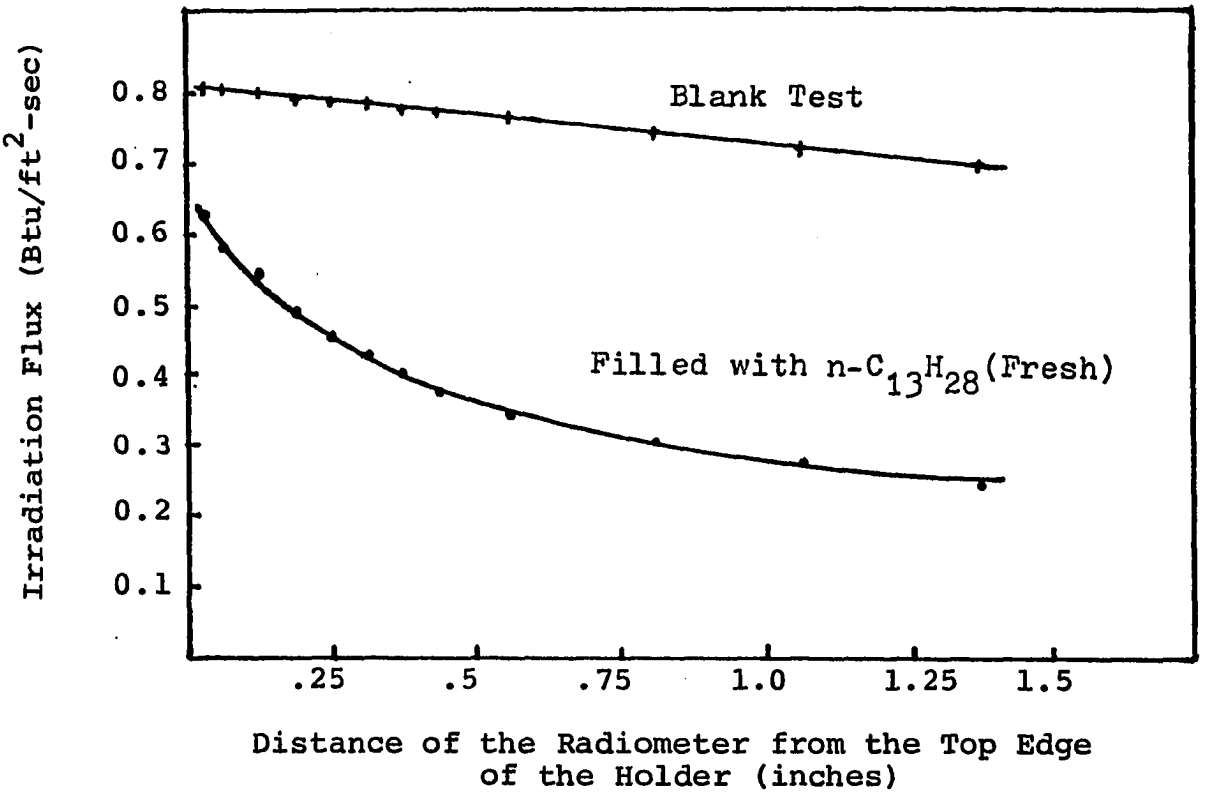

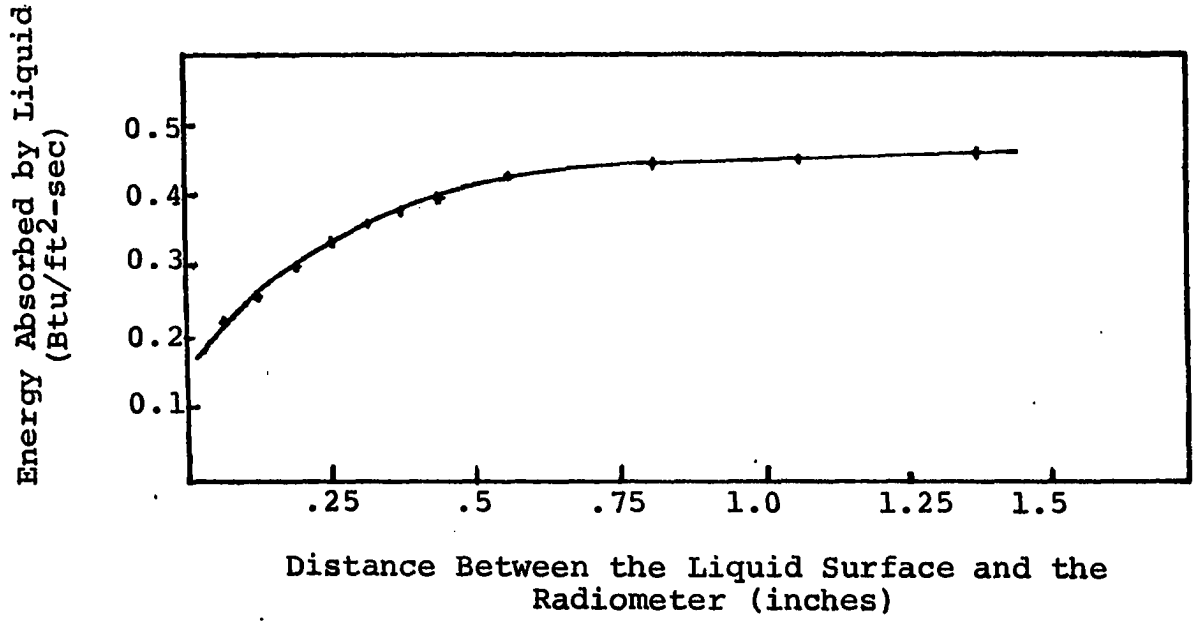

Figure 4-12-C. The Variation of Radiation Absorbed by Fuel B (Fresh) with Liquid Depth

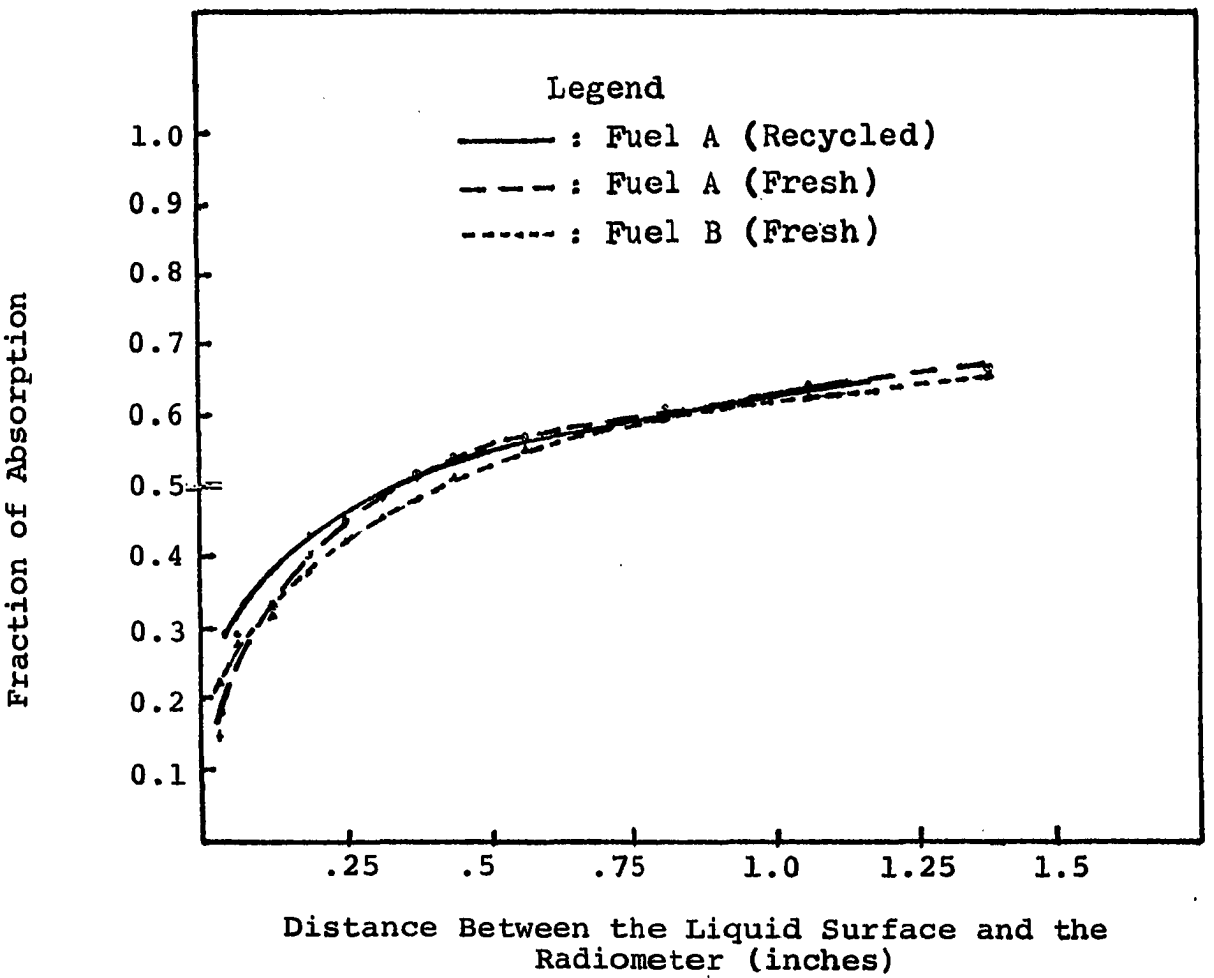

Figure 4-12-D. The Net Fraction of Radiation Absorbed by the Fuels with Liquid Depth

penetration) are shown in Figure 4-12-D for all three fuels. The similarities are not unexpected considering the closeness in molecular structures of n-tridecane and n-tetradecane. The fact that the recycled fuel shows almost identical absorption characteristics to fresh Fuel A and B justifies its use in experimentation. Thus, the virtual identical absorption characteristics of these fuels adds to the validation of why Fuels B, C, D, E and F have similar minimum incident radiative fluxes for ignition which are closely related to the center-point, piloted ignition temperature, and demonstrate the same trends for ignition time as a function of incident irradiation.

Table 4-6, showing the relationship between the thickness of fuel bed and the radiative absorption, was obtained by curve fitting the data in Table 4-5 and by extrapolating to a zero thickness of liquid bed, i.e. on the surface. From this result it appears that almost 17.4 percent of the incident irradiance was reflected away at the liquid surface and approximately 40 percent of the incident irradiance was absorbed by the fuel bed down to a depth of penetration of 1.66 cm (corresponding to 200 ml of liquid in the sample dish). It is evident from Figure 4-12-D that further increases in the depth of penetration would not increase the fraction absorbed. The absorption of infrared radiation depends on the increase in the energy of vibration or rotation associated with the covalent bond, provided that such an increase results in a change in the dipole moment of

TABLE 4-6

RADIATION ABSORPTION AND FUEL BED THICKNESS

Bed Thickness (cm)	Avg. Fraction* of Absorption	Net Absportion** Fraction
1.66	0.5782	0.4046
1.25	0.5506	0.3770
0.83	0.4901	0.3166
0.42	0.3759	0.2023
0.00	0.1736	0.0000

*This is the curve fitting result based on the data given in Figure 4-12-D.

**The net absorption fraction is computed by taking the difference between the average fraction of absorption at the specified depth and the average fraction of absorption at zero depth. Note that the average fraction of absorption at zero depth represents the reflection at the surface since the absorption at the surface is zero.

the molecules for normal paraffins. The absorption bands associated with the modes are given in Table 3-1. The lamp is assumed to be a black-body with a filament temperature of 2450°K (35) and a continuous emission spectra. From these assumptions, the band absorption can be calculated by using approximate equations (Equations II-17, II-18 and II-19) from Chapter II. The calculated absorption fraction is about 33.7 percent, compared to the experimental result of 40 percent; the discrepancy is not unreasonable.

Calculated Ignition Temperature

An exact mathematical model is not available for calculating adequately the surface ignition temperature for this small scale liquid ignition test. This contention will be demonstrated by comparing the results of applying two models discussed in Chapter II with experimental measurements obtained in this work. The designation, Model A, is assigned to the pure conduction model (Equation II-31) from Carslaw and Jaeger and Model B to the convection model from Viskanta and Grosh or Noble (substituting the effective thermal conductivity, Equation II-25, for the true thermal conductivity in Equation II-31, thereby including the convective effect). Since the radiative energy absorption mechanism for liquids is not well understood, it is a major problem to determine how much energy is actually absorbed in the liquid fuel. The experimental radiative energy absorptions and reflection for the fuels used in this study were presented in an earlier

section of this chapter. Based on those results, three hypothetical energy inputs were chosen for these two models. They are: case (i), all the radiative energy from the tungsten lamp is absorbed by the fuel bed, case (ii), all of the energy is absorbed except for the 17.4 percent which is reflected from the liquid surface, case (iii), only the net absorption corresponding to the fuel bed thickness is considered as given in Table 4-6. Comparison of the six sets of (the three cases for each of Models A and B) calculated surface ignition temperatures with the experimental results is presented in Table 4-7 from which the following conclusions are drawn:

1. The results of Model B which includes radiation penetrating into the liquid are much better than that of Model A which takes into account only surface absorption--not unexpected.

2. For Model A, the results of the case iii are better than other two cases. In Model B, case ii gives better results than others. Case i of Model B gives a value which is too high to be real and case iii gives unrealistically low results--again as would be expected.

3. In case ii of Model B, the calculated temperature for piloted ignition gives better agreement with experiment than unpiloted ignition does. Further, for piloted ignition, a sample volume of 100 ml gives closer correspondence

TABLE 4-7

COMPARISONS OF THE CALCULATED AND MEASURED MAXIMUM SURFACE TEMPERATURES

					C.J. APPROACH		V.G. OR N. APPROACH			C.J. APPROACH		V.G. OR N. APPROACH			C.J. APPROACH		V.G. OR N. APPROACH		
FUEL	VOL (ML)	EX.TI (SEC)	EX.TE DEG.F	FLUX	CA.TE DEG.F	ERROR %	CA.TE DEG.F	ERROR %	FLUX	CA.TE DEG.F	ERROR %	CA.TE DEG.F	ERROR %	FLUX	CA.TE DEG.F	ERROR %	CA.TE DEG.F	ERROR %	P. OR U.
A	100.	103.6	213.0	0.34	715.3	235.8	283.2	33.0	0.28	572.1	168.6	215.1	1.0	0.11	223.5	4.9	86.7	-59.3	(P.)
A	100.	69.7	207.0	0.46	787.1	280.2	270.9	30.9	0.38	634.1	206.3	207.5	0.2	0.15	250.2	20.9	86.7	-58.1	(P.)
A	100.	74.3	218.5	0.52	905.3	314.3	310.6	42.1	0.43	726.4	232.4	234.9	7.5	0.16	279.5	27.9	91.2	-58.3	(P.)
A	100.	60.0	216.5	0.61	960.3	343.5	305.7	41.2	0.51	773.2	257.1	232.3	7.3	0.19	299.0	38.1	91.7	-57.6	(P.)
A	100.	43.9	198.3	0.64	862.8	335.1	257.2	29.7	0.53	700.0	253.0	199.5	0.6	0.20	279.2	40.8	87.4	-55.9	(P.)
A	100.	49.0	215.5	0.73	1021.9	374.2	303.7	40.9	0.60	825.2	282.9	231.7	7.5	0.23	320.1	48.5	92.7	-57.0	(P.)
A	100.	29.7	206.5	1.01	1101.8	433.6	285.8	38.4	0.83	895.9	333.9	221.6	7.3	0.32	352.4	70.7	94.1	-54.4	(P.)
A	100.	92.3	334.3	0.71	1350.9	304.1	469.9	40.6	0.59	1071.9	220.7	343.9	2.9	0.22	386.3	15.6	107.4	-67.9	(P.)
A	100.	96.6	328.0	0.79	1556.6	374.6	555.8	69.4	0.65	1230.1	275.0	403.0	22.9	0.25	433.5	32.2	116.7	-64.4	(U.)
A	100.	68.8	305.8	0.96	1598.0	424.0	502.2	64.6	0.78	1273.2	317.4	367.6	20.5	0.30	460.1	50.8	113.1	-62.9	(U.)
A	100.	51.8	292.0	1.18	1707.2	484.7	483.7	65.6	0.98	1367.5	368.3	356.4	22.1	0.37	500.8	71.5	113.4	-61.2	(U.)
A	100.	37.3	281.5	1.56	1907.8	577.7	482.4	71.4	1.29	1535.9	445.6	357.9	27.2	0.49	568.2	101.9	116.9	-58.5	(U.)
A	150.	71.9	300.5	0.96	1638.9	445.4	399.3	32.9	0.79	1324.5	340.8	300.1	-0.1	0.36	589.6	96.2	122.3	-59.3	(U.)
A	150.	49.2	282.0	1.17	1651.8	485.7	368.8	30.5	0.97	1341.9	375.8	280.9	-0.4	0.44	605.4	114.7	121.4	-56.9	(U.)
A	150.	39.6	286.5	1.57	1976.1	589.8	410.5	43.3	1.30	1607.2	461.0	313.4	9.4	0.59	723.3	152.5	133.1	-53.6	(U.)
A	200.	96.8	315.5	0.79	1558.1	393.8	353.9	12.2	0.65	1264.7	300.8	269.6	-14.6	0.32	610.4	93.5	123.2	-61.0	(U.)
A	200.	66.8	297.0	0.95	1567.7	427.8	331.4	11.6	0.79	1278.1	330.3	256.4	-13.7	0.38	623.5	109.9	123.3	-58.5	(U.)
A	200.	47.1	279.0	1.17	1617.8	479.9	326.6	17.1	0.97	1323.2	374.3	256.2	-8.2	0.47	650.0	133.0	127.6	-54.3	(U.)
A	200.	36.7	285.0	1.56	1894.5	564.7	363.0	27.4	1.29	1550.9	444.2	285.3	0.1	0.63	760.3	166.8	140.7	-50.6	(U.)
B	50.	57.2	208.0	0.49	771.6	270.9	401.2	92.9	0.41	601.1	189.0	295.0	41.8	0.10	151.6	-27.1	76.7	-63.1	(P.)

B	100.	61.1	203.5	0.51	812.3	299.2	268.3	31.8	0.42	655.7	222.2	206.1	1.3	0.16	259.2	27.4	87.0	-57.2	(P.)
B	100.	62.4	198.5	0.51	823.2	314.7	273.3	37.7	0.42	664.0	234.5	209.6	5.6	0.16	261.7	31.8	87.6	-55.9	(P.)
B	100.	49.1	200.0	0.60	862.3	331.1	269.3	32.6	0.50	698.1	249.1	204.8	2.4	0.19	276.8	38.4	87.8	-56.1	(P.)
B	100.	54.4	202.5	0.60	907.2	348.0	284.7	40.6	0.50	732.5	261.7	218.0	7.7	0.19	286.8	41.6	89.7	-55.7	(P.)
B	100.	39.3	197.0	0.72	914.8	364.4	263.2	33.6	0.59	742.7	277.0	204.2	3.6	0.23	295.2	49.8	88.9	-54.9	(P.)
B	100.	42.9	200.0	0.72	958.1	379.0	279.3	39.7	0.60	776.1	288.0	215.2	7.6	0.23	302.4	52.7	90.5	-54.8	(P.)
B	100.	32.8	195.0	0.90	1034.7	419.9	278.8	40.1	0.74	840.8	322.5	216.1	8.6	0.28	331.6	66.7	92.3	-53.6	(P.)
B	150.	70.6	203.0	0.65	935.6	360.9	253.3	24.8	0.45	762.0	275.4	198.1	-2.4	0.21	355.0	74.9	97.8	-51.8	(P.)
B	150.	56.3	198.5	0.65	986.0	396.7	253.0	27.4	0.54	804.9	305.5	199.1	0.3	0.24	376.0	89.4	99.6	-49.8	(P.)
B	150.	46.4	200.5	0.80	1097.5	447.4	266.6	33.0	0.66	896.6	347.2	210.0	4.7	0.30	417.4	108.2	104.2	-48.0	(P.)
B	150.	36.2	200.0	0.99	1190.3	495.1	275.1	37.6	0.82	974.1	387.0	217.8	8.9	0.37	452.7	126.8	108.7	-45.7	(P.)
B	200.	59.7	197.5	0.55	866.3	339.6	212.8	7.8	0.45	714.2	261.6	172.5	-12.6	0.22	364.2	64.4	99.0	-49.9	(P.)
B	200.	53.2	201.5	0.66	972.8	382.8	229.3	13.8	0.54	799.6	296.8	185.2	-8.1	0.27	404.9	100.9	104.1	-48.3	(P.)
B	200.	44.4	204.0	0.80	1075.3	427.1	244.3	19.8	0.66	884.1	333.4	197.4	-3.2	0.32	446.0	116.6	109.8	-46.2	(P.)
B	100.	137.7	348.5	0.67	1596.4	358.7	659.1	69.1	0.56	1249.0	258.4	472.8	35.7	0.21	423.3	21.5	125.9	-63.9	(U.)
B	100.	91.2	312.0	0.78	1508.8	383.6	531.2	70.3	0.64	1194.2	282.8	386.3	23.8	0.25	423.9	35.9	114.4	-63.3	(U.)
B	100.	62.7	289.5	0.94	1517.6	424.2	466.4	61.1	0.78	1211.9	318.6	343.3	18.6	0.30	442.5	52.8	109.7	-62.1	(U.)
B	100.	64.7	291.0	0.95	1548.4	432.1	480.2	65.6	0.78	1235.6	324.6	352.7	21.2	0.30	449.3	54.4	111.1	-61.8	(U.)
B	100.	49.8	295.0	1.17	1669.9	466.1	469.2	59.1	0.97	1338.6	353.8	346.4	17.4	0.37	492.0	66.8	111.8	-62.1	(U.)
B	100.	51.8	291.5	1.18	1715.9	488.6	487.7	67.3	0.98	1374.1	371.4	359.2	23.2	0.37	502.7	72.4	113.8	-60.9	(U.)
B	100.	38.4	279.0	1.56	1944.8	597.0	497.2	78.2	1.29	1564.3	460.7	368.1	31.9	0.49	576.8	106.7	118.6	-57.5	(U.)
B	100.	38.6	294.0	1.56	1949.7	863.1	497.0	69.0	1.29	1568.1	433.4	367.6	25.0	0.49	577.9	96.6	118.0	-59.9	(U.)
B	150.	63.0	291.0	1.04	1666.5	473.7	393.9	35.4	0.86	1351.8	364.4	297.3	2.2	0.39	603.8	107.5	122.9	-57.8	(U.)
B	150.	48.0	279.5	1.27	1775.6	535.3	391.1	39.9	1.05	1441.8	415.9	297.7	6.5	0.48	648.2	131.9	126.3	-54.8	(U.)
B	150.	38.0	284.5	1.62	2007.0	605.5	414.2	45.6	1.34	1632.8	473.9	316.4	11.2	0.61	734.9	158.3	134.4	-52.8	(U.)
B	200.	80.8	289.5	0.85	1546.3	434.1	341.9	18.1	0.70	1257.9	334.5	262.6	-9.3	0.34	610.6	110.9	123.3	-57.4	(U.)
B	200.	64.3	292.0	1.03	1670.5	472.1	349.0	19.5	0.85	1361.9	366.3	269.5	-7.7	0.42	662.5	126.9	127.9	-56.2	(U.)
B	200.	46.9	280.5	1.27	1756.2	526.1	350.1	24.8	1.05	1436.3	411.7	273.4	-2.5	0.51	702.2	150.3	133.3	-52.5	(U.)
B	200.	37.7	283.0	1.64	2024.6	615.4	386.3	36.8	1.34	1856.2	485.2	302.3	6.8	0.66	809.1	185.9	146.3	-48.3	(U.)
C	100.	50.6	195.7	0.60	870.1	344.6	269.5	37.7	0.50	704.9	289.7	207.7	6.1	0.19	278.4	42.3	88.3	-54.9	(P.)

C	100.	43.6	201.7	0.72	962.2	380.0	282.7	40.2	0.60	784.0	288.7	217.5	7.8	0.23	307.9	52.6	90.6	-55.8	(P.)
C	100.	34.1	198.0	0.89	1049.5	430.0	284.7	43.8	0.74	852.2	330.4	220.1	11.2	0.28	338.1	65.2	92.9	-53.1	(P.)
C	100.	86.4	301.0	0.77	1459.5	384.9	504.9	67.8	0.64	1157.3	284.8	368.5	22.4	0.24	414.1	37.6	111.9	-62.6	(U.)
C	100.	64.2	288.3	0.95	1841.0	434.8	476.6	65.3	0.78	1229.9	326.6	350.3	21.5	0.30	447.8	55.3	110.8	-61.6	(U.)
C	100.	48.4	283.5	1.17	1645.3	480.4	459.5	62.1	0.97	1319.9	365.6	339.9	19.9	0.37	486.8	71.8	111.1	-60.8	(U.)
C	100.	37.9	284.3	1.56	1930.3	579.0	490.8	72.6	1.29	1553.2	446.3	363.8	27.9	0.49	573.4	101.7	117.7	-58.6	(U.)
D	100.	56.1	203.0	0.60	910.3	348.4	288.0	41.9	0.49	734.5	261.8	220.2	8.5	0.19	287.0	41.4	90.0	-55.7	(P.)
D	100.	45.0	200.0	0.73	992.4	366.2	291.4	45.7	0.60	802.8	301.4	223.5	11.8	0.23	313.8	56.9	91.8	-54.1	(P.)
D	100.	34.7	196.3	0.91	1078.1	449.2	292.7	49.1	0.75	874.8	345.6	225.8	15.0	0.29	342.6	74.5	94.0	-52.1	(P.)
D	100.	26.7	196.3	1.12	1160.3	491.1	293.7	49.6	0.93	944.1	381.0	227.9	16.1	0.35	370.7	88.9	96.3	-50.9	(P.)
D	100.	99.7	324.7	0.79	1592.2	360.4	577.2	77.8	0.65	1256.5	287.0	417.7	28.6	0.25	440.2	35.8	118.9	-63.4	(U.)
D	100.	69.0	297.0	0.96	1611.5	442.8	509.2	71.4	0.79	1283.4	332.1	372.5	25.4	0.30	462.0	55.9	114.0	-61.6	(U.)
D	100.	51.7	287.0	1.18	1714.2	497.3	487.4	69.8	0.98	1372.8	378.3	359.0	25.1	0.37	502.3	75.0	113.9	-60.3	(U.)
D	100.	39.2	285.0	1.56	1964.1	589.2	504.0	76.9	1.29	1579.2	454.1	372.6	30.7	0.49	581.2	103.9	119.0	-58.3	(U.)
E	100.	50.3	192.7	0.63	905.8	370.0	279.3	45.0	0.52	732.3	280.0	214.6	11.4	0.20	287.9	49.4	89.8	-53.5	(P.)
E	100.	40.4	192.0	0.72	934.4	386.7	270.6	40.9	0.60	757.9	294.7	209.3	9.9	0.23	299.9	56.2	89.6	-53.2	(P.)
E	100.	30.2	186.0	0.90	998.4	438.8	267.6	43.9	0.74	812.8	336.9	206.7	12.2	0.28	322.9	73.6	91.5	-50.8	(P.)
E	100.	24.8	191.5	1.12	1124.0	487.0	282.9	47.7	0.93	915.8	378.2	220.7	15.2	0.35	361.7	88.9	95.4	-50.2	(P.)
E	100.	93.7	314.0	0.79	1547.3	392.8	550.9	75.5	0.65	1223.2	289.6	399.8	27.3	0.25	431.9	37.5	116.4	-62.9	(U.)
E	100.	62.0	279.0	0.95	1522.6	445.7	468.1	67.8	0.78	1216.0	335.8	344.6	23.5	0.30	443.9	89.1	110.1	-60.5	(U.)
E	100.	50.7	288.7	1.18	1704.4	490.4	482.8	67.2	0.98	1365.4	372.9	355.8	23.3	0.37	500.2	73.3	113.4	-60.7	(U.)
E	100.	39.0	283.0	1.56	1966.6	594.9	505.3	78.6	1.29	1581.1	458.7	373.5	32.0	0.49	581.8	105.6	119.2	-57.9	(U.)
F	100.	56.1	204.0	0.60	908.6	345.4	287.2	40.6	0.49	733.2	259.4	219.6	7.7	0.19	286.6	40.5	89.9	-55.9	(P.)
F	100.	44.0	197.5	0.73	973.9	363.1	285.0	44.3	0.60	788.5	299.2	219.2	11.0	0.23	309.3	56.6	91.2	-53.8	(P.)
F	100.	34.9	196.8	0.90	1073.4	439.4	291.5	46.5	0.75	871.0	337.7	224.8	13.0	0.29	341.3	71.5	93.7	-52.9	(P.)
F	100.	29.0	202.0	1.12	1204.4	496.2	307.3	52.1	0.93	978.5	384.4	237.1	17.4	0.35	381.6	88.9	97.5	-51.7	(P.)
F	100.	87.9	299.0	0.78	1673.5	392.8	512.4	71.4	0.64	1167.9	290.6	373.6	25.0	0.25	417.0	39.5	112.7	-62.3	(U.)
F	100.	69.4	293.0	0.96	1615.7	451.4	511.0	74.4	0.79	1286.7	339.2	373.8	27.6	0.30	464.0	58.4	114.2	-61.0	(U.)
F	100.	52.3	287.5	1.18	1720.0	498.3	490.0	70.4	0.98	1377.2	379.0	360.8	25.5	0.37	503.6	75.2	114.2	-60.3	(U.)
F	100.	40.1	278.5	1.57	1993.8	618.9	814.9	84.9	1.30	1602.4	475.4	380.2	36.5	0.50	588.6	111.3	120.4	-56.8	(U.)

REFRACTIVE INDEX = 1.4268

EXTINCTION COEFFICIENT = 0.1363

P. = PILOTED IGNITION

U. = UNPILOTED IGNITION

VOL = VOLUME IN ML: 50., 100., 150., 200.

EX.TI = EXPERIMENTAL IGNITION TIME IN SEC.

EX.TE = MEASURED IGNITION TEMPERATURE IN FAHRENHEIT

FLUX = INCIDENT IRRADIANCE IN CAL/CM**2-SEC

CA.TE = CALCULATED MAXIMUM IGNITION TEMPERATURE IN FAHRENHEIT

ERROR = ERROR PERCENTAGE

C.J. APPROACH = CARSLAW AND JAEGER APPROACH, CONDUCTION APPROACH

V.G. OR N. APPROACH = VISKANTAAND GROSH OR NOBLE APPROACH, CONVECTION APPROACH

VOLUME (ML)	THICKNESS (CM)	FRACTION OF ABSORPTION				COMPOSITION OF FUELS					
						FUEL A	FUEL B	FUEL C	FUEL D	FUEL E	FUEL F
50.0	0.42	1.0000	0.8264	0.2023	N-DODECANE	0.000	0.000	0.124	0.025	0.716	0.036
100.0	0.83	1.0000	0.8264	0.3166	N-TRIDECANE	0.000	1.000	0.520	0.931	0.170	0.496
150.0	1.25	1.0000	0.8264	0.3770	N-TETRADECANE	1.000	0.000	0.356	0.044	0.114	0.447
200.0	1.66	1.0000	0.8264	0.4046	N-PENTADECANE	0.000	0.000	0.000	0.000	0.000	0.021

to the experimental values than the other volumes: 50 ml, 150 ml and 200 ml.

If the error is defined as the percentage of the ratio of the difference of the calculated and experimental ignition temperatures versus the experimental ignition temperature, then in case ii for Model B the distribution of error is as follows:

1. In the piloted ignition tests, the calculated error for a volume of 100 ml is approximately in the range from 0.2 to 15.0 percent; for a volume of 150 ml it is -2.4 to 9.4 percent; and for a volume of 200 ml, it is about -10 percent. For a volume of 50 ml, there is only one calculated result, which is about 40 percent in error.

2. In the unpiloted ignition tests the calculated error for a volume of 100 ml is about 20 percent; for a volume of 150 ml it is from 2.0 to 10.0 percent; and for a volume of 200 ml it is about -14.6 to 6.8 percent.

The errors are not surprising considering the gross simplifications and assumptions in the models. Many of the parameters, such as the physical constants are functions of temperature, heat of evaporation, heat loss from the walls, wall heating effect, etc. which have not been taken into account. In the piloted ignitions, the sample volume of 50 ml resulted in the errors because the smaller the sample mass (and therefore heat capacity) the more pronounced (relatively) the wall heating effect. For a volume of 100 ml,

the combined effects of mass, heating effect from the sample container walls and the adiabatic assumption might be in balance. If so, then for samples of 150 ml and 200 ml these aforementioned compensating effects could then be out of balance in the reverse sense which would explain why the sample volume of 200 ml is more in error than the 150 ml sample. The same explanation can also be applied in the error analysis of the unpiloted ignition tests. In the calculations, it was assumed that there was no heat loss (adiabatic) from the base of the sample dish. Longer heating times result in higher calculated ignition temperatures; a typical comparison of the temperature-time relationship for piloted and unpiloted ignition, as extracted from Table 4-7, are given below. Note particularly the larger error for unpiloted ignition.

Type	Sample Volume (ml)	Type of Ignition	Ignition Time (sec)	Ignition Temp (°F)		Flux $\frac{cal}{cm^2\text{-}sec}$	Error (%)
				Calc'd (Model B)	exp.		
A	100	Piloted	49.0	231.7	215.0	0.60	7.5
A	100	Unpiloted	96.6	403.0	328.0	0.65	22.9

It is obvious from the above tabulation that the predictions from Model B are not encouraging; Model A is even worse. At equal irradiant fluxes, the ignition times for unpiloted ignition are almost double that of piloted ignition. The calculated unpiloted ignition temperature is also considerably higher than the calculated piloted ignition temperature,

the same is true for the measured values but to a much lesser extent. The only explanation for the failure in the models must be in the simplifying assumptions.

Effects of Thickness and Density on Piloted Ignition

In Chapter II an analytical solution for the infinite slab of an inert, opaque material exposed to a constant heat flux on one face and no heat loss on the opposite face was given as (44)

$$\frac{\Delta T_s \rho c L}{H_i t} = 1 + \frac{1}{F}\left(\frac{1}{3} - \frac{2}{\pi^2}\sum_{n=1}^{\infty}\frac{1}{n^2} e^{-n^2\pi^2 F}\right) \qquad \text{(II-31)}$$

This solution can also be expressed as follows (18):

$$\Delta T_s = \frac{2H_i t^{1/2}}{(\alpha\rho c)^{1/2}} \sum_{n=0}^{\infty}\left[\text{ierfc}\ \frac{2nL}{2(\alpha t)^{1/2}} + \text{ierfc}\ \frac{(2n+2)\ L}{2\ (\alpha t)^{1/2}}\right] \qquad \text{(IV-1)}$$

where

ΔT_s = surface temperature rise at ignition

t = time

c = heat capacity

L = thickness of the slab

ρ = density

H_i = heat on the surface

α = thermal diffusivity

F = Fourier number $\alpha t/L^2$

ierfc = the first integral of the complementary error function

From experimental data on the ignition times of different woods at various levels of irradiation from both flames and tungsten lamps Wesson et al (80, 81) concluded that the front surface temperature of wood at the moment of ignition is constant. Assuming further that the thermal conductivity of dry wood is linearly dependent on its density and that the specific heat of wood is approximately constant, they represented Equation IV-1 in functional form as

$$t_i = f\{\rho, H_i, \text{erf}[L/2(kt)^{1/2}]\} \qquad \text{(IV-2)}$$

and in correlating form by

$$t_i = \frac{\kappa \rho^a \{\text{erf}(x)\}^b}{(\bar{\alpha} H_i)^d} \qquad \text{(IV-3)}$$

where

t_i = measured ignition time (piloted ignition)

$\bar{\alpha}$ = average absorptance of the wood surface which takes into account the spectral emissivity of the irradiation source and the spectral absorptivities of the various woods.

x = a parameter $[L/2\ (kt)^{0.5}]$ which is the Fourier modulus.

κ = a constant

The exponents a, b and d were then determined empirically by systematic trial and error plotting until an acceptable single

correlation of ignition time and the function $\rho^a[\text{erf}(x)]^b/\bar{\alpha}\bar{H}_i^d$ was found, which resulted in assigning the values of a =1/3, b = 3/4 and d = 1.

Although in Wesson's work the various woods tested had different average absorptivities, in this study the variation in radiant energy absorption characteristics of the liquids was not discernible. Therefore, absorptivity is not an identifiable parameter, as such, in this work, which leaves only thickness and density, plus possibly some other parameters yet to be identified, for consideration.

Effect of Thickness

Wesson found in his study on a variety of woods that as the thickness of the wood sample increased beyond 3/4 to 1 inch, thickness became an insensitive parameter. This cut-off thickness is often referred to as "thermally-thick" which infers that the fraction of energy absorbed as it traverses through the sample increases with path length or thickness up to an asymptotic limit. Similarly, in this study on ignition of liquids, it was found that the fraction of energy absorbed as a function of depth of penetration approaches an apparent asymptotic limit, as demonstrated by Figure 4-12-D. In this case, thicknesses beyond about 0.5 inches do not contribute materially to the fraction of energy absorbed and consequently to the ignition time.

In this study, thickness of the fuel bed was defined as the volume of the liquid sample divided by the constant cross-sectional area of the sample container. Thus

Volume of Sample in ml	Thickness of Fuel in inches
50	0.17
100	0.34
150	0.51
200	0.68

Figures 4-4-A and -B clearly indicate that the ignition times do vary with volume of sample (or thickness) at least for 50 ml and to a lesser degree for 100 ml, whereas the differences between 150 ml and 200 ml are not detectable within the limits of experimental scatter. These thickness limits correspond with the fraction of energy absorbed as indicated in Figure 4-12-D.

The first objective then is to determine if the three ignition lines of Figures 4-4-A and -B, for volume of sample as a parameter, can be collapsed into a single line by introducing the error function of the Fourier modulus as a second independent variable. Following Wesson's choice of incorporating the error function to the 3/4 power, Figures 4-13-A and -B do indicate that Figures 4-4-A and -B can be reduced to a single line.

Effect of Density

Although the range of densities covered by this study were very small, 0.730 to 0.742, it is quite evident from Figure 4-5-B that the ignition time for a prescribed level of incident radiant flux and a constant sample volume varies with the fuel. Looking at the extremes, the least dense fuel

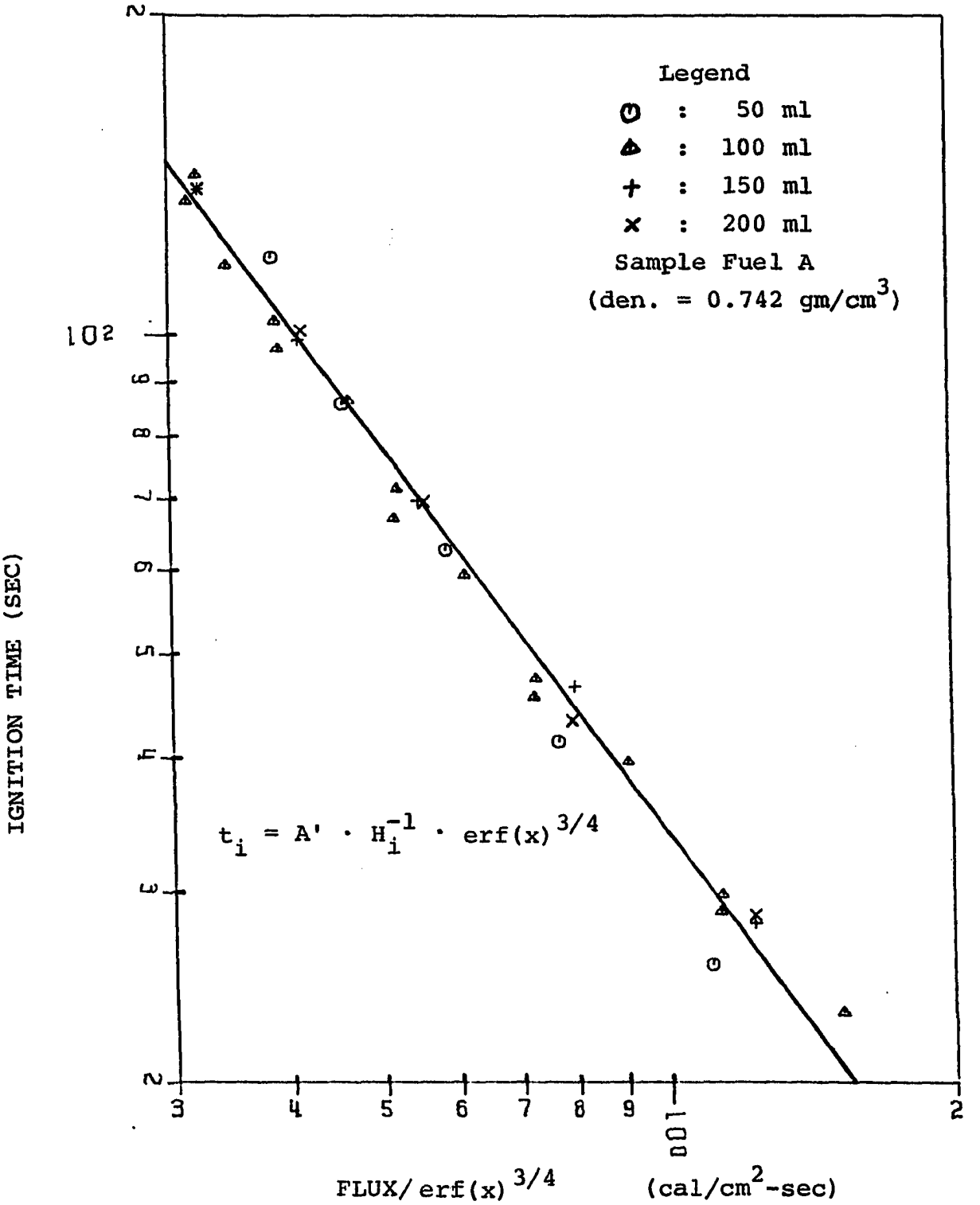

Figure 4-13-A. Correlation of Fuel A Piloted Ignition Data for Surface Irradiation by Tungsten Lamps

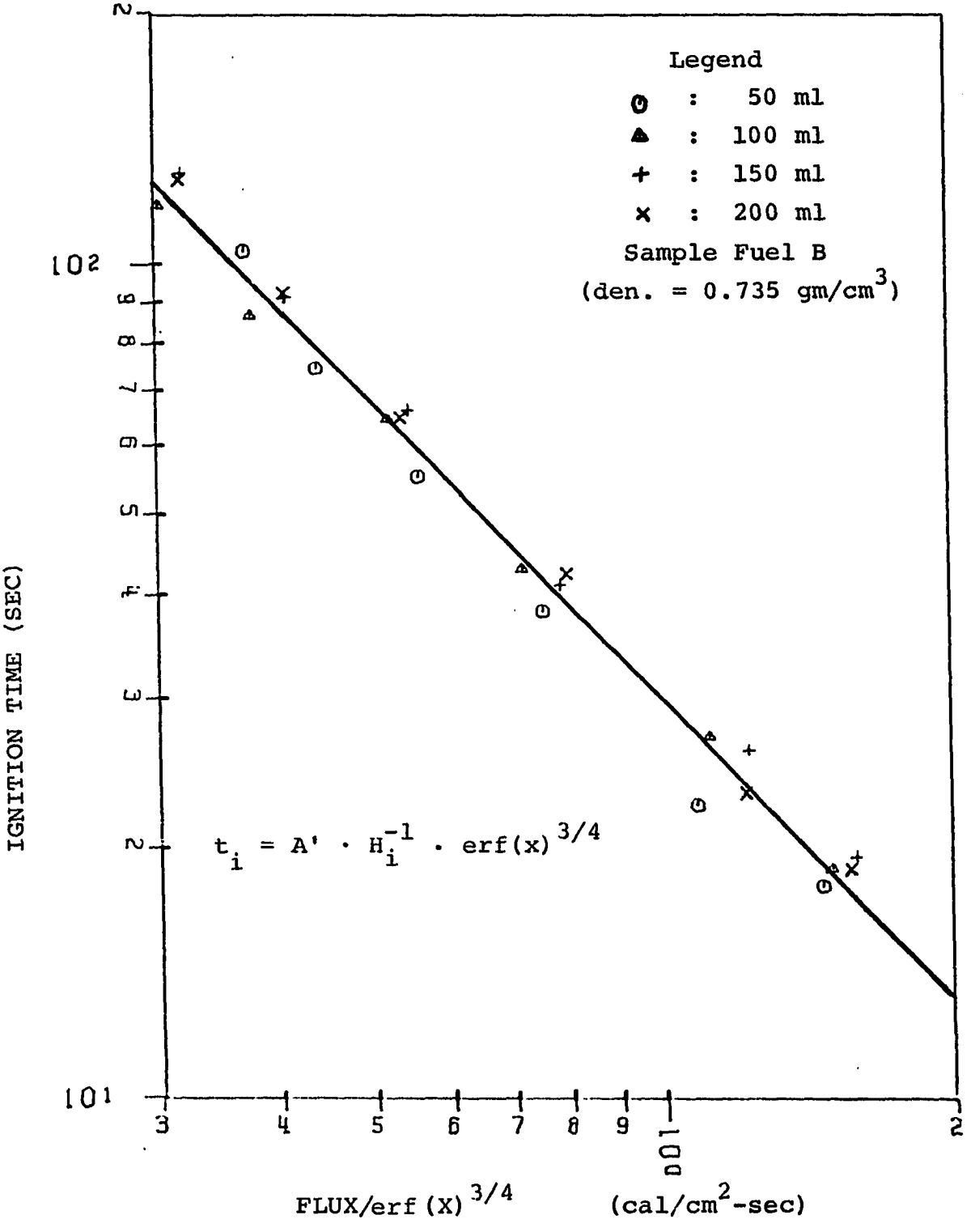

Figure 4-13-B. Correlation of Fuel B Piloted Ignition Data for Surface Irradiation by Tungsten Lamps

(Fuel E, 0.730 gm/ml^3) gives the lowest ignition time whereas the most dense fuel (Fuel A, 0.742 gm/ml^3) requires the highest (about 50 percent higher) ignition time. Thus, it would appear at first that ignition time is very sensitive to small changes in density, which implies that density would have to be raised to a very high power to compensate for the very small differences in density. The result of applying the two functional forms

$$t_i = A\, H_i^{-1}\, \rho^{1/3}$$

and

$$t_i = A\, H_i^{-1}\, \rho^{7}$$

are shown in Figures 4-14-A and 4-14-B, respectively, for the six fuels at a constant volume of 100 ml (constant thickness). It is apparent that as the exponent on density is increased, the three lines of Figure 4-14-A tend to merge into a single correlation. However, raising density to a large power, such as 7 or greater, to achieve correlation is difficult to justify on physical grounds. For this reason another physical parameter which can characterize the different fuels will be sought.

Effect of Heat of Vaporization on Piloted Ignition

Since ignition is initiated in the vapor phase near the surface of the liquid, it is reasonable to consider the relative ease of volatilizing the different fuels as a possible parameter for ignition. Accordingly, the molal average

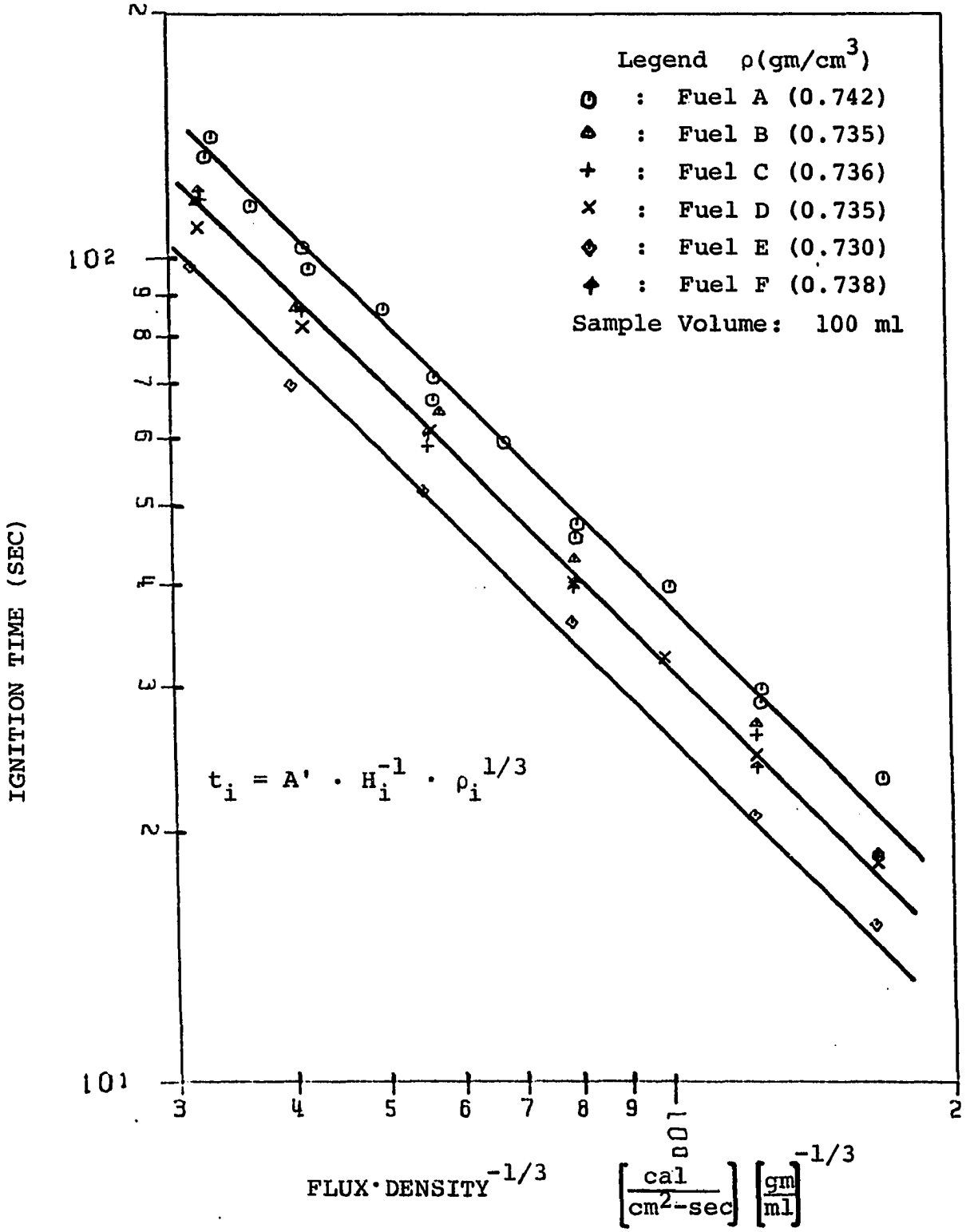

Figure 4-14-A. Correlation of Piloted Ignition Time vs $Flux^{-1} \cdot Density^{1/3}$ for a Six Fuels Having a Volume of 100 ml for Surface Irradiation by Tungsten Lamps

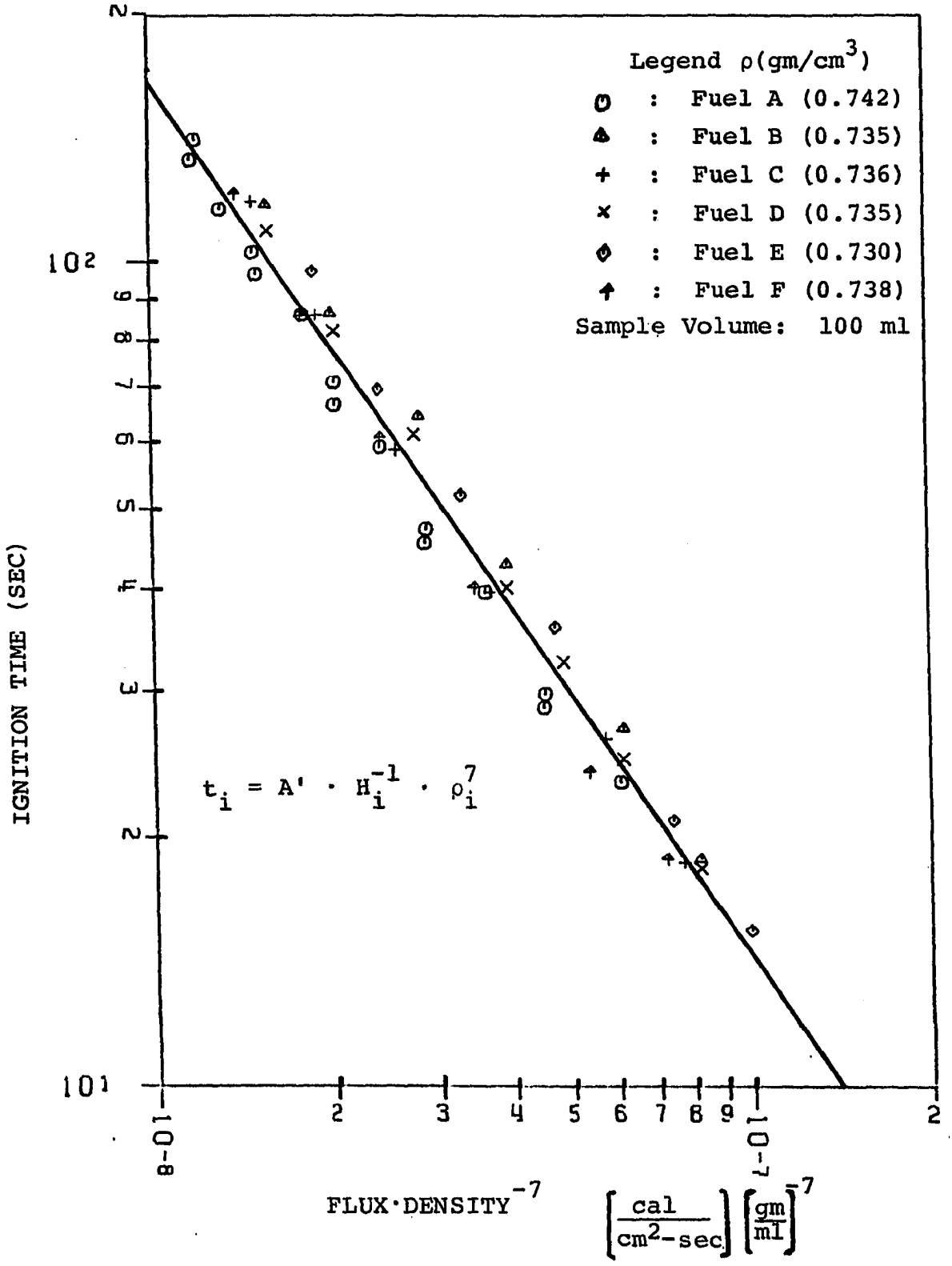

Figure 4-14-B. Correlation of Piloted Ignition Time vs Flux^{-1}·Density^{7} for Six Fuels Having a Volume of 100 ml for Surface Irradiation by Tungsten Lamps

heat of vaporization was evaluated as a correlating variable. The result of applying the functional form

$$t_i = A\, H_i^{-1}\, (\Delta H_{vap})^2$$

is shown in Figure 4-15 for all six fuels at a volume of 100 ml. It is immaterial whether the heat of vaporization is taken at the normal boiling points or some other fixed temperature. Thus, the three lines of Figure 4-5-B representing the various fuels have been collapsed into a representative, single line.

Final Correlation

As a result of investigating the effect of thickness and heat of vaporization on the piloted ignition times, the best final correlation is

$$t_i = A\, H_i^{-1}\, (\Delta H_{vap})^2\, [\mathrm{erf}(x)]^{3/4}$$

as shown in Figure 4-16. Note that the exponents on these independent variables which actually appear in the abscissa of this figure are arbitrarily assigned other values simply to fit within two cycles on the graph.

To summarize, in the piloted ignition of liquids by surface irradiation with tungsten lamps, the ignition time at any prescribed flux level is dominated primarily by the thickness of the fuel (or volume of sample), to a lesser extent by the latent heat of vaporization and to a much, much lesser extent--if any--by density.

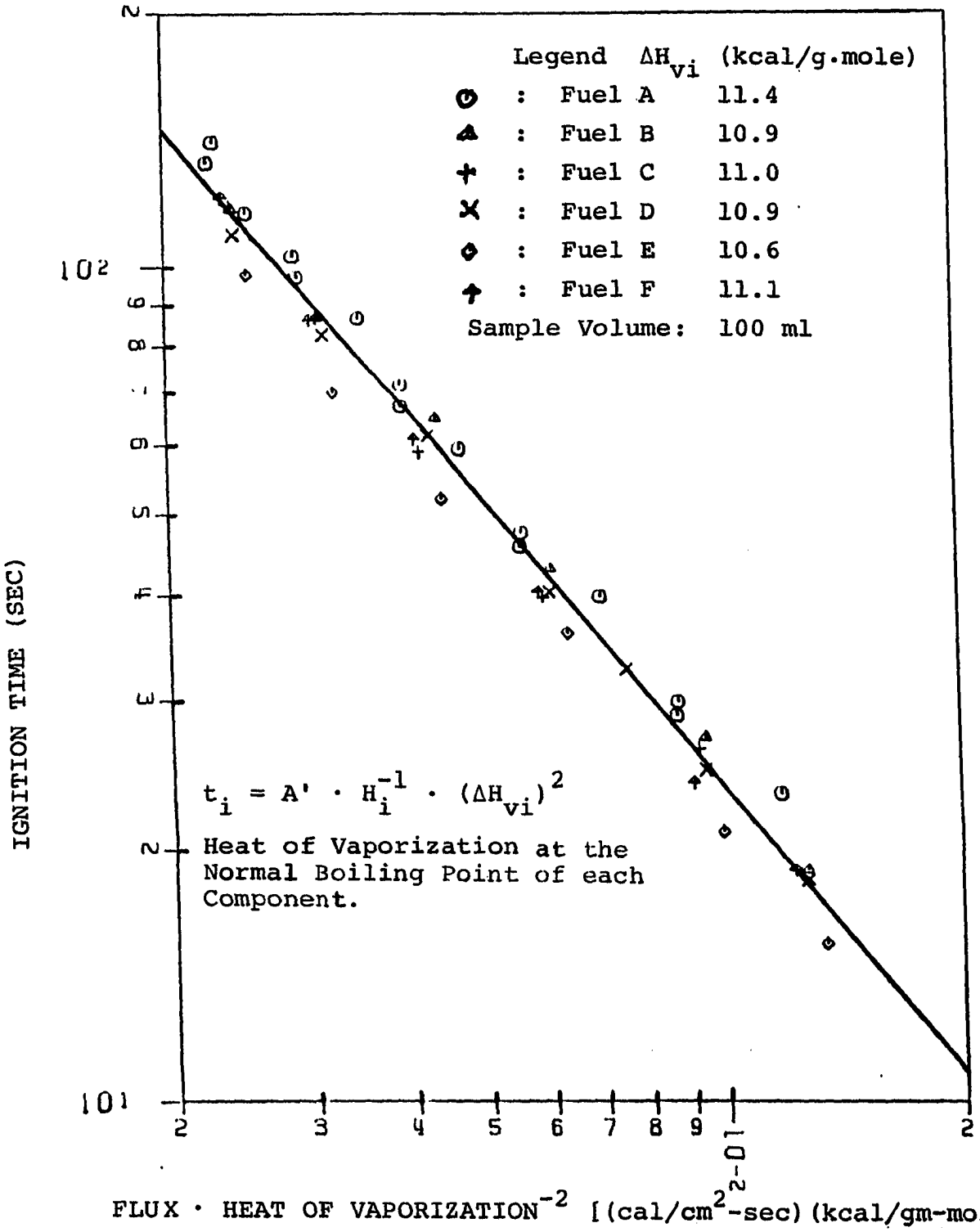

Figure 4-15. Correlation of Piloted Ignition Time vs Flux^{-1} · $(\Delta H_{vi})^2$ for Six Fuels Having a Volume of 100 ml for Surface Irradiation by Tungsten Lamps

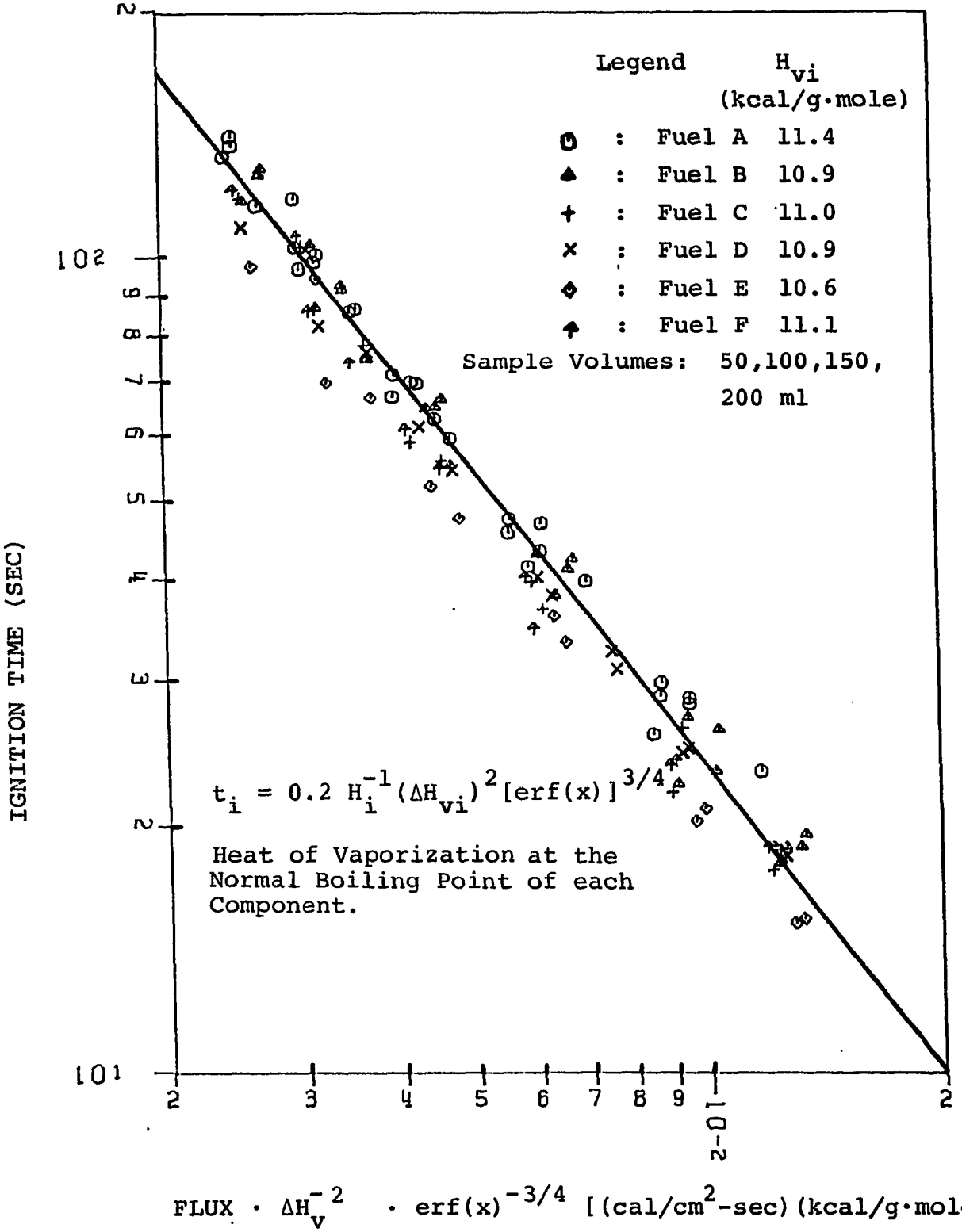

Figure 4-16. Correlation of Piloted Ignition Time with Heat of Vaporization (B.P.) and Thickness for Surface Irradiation by Tungsten Lamps

Effect of the Material of the Container

A cursory examination of the effect of vessel material on the ignition time was made during the preliminary test period. The base part of a pyrex glass petri dish, its top part (its cover), an aluminum petri dish (base part), and two specially fabricated brass trays were used. The specifications and physical properties of these five containers are given in Table 4-8. In each test 50 ml of liquid n-tetradecane were used. Piloted ignition times for various lamp heights are presented in Table 4-9 and in Figure 4-17. There are two curves that can be drawn to represent the data; time-intensity relationship data, one for pyrex petri dish parts and aluminum petri dish and the other for brass trays. Data obtained with the stainless steel containers used to obtain most of the data in this study are also included for comparison. Since pyrex and aluminum petri dishes have much lower thermal capacities, they can be heated much faster than either of the brass trays. When these data are compared to those of the piloted ignition with a stainless steel sample dish with 50 ml of testing liquid and with the radiometer protruding into the liquid about 1 inch above the base of the sample dish, the measured piloted ignition times match with those of the brass trays. When the radiometer is level with the base of the sample dish, the data with stainless steel match the data for pyrex glass and aluminum petri dishes.

TABLE 4-8

SPECIFICATIONS AND PHYSICAL PROPERTIES OF CONTAINERS

Container	Mass (gm)	Diameter (cm)	Height (cm)	C_p@	k@ ($*10^3$)	m C_p
Base of Pyrex Glass Petri Dish	40.0	9.0	1.90	0.2	1.86	8.00
Top of Pyrex Glass Petri Dish	38.7	9.5	1.76	0.2	1.86	7.74
Base of Aluminum Petri Dish	16.2	9.0	1.66	0.208	484.0	3.37
Brass Tray I	314.6	10.2	1.27	0.902	232.	28.94
Brass Tray II	435.4	10.2	2.54	0.902	232.	40.06
Stainless Steel Dish**	--	12.38	3.17	0.11	33.	--

@ At Temperature of 0°C

** For Reference Only

C_p Specific Heat Content in cal/gm-°C

k Thermal Conductivity Coefficient in cal/cm-°C-sec

m C_p Thermal Capacity of Container in cal/°C

TABLE 4-9

EXPERIMENTAL IGNITION DATA OF FUEL A WITH THE MATERIAL EFFECT OF THE CONTAINERS

Distance (inches)	T_{BGPD}	T_{TGPD}	T_{LBT}	T_{MBT}	T_{APD}
	Ignition Time (sec)				
3	16.8	17.6	16.7	17.5	13.4
4	24.9	24.5	29.6	23.7	20.6
5	31.2	28.2	40.1	28.5	30.0
6	41.5	39.0	41.0	44.4	40.1
7	53.7	53.9	65.2	58.2	55.6
8	64.7	63.9	76.6	72.9	71.5
9	67.1	72.2	93.2	89.6	67.8
10	96.9	83.0	107.0	120.3	95.2
11	104.8	100.9	139.6	116.6	111.6
12	123.9	116.5	154.2	164.2	131.0

APD Aluminum Petri Dish

TGPD Top Pyrex Glass Petri Dish

BGPD Bottom Pyrex Glass Petri Dish

LBT Large Brass Tray (II)

MBT Medium Brass Tray (I)

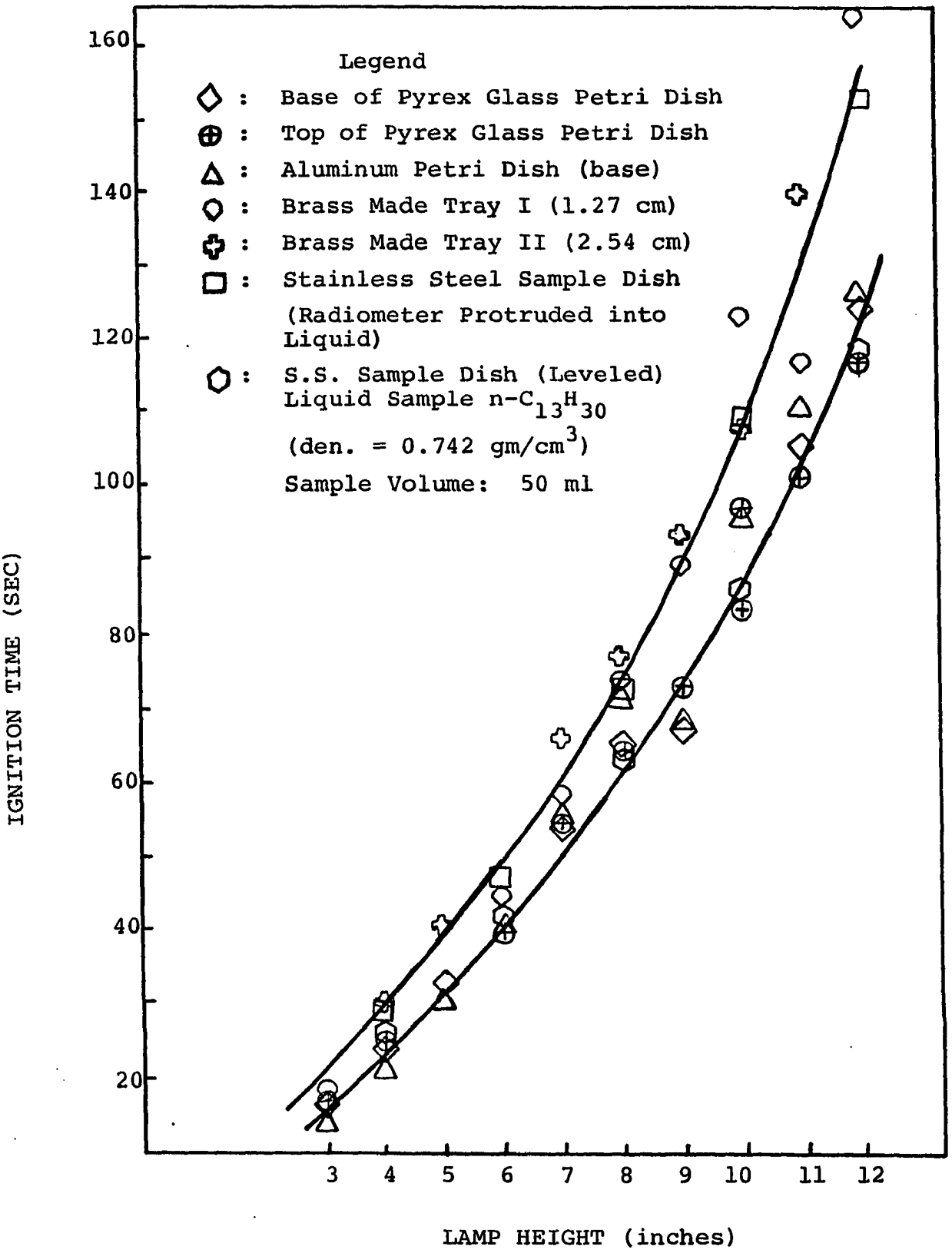

Figure 4-17. Variation of Piloted Ignition Time with Lamp Height

Water Sublayer Substitution

During the preliminary testing period, it was realized that a large amount of fuel was going to be needed for this experiment. To conserve on fuel, experiments were run in which the fuel was floated on a lower layer of water. For example, in one run 50 ml of n-tetradecane floating on 50 ml of water were used. The ignition time was shorter than for tetradecane alone. A possible explanation is that n-tetradecane and water have different infrared absorption bands (refer back to Table 2-1) so that the same amount of radiative energy absorbed by the two component system is greater than for the single component. In addition, as the water layer gains heat from the bottom of the sample dish, it begins to vaporize (since it has a much lower boiling point, or higher vapor pressure, than n-$C_{14}H_{30}$ does). In so doing, it not only entrains fuel molecules during the preheating period but also induces a "steam distillation" effect. Rather than having to contend with these additional variable, using water to conserve fuel was abandoned.

Durability of Lamp Filament

Many lamp filaments had to be replaced during the experiment; the average life of the lamps was 20 hours as compared to the manufacturer's estimation of 5000 hours. This drastic reduction in life was not encountered by previous investigators in solid ignition tests. One explanation is that in the unpiloted ignition tests flashing was initiated

near the surface of the lamp. The flashing phenomenon can be likened to a small scale explosion, judging from the nature of the sound waves produced. The localized over-pressures generated could conceivably have been of sufficient magnitude to set the fragile lamp filament into vibration and eventually failure. In addition, it was observed that the ends of some used filaments were corroded.

Pyrolysis of Liquid Fuel

The kinetic order for the combustion reactions of n-paraffins in the air, as determined by many experiments, is approximately equal to two. These paraffins pyrolyze into smaller molecular compounds (CH_4, C_2H_2, H_2, and etc.), atoms (C and H), radicals ($-CH_3$, $:CH_2$, $\cdot H$, and etc.) and into many other active species at a temperature of about 400°C and one atmosphere pressure. The observed combustion processes of n-paraffins are actually the superimposed reactions of the active species. The burning zone of the wick flame or the envelope and wake flames of a liquid droplet in combustion always shows a black pyrolyzing zone in the inner region of the flame. In the present unpiloted ignition experiments, a black, misty zone was observed in front of the lamp reflector which probably was from the products of the pyrolyzing fuel. Flashing back to the fuel surface was never observed until the black, misty pyrolyzing zone appeared. The time delay between those two phenomena was very short. For piloted ignition, a similar phenomenon was not observed. Either there

was one pyrolyzing zone around the pilot flame before ignition, which was too tiny or too short to be seen, or the complicated ignition mechanism of the propane pilot flame (thermal and radical effects involved in this process) masked the pyrolyzing zone which might have been present.

Chemical and Physical Properties of the Fuels

The chemical properties of a substance are dependent on the distribution of valent electrons in the molecule. For $n\text{-}C_{12}H_{26}$ up to $n\text{-}C_{15}H_{32}$, their chemical properties are dominated by the distribution of the covalent charges in the C-H and C-C bonds; thus little differences in properties would be possible. Physical properties in the paraffin family are primarily affected by their molecular weights. However, even though the spread in molecular weights for the four compounds constituting the test fuels was 42 (170 to 212) at these molecular weight levels, the variation in physical properties was not significant. For example,

1. Refractive Index (64)

	$n\text{-}C_{12}H_{26}$	$n\text{-}C_{13}H_{28}$	$n\text{-}C_{14}H_{30}$	$n\text{-}C_{15}H_{32}$
20°C	1.4216	1.4256	1.4289	1.4319
25°C	1.4195	1.4234	1.4268	1.4298

2. Specific Heat Content (64)

$n\text{-}C_{12}H_{26}$	0.498 cal/g°C (0~50°C)
$n\text{-}C_{13}H_{28}$	0.499 cal/g°C (0~50°C)
$n\text{-}C_{14}H_{30}$	0.497 cal/g°C (0~50°C)
$n\text{-}C_{15}H_{32}$	0.497 cal/g°C (0~50°C)

3. Thermal Conductivity (36)

	$n\text{-}C_{12}H_{26}$	$n\text{-}C_{13}H_{28}$	$n\text{-}C_{14}H_{30}$	$n\text{-}C_{15}H_{32}$
30°C	3.37×10^{-4}	3.39×10^{-4}	3.49×10^{-4}	3.52×10^{-4}

[cal/cm·sec°C]

4. Density (64)

	$n\text{-}C_{12}H_{26}$	$n\text{-}C_{13}H_{28}$	$n\text{-}C_{14}H_{30}$	$n\text{-}C_{15}H_{32}$
30°C	0.7416	0.7492	0.7557	0.7615
50°C	0.7271	0.7349	0.7417	0.7476

[gm/cm^3]

Since both their chemical and physical properties are so close, the test results do not show, any difference in the minimum incident radiations for ignition, ignition times, and ignition temperatures among the six fuel samples other than the effect which was compensated by introducing heat of vaporization. It should be understood that the objective of this study was to devise an experimental technique for investigation of the ignition times of liquids exposed to external radiation. The selection of the fuels was on the basis of ready availability, cost, safety from the standpoint of having a high flash point temperature and reliable data on flash points by conventional techniques which could be used for comparisons with the results of this work. Now that a technique for measuring the ignition behavior of liquids has been developed, subsequent studies can be made on fuels of widely different properties to obtain more definitive information on the parameters which affect the ignition process.

CHAPTER V

CONCLUSIONS

From the data obtained in this study the following conclusions were drawn:

1. Experimental equipment and procedures have been developed for measuring ignition times of liquids subjected to an external irradiation flux, and for measuring the radiant energy absorption of liquid fuels. The results of this study indicate that this design for liquid flammability tests is satisfactory and promising.

2. A correlation form with parameters; such as the piloted ignition time t_i, the incident irradiation flux H_i, heat of vaporization of liquid fuel ΔH_v, and the error function of Fourier modulus erf (x), has been obtained:

$$t_i = 0.2 * H_i^{-1} * (\Delta H_v)^2 * [\text{erf } (x)]^{3/4}$$

3. For both piloted and unpiloted ignition experiments, increasing the incident irradiance decreases the ignition time. At lower incident irradiance levels, higher ignition times are required for an increased volume of the liquid fuel. This effect is much more pronounced in the unpiloted ignition tests than in the piloted ignition tests.

4. Minimum incident irradiance required for piloted ignition of n-tridecane and n-tetradecane are 0.06 and 0.078 cal/cm^2-sec, respectively.

5. Maximum piloted surface ignition temperatures of n-tridecane and n-tetradecane are 200 and 210°F, respectively. The various compositions of mixtures of four normal paraffins, from n-dodecane to n-pentadecane, have maximum surface ignition temperatures in the range of 190 to 200°F. However, the heating rates, or the intensities of incident irradiance will not effect the piloted ignition temperature readings in this test apparatus.

6. Comparing unpiloted ignition to piloted ignition tests, the former tests always need longer ignition times at the same incident irradiance and the ignition time and maximum surface ignition temperatures vary with distance between the ignition source and the fuel.

7. Placing the radiometer inside the liquid alters the measured ignition times for both piloted and unpiloted ignition tests because the water-cooled radiometer abstracts heat through its wetted walls.

8. Radiation energy absorbed by the liquid increases as the liquid depth is increased but levels off beyond a depth of penetration of about 1 cm. Of the incident irradiance on the liquid surface, 17.4 percent was reflected away, and about 40 percent of the energy incident on the surface (before reflection) was absorbed by the liquid fuel within the first 1.7 cm of penetration.

REFERENCES

1. Adomeit, G., "Ignition of Gases at Hot Surfaces Under Non Steady-State Conditions," Tenth Symposium (International) on Combustion, 237 (1965).

2. Affens, W. A., "Flammability Properties of Hydrocarbon Fuels," J. of Chem. Engr. Data, 11, 197 (1966).

3. Affens, W. A. and McLaren, G. M., "Flammability Properties of Hydrocarbon Solution in Air," J. of Chem. Engr. Data, 17, 482 (1972).

4. Akita, K. and Yumoto, T., "Heat Transfer in Small Pools and Rates of Burning of Liquid Methanol," Tenth Symposium (International) on Combustion, 943 (1965).

5. Alkidas, A. and Durbetaki, P., "Ignition Characteristics of A Stagnation Point Combustible Mixture," Comb. Sci. and Tech., 3, 187 (1971).

6. Alkidas, A. and Durbetaki, P., "Stagnation-Point Heat Transfer: The Effect of the First Damkohler Similarity Parameter," J. of Heat Transfer, 94, Series C, 410 (1972).

7. Alkidas, A. and Durbetaki, P., "Ignition of a Gaseous Mixture by a Heated Surface," Comb. Sci. and Tech., 7, 135 (1973).

8. Alvares, N. J., Blackshear, P. L., Jr. and Kanury, A. M., "The Influence of Free Convection on the Ignition of Vertical Cellulosic Panels by Thermal Radiation," Comb. Sci. and Tech., 1, 407 (1970).

9. Andersen, W. H., Garfinkle, D. R., Carpenter, G. E. and Brown, R. E., "Energy Absorption Near and Below the Burning Surface of Hydrocarbon Pools," 1969 Meeting, Central State Section/The Comb. Inst., March 18-19, 1969.

10. Barnett, H. C. and Hibbard, R. R., "Basic Considerations in the Combustion of Hydrocarbon Fuels with Air," NACA Report 1300 (1957)

11. Berl, W. G., "International Symposium on the Use of Models in Fire Research," NAS-NRC, Publication 786, Washington, D.C. (1961).

12. Bridgeman, O. C. and Marvin, C. F., Jr., "Auto Ignition Temperature of Liquid Fuels," Ind. and Engr. Chem., 20, 1219 (1928).

13. Brown, C. R., "The Determination of the Ignition Temperatures of Solid Materials," Fuel, 14, 14 (1935).

14. Burgoyne, J. H., Roberts, A. F. and Quinton, P. G., "The Spread of Flame Across a Liquid Surface: I. The Induction Period," Proc. Royal Soc., London, A308, 39 (1969).

15. Burgoyne, J. H. and Roberts, A. F., "The Spread of Flame Across a Liquid Surface: II. Steady-State Conditions, and III. A Theoretical Model," Proc. Royal Soc., London, 55 and 69 (1969).

16. Burgoyne, J. H. and Williams-Leir, G., "Inflammability of Liquids," Fuel, 28, 145 (1949).

17. Butler, R. M., Cooke, G. M., Lukk, G. G. and James, B. G., "Prediction of Flash-Point of Middle Distillates," Ind. & Engr. Chem, 48, 808 (1956).

18. Carslaw, H. S. and Jaeger, J. C., Conduction of Heat in Solids, Clarendon Press (1959).

19. Chambre, P. L., "On the Ignition of a Moving Combustible Gas Stream," J. of Chem. Phys., 25, 417 (1956).

20. Constam, E. J. and Schlapfer, P., "Determination of the Self Ignition Temperature of Motor Oils," Z. Ver. Deut. Ing., 57, 38 (1913).

21. Corlett, R. C. and Fu, T. M., "Some Recent Experiments with Pool Fires," Pyrodynamics, 4, 253 (1966).

22. Coward, H. F. and Jones, G. W., "Limits of Flammability of Gases and Vapors," Bulletin 503, Bureau of Mines, Washington, D. C. (1952).

23. Dixon, H. B. and Coward, H. F., "Ignition Temperature of Gases," J. Chem. Soc., London, 95, 514 (1909).

24. Dykstra, F. J. and Edgar, G., "Spontaneous Ignition Temperature of Liquid Hydrocarbons at Atmospheric Pressure," Ind. & Engr. Chem., 26, 509 (1934).

25. Ewing, G. W., Instrumental Methods of Chemical Analysis, McGraw-Hill, New York (1969).

26. Falk, K. G., "The Ignition Temperature of Hydrogen-Oxygen Mixtures," J. Amer. Chem. Soc., 28, 1517 (1906).

27. Frank, C. E. and Blackham, A. U., "Spontaneous Ignition of Organic Compounds," Ind. Engr. Chem., 44, 862 (1952).

28. Glassman, I. and Hansel, J. G., "Some Thoughts and Experiments on Liquid Fuel Spreading, Steady Burning and Ignitability in Quiescent Atmospheres," Fire Research Abstracts and Reviews, 10, 217 (1968).

29. Glassman, I., Hansel, J. G. and Eklund, T., "Hydrodynamic Effects in the Flame Spreading, Ignitability and Steady Burning of Liquid Fuels," Comb. and Flame, 13, 99 (1969).

30. Goldman, G. W. and Heyt, J. W., "Radiation in the Reacting Boundary Layer," Comb. Sci. and Tech., 6, 71 (1972).

31. Goto, R. and Nikki, M., "Vapor Pressures and Inflammation Limits of Organic Volatile Substances," Kyoto Univ., Univ. Institute for Chem. Research Bulletin, 28, 68 (1952).

32. Hallman, J. R., "Ignition Characteristics of Plastics and Rubbers," Ph.D. Dissertation, Univ. of Oklahoma, Norman, OK (1971).

33. Holm, H., "Kindling Temperatures," Z. Angeu. Chem., 26, 273 (1913).

34. Hottel, H. C., "Review of'Certain Laws Governing Diffusive Burning of Liquid,'" Fire Research Abstracts and Reviews, 1, 41 (1958).

35. Infrared Heating, Lamp Business Division, General Electric, TP-142 (1974).

36. Jamieson, D. T., Irving, J. B. and Tudhope, J. S., "Liquid Thermal Conductivity: A Data Survey to 1973," National Engr. Lab., Her Majesty's Stationary Office, Edinburg (1975).

37. Jentzsch, H., "Self-Ignition of Oils and Fuels," Z. Ver. Deut. Ing., 68, 1150 (1924).

38. Kanury, A. M., "Ignition of Celulosic Solids--A Review," Tech. Report, FMRC Serial No. 19721-7 (1971).

39. Kashiwagi, T., "A Radiative Ignition Model of a Solid Fuel," Comb. Sci. and Tech., 8, 225 (1974).

40. Kashiwagi, T., "Experimental Observation of Radiation Ignition Mechanism," Comb. and Flame, 34, 231 (1979).

41. Kindelan, M. and Williams, F. A., "Theory for Endothermic Gasification of a Constant Energy Flux," Comb. Sci. and Tech., 10, 1 (1975).

42. Kindelan, M. and Williams , F. A., "Radiant Ignition of a Combustible Solid with Gas-Phase Exothermicity," ACTA Astronautica, 2, 955 (1975).

43. Kindelan, M. and Willaims, F. A., "Gas-Phase Ignition of a Solid with In-Depth Absorption of Radiation," Comb. Sci. and Tech., 16, 47 (1977).

44. Koohyar, A. N., "Ignition of Wood by Flame Radiation," Ph.D. Dissertation, Univ. of Oklahoma, Norman, OK (1967).

45. Kumagai, S. and Kirmura, I., "Ignition of Flowing Gases by Heated Wires," Sixth Symposium (International) on Combustion, 554 (1957).

46. Kumar, R. K. and Hermance, C. E., "Role of Gasphase Reactions During Radiant Ignition of Solid Propellants," Comb. Sci. and Tech., 14, 169 (1976).

47. Lang, N. A., Handbook of Chemistry, 10th ed., McGraw-Hill (1961).

48. Law, C. K., "On the Stagnation-Point Ignition of a Premixed Combustible," Int. J. Heat and Mass Transfer, 21, 1363 (1978).

49. Law, C. K., "Ignition of a Combustible Mixture by a Hot Particle," AIAA J., 16, 628 (1978).

50. Lenoir, J. M., "Predict Flash Points Accurately," Hydrocarbon Processing, 54, 95 (1975).

51. Leu, J. C., "Modelling of the Pyrolysis and Ignition of Wood," Ph.D. Dissertation, Univ. of Oklahoma, Norman, OK (1975).

52. Lewis, B. and von Elbe, G., Combustion, Flames and Explosions of Gases, Academic Press, New York (1961).

53. Mackinven, R., Hensel, J. G. and Glassman, I., "Influence of Laboratory Parameters on Flame Spread Across Liqid Fuels," Comb. Sci. and Tech., 1, 293 (1970).

54. Moore, H., "spontaneous Ignition Temperatures of Liquid Fuels for Internal Combustion Engines," J. Soc. Chem. Ind., London, 36, 109 (1917).

55. Mullen, J. W., Penn, J. B. and Irby, M. R., "Ignition of High Velocity Streams of Combustible Gases by Heated Cylindrical Rods," Third Symposium on Combustion, Flame, and Explosion Phenomena, 317 (1949).

56. Mullins, B. P., Spontaneous Ignition of Liquid Fuels, Butterworths Scientific Publications, London (1955).

57. Mullins, B. P., "Bubble Points, Flammability Limits and Flash Points of Petroleum Products," Combustion Researches and Reviews, AGARDOgraph 15, pp 55-75, Butterworths Scientific Publications, London (1957).

58. Murad, R. J., Lamendola, J., Isoda, H. and Summerfield, M., "A Study of Some Factors Influencing the Ignition of a Liquid Fuel Pool," Comb. and Flame, 15, 289 (1970).

59. Noble, J. J., "The Effect of Radiative Transfer on Natural Convection in Enclosures: A Numerical Investigation," Ph.D. Dissertation, M. I. T. (1968).

60. Ormandy, M. R. and Craven, E. C., "Further Experiments with the Moore Ignition Meter," J. Instn. Petrol. Tech., 12, 650 (1926).

61. Penner, S. S. and Mullins, B. P., Explosion Detonation, Flammability and Ignition, Pergamon Press (1959).

62. Perry, R. H., Chemical Engineer's Handbook, Third Ed., McGraw-Hill, New York (1950).

63. Rix, H. D., Strother, G. K. and Woodbridge, C. L., "A Literature Survey of Combustion Flames," AF 19(604)-1885, Haller, Raymond and Brown, Inc., State College, PA (1957).

64. Rossini, F. D. et al, Selected Values of Physical and Thermodynamic Properties of Hydrocarbons and Related Compounds, American Petroleum Institute (1953).

65. Scott, G. S., Jones, G. W. and Scott, F. E., "Determination of Ignition Temperatures of Combustible Liquids and Gases," Analyt. Chem., 20, 238 (1948).

66. Sharma, O. P. and Sirignano, W. A., "Ignition of Stagnation Point Flow by a Hot Body," Comb. Sci. and Tech., 1, 95 (1969).

67. Siegel, R. and Howell, J. R., Thermal Radiation Heat Transfer, McGraw-Hill, New York (1972).

68. Sirignano, W. A. and Glassman, I., "Flame Spreading Above Liquid Fuels: Surface-Tension-Driven Flows," Comb. Sci. and Tech., 1, 307 (1970).

69. Sirignano, W. A., "A Critical Discussion of Theories of Flame Spread Across Solid and Liquid Fuels," Comb. Sci. and Tech., 6, 95 (1972).

70. Smith, H. W., Schmitz, R. A. and Ladd, R. G., "Combustion of a Premixed System in Stagnation Flow: I. Theoretical," Comb. Sci. and Tech., 4, 131 (1971).

71. Sortman, C. W., Beatty, H. A. and Heron, S. D., "Spontaneous Ignition of Hydrocarbons: Zone of Non-ignition," Ind. & Engr. Chem., 33, 357 (1941).

72. Steinberg, M. and Kaskan, W. E., "The Ignition of Combustible Mixtures by Shock Waves," Fifth Symposium (International) on Combusiton, pp 664-671 (1955).

73. Sullivan, M. V., Wolfe, J. K. and Zisman, W. A., "Flammability of the Higher Boiling Liquids and Their Mists," Ind. & Engr. Chem., 39, 1607 (1947).

74. Thompson, N. J., "Auto-Ignition Temperatures of Flammable Liquids," Ind. & Engr. Chem., 21, 134 (1929).

75. Torrance, K. E., "Surface Flows Preceding Flame Spread Over a Liquid Fuel," Comb. Sci. and Tech., 3, 133 (1971).

76. Torrance, K. E. and Mahajan, R. L., "Fire Spread Over Liquid Fuels: Liquid Phase Parameters," 15th Symposium (International) on Combustion, 281 (1974).

77. Viskanta, R. and Grosh, R. J., "Boundary Layer in Thermal Radiation Absorbing and Emitting Media," Int. J. Heat Mass Transfer, 5, 795 (1962).

78. Welker, J. R., Wesson, H. R. and Sliepcevich, C. M., "Ignition of Alpha-Cellulose and Cotton Fabric by Flame Radiation," Fire Technology, 5, 59 (1969).

79. Wesson, H. R., "The Piloted Ignition of Wood by Radiant Heat," Ph.D. Dissertation, Univ. of Oklahoma, Norman, OK (1970).

80. Wesson, H. R., Sliepcevich, C. M. and Welker, J. R., "The Piloted Ignition of Wood by Radiant Heat," Internal Memorandum 1578-IM-6, OURI Project 1578 (July 1970).

81. Wesson, H. R., Welker, J. R. and Sliepcevich, C. M., The Piloted Ignition of Wood by Thermal Radiation," Comb. and Flame, 16, 303 (1971).

82. Williams, C. G., "Fuels and Lubricants for Aero Gas Turbines," J. Instn. Petrol., 33, 267 (1947).

83. Yumoto, T., Takahashi, A. and Handa, T., "Combustion Behavior of Liquid Fuel in a Small Vessel: Effect of Convective Motion in the Liquid on Burning Rate of Hexane in the Early Stage of Combustion," Comb. and Flame, 30, 33 (1977).

84. Zabetakis, M. G., "Flammability Characteristics of Combustible Gases and Vapors," Bulletin 627, Bureau of Mines, Washington, D. C. (1965).

85. Zabetakis, M. G. and Burgess, D. S., "Research on the Hazards Associated with the Production and Handling of Liquid Hydrogen," Report of Investigations 5707, Bureau of Mines, Washington, D. C. (1961).

86. Zabetakis, M. G. and Richmond, J. K., "The Determination and Graphic Representation of the Limits of Flammability of Complex Hydrocarbon Fuels at Low Temperatures and Pressures," Fourth Symposium (International) on Combustion, pp 121-126 (1953).

APPENDIX

Chronology of Modifications in the Apparatus

It took almost four months from the completion of fabrication of the test cabinet to the point where reliable data could be collected. During this "shakedown" period, essential details for the experimental procedure were devised.

Liquid Removal System

Rapid and safe removal of the hot liquid fuel after each ignition test is required. At first, allowing the liquid to cool naturally and then reusing it was contemplated but it proved to be too time consuming, which led to the institution of the vacuum removal system shown in Figure 3-5. It performed this task efficiently.

Starting Temperature Control

Scattering of data was one of the major problems encountered in the early work. After performing a number of trial runs it became evident that the starting temperature for the sample dish and holder and the lamp housing assembly had to be maintained within certain limits in order to minimize the introduction of bias in the measurement of pre-heating time which represents the time required to raise the fuel from a specified ambient temperature such as 20°C to the

ignition temperature which for this study was around 200°C. To expedite cooling of the sample container assembly to essentially ambient condition, cooling water was passed through 1/8 inch copper tubing which was wrapped around it. A thermocouple was attached to the outside bottom of the sample dish to monitor the temperature. As a further precaution the fuel added to the sample dish was always at ambient temperature. In addition, provision was made to cool the lamp holder assembly with a bank of S-bend copper tubing (1/8 inch) by circulating tap water. A thermocouple monitor was attached to a metal bar which supports the lamp holder assembly. Since the entire lamp assembly is relatively massive, its temperature can affect the initial environmental conditions in the test enclosure. Furthermore, since the temperature of the lamp continues to increase with preheating time, a higher starting temperature for the lamp holder assembly eventually results in a higher temperature at the end of the test which could affect the results. It was found that a starting reference temperature of 40 to 50°C for the lamp holder would simultaneously assure that the temperature of the sample dish assembly had dropped to ambient and at the same time had reduced the temperature of the lamp holder assembly to the point where it no longer biased the experimental measurements on ignition time.

As a result of these provisions the variance of the final data is approximately 5 percent of its mean value over

5 to 10 repeated runs. Most of the final data reported herein represented the average value of multiple runs--usually 3 to 5.

Temperature of Environment

Most of the data were taken in the winter when the room temperature could be maintained at 60 ± 10°F. The experimental data reported herein were taken within this range of room temperatures.

Ventilation

A blower, installed vertically over the vent of the test cabinet, which was used to exhaust the hot gases produced during the test period. It was observed during the early tests that the rate at which these gases were exhausted had a material affect on the measured times to ignition. By installing a baffle board between the vent and the duct and by trial and error adjusting of the distance between the baffle board and duct, it was possible to obtain a condition whereby the gases could be exhausted at a uniform rate which was also sufficient to prevent an accumulation of flammable gases in the test enclosure that could lead to a hazardous condition. The proper venting rate could be monitored adequately by visual observation of the accumulation of gases in the enclosure and by their odor which could be detected outside the cabinet if the vent rate was inadequate. In essence, adjustment of the baffle board removed venting rate as an extraneous variable in the ignition measurements.

Pilot

The propane pilot light which was fabricated from 1/16 inch stainless steel tubing was initially installed in a fixed position above the edge of the sample dish during the preheating period. During the early tests it was observed that in this configuration the ignition was dependent on the establishment of a localized flammable mixture near the pilot which depended on convection currents near the surface. By installing the pilot on a moveable arm which allowed it to be swept over the surface of the liquid, the effect of localized fluctuations was eliminated and the reproducibility of the ignition measurements was improved markedly.

Position of Center Radiometer

Many experiments were conducted to determine the optimum location of the center radiometer for monitoring the heat flux to the fuel. Since the radiometer had to be water-cooled, and because of its relative mass, it exerted a significant cooling effect on the fuel when it protruded into it from the base of the sample dish. Eventually it was determined that if the top surface of the radiometer was set flush with the base of the sample dish, the extraneous heat transfer mechanism, which would complicate the analysis of the data, was minimized; above all, with the radiometer in this flush-bottom position the runs were much more reproducible.

The Position of Thermocouples

One of the objectives of this work was to compare the temperature of the liquid at ignition with conventional flash point measurements obtained previously by others. At first, two thermocouple probes were arranged as shown in Figure A-1(a). They were placed above the sample dish (in an inverted "L" shape) with their tips close to the liquid surface. The ignition temperatures, both piloted and unpiloted ignition processes, obtained by this configuration were higher than what was anticipated based on conventional flash point data; apparently absorbed enough radiant energy to affect the temperature readings. The thermocouple probes were then adjusted as in Figure A-1(b), with their tips slightly above the liquid surface, initially. The distance was set to compensate for the expansion of the liquid fuel during the preheating period; ideally the tip would be level with the liquid surface when flame first appeared on the sample dish. Using this configuration, the measured surface piloted ignition temperatures were very close to the published flash point for that fuel. Based on these findings a new fuel dish was fabricated to accommodate better these requirements for temperature measurement [see Figures 3-1(c) and 3-3 of Chapter III].

Liquid Selection

The choice of liquid fuels was based on four factors: safety (the flash point should be above 100°F), economy,

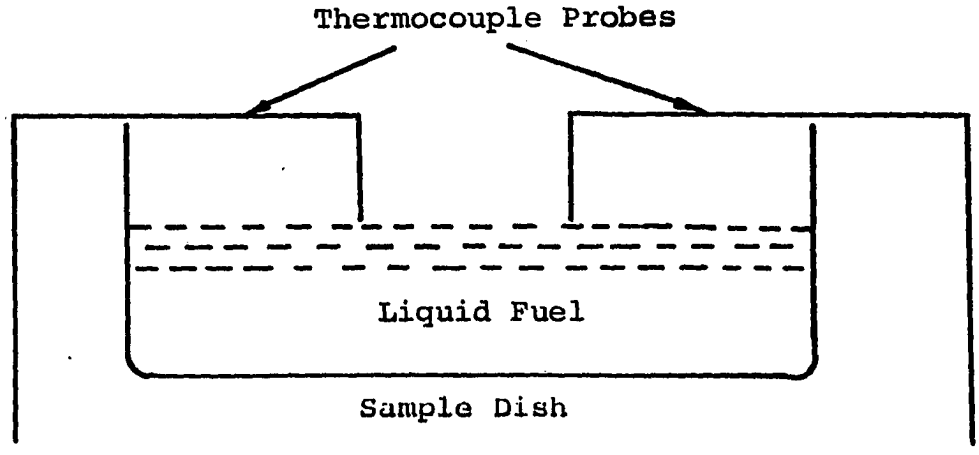

(a) Thermocouple Probes were Set above the Liquid Surface

(Temporary)

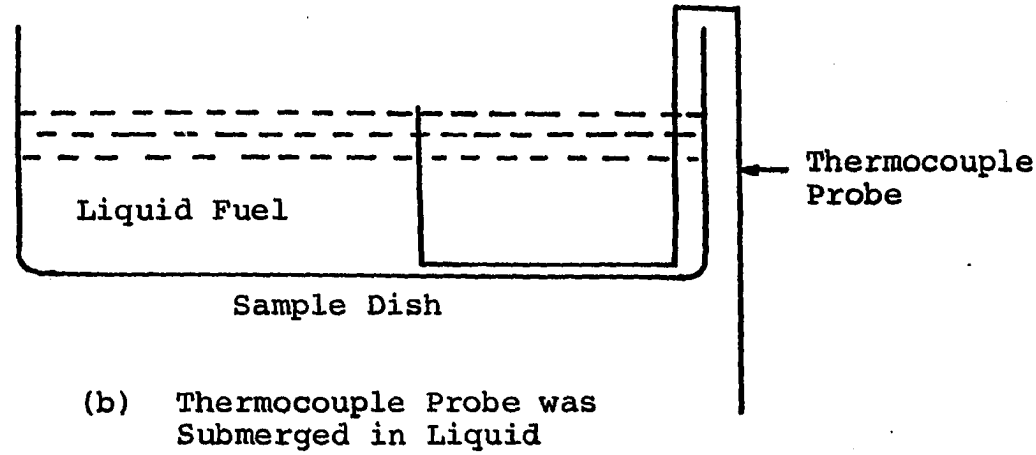

(b) Thermocouple Probe was Submerged in Liquid

(Temporary)

Figure A-1. The Position of Thermocouple Probe in the Sample Dish

availability and reliable data on flash point measurements. Mixtures of components commonly present in kerosene was the expedient choice. Testing volumes of 50 ml, 100 ml, 150 ml and 200 ml were selected as being reasonable and consistent with the size of the test apparatus envisioned. Although the 50 ml volume is obviously the most economical, it was found that the wall heating effects, which depend on the surface to volume ratio, were too dominant and introduced the need for applying a correction factor to the ignition measurements, which was difficult to assess. Consequently most of the data reported herein is for a volume of 100 ml which represents a reasonable compromise between economy and unaccountable, extraneous wall heating effects which introduce experimental bias into the ignition temperature measurements.

Limit of Experimental Ignition Times

The incident irradiation is a function of the distance between the lamp and the liquid surface. In this experiment, the distance was varied from three inches to twelve inches, corresponding to approximate radiation fluxes of 1.65 cal/cm^2-sec to 0.25 cal/cm^2-sec. In this range of incident irradiances, the measured piloted ignition times were always less than three minutes. Longer sustained pre-heating times have a very adverse effect on the life of the tungsten lamps since their filament temperature continues to increase with time. Unfortunately, the three minute restriction

limited the range of variables that could be investigated in unpiloted ignitions. However, piloted ignitions are of more immediate interest because of their comparability to conventional flash point measurements.

One-Man Operation

Since one of the requirements for the test apparatus was that it could be operated by one individual, a substantial amount of time was devoted to rearranging the equipment compactly and revising the procedures in such a way that all exercises could be performed by one person without undue scrambling.

The Distribution of Incident Irradiance

Since the temperature distribution on the surface of tungsten lamps is not uniform, the thermal radiation intensity emitted from the lamp to the sample surface is not uniform. To measure the distribution of the incident irradiance on the sample surface, a calibrated radiometer was located at different transverse positions, but at one level, in the empty sample dish. These positions are identified on Figure A-2 by the letters inside the circles. The distribution of radiation over the surface of the liquid in the sample dish also varies with the lamp heights.

The vertical location of the radiometer was always 5/16 inches below the top edge of the sample dish for every horizontal traverse. There is nothing profound about the 5/16-inch dimension other than it is a reasonable

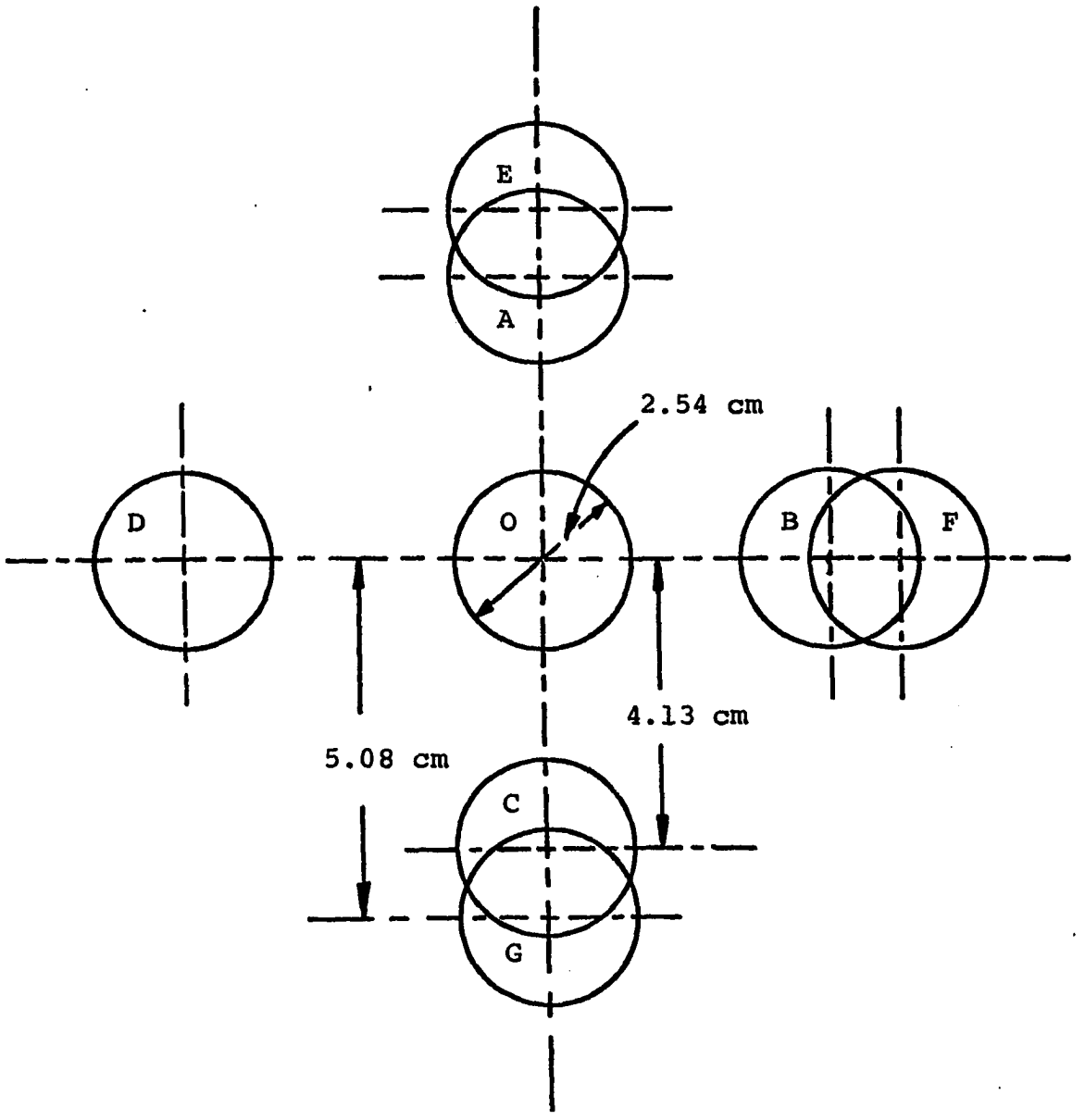

Figure A-2. Positions of Radiometer in the Calibration of Incident Irradiance on the Fuel Surface

representation of the level of the liquid surface during tests. Obviously, because of the diameter of the radiometer, the proximity of measurements to the walls of the dish was limited. Eight horizontal positions were chosen to measure the distribution of the incident irradiance for each of three lamp settings at 5, 8, and 10 inches above the dish holder. Complete data are tabulated in Table A-1, from which three principal conclusions were drawn:

1. The lamp and the dish holder were not parallel to each other so that the flux readings were not exactly symmetrical around the center point.

2. The maximum radiometer readings were always at the center position, 0, and/or at position F. The latter is near the wall of the dish and indicates some reflection of energy from the walls.

3. The difference between the maximum and minimum readings at each level was about 7 percent, which for all practical purposes represents a reasonably uniform distribution. For convenience, the center radiometer reading was adopted as the indicator for the radiation flux reaching the liquid surface.

Fuel Compositions

Six different compositions of normal paraffins (from C_{12} to C_{15}) were used in this experiment. Analyses from a gas chromatograph are presented in Table A-2.

TABLE A-1

THE DISTRIBUTIONS OF INCIDENT IRRADIANCE OF EIGHT POSITIONS OF A SIMULATED LIQUID SURFACE AT THREE RADIATION ENERGY LEVELS

Position	0	A	B	C	D	E	F	G
5 inches	.925	.855	.914	.876	.878	.863	.926	.866
8 inches	.485	.463	.481	.487	.468	.468	.484	.478
10 inches	.342	.317	.338	.334	.333	.329	.343	.338

TABLE A-2

COMPOSITION OF FUELS

(in Mole Fraction)

Fuel	Component $n\text{-}C_{12}H_{26}$	$n\text{-}C_{13}H_{28}$	$n\text{-}C_{14}H_{30}$	$n\text{-}C_{15}H_{32}$	Density gm/cm^3 at 50° C*
	Boiling Point, °C				
	214.5	234	252.5	270.5	
A	--	--	1.000	--	0.742
B	--	1.000	--	--	0.735
C	0.124	0.520	0.356	--	0.736
D	0.025	0.931	0.044	--	0.735
E	0.716	0.170	0.114	--	0.730
F	0.036	0.496	0.447	0.021	0.738

*The density at a temperature of 50° C is probably representative of the average density of the fuel at ignition.